

AD-A013 927

EVALUATION OF 3-D TURBULENCE TECHNIQUES FOR DESIGNING
AIRCRAFT

Frederick D. Eichenbaum

Lockheed-Georgia Company

Prepared for:

Air Force Flight Dynamics Laboratory

January 1975

DISTRIBUTED BY:

NTIS

National Technical Information Service
U. S. DEPARTMENT OF COMMERCE

245099

AFFDL-TR-74-151

AD A013927

EVALUATION OF 3-D TURBULENCE TECHNIQUES FOR DESIGNING AIRCRAFT

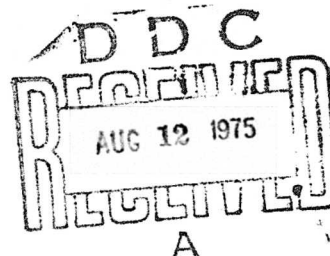
LOCKHEED-GEORGIA COMPANY

TECHNICAL REPORT AFFDL-TR-74-151

MARCH 1975

Approved for public release; distribution unlimited.

Reproduced by
NATIONAL TECHNICAL
INFORMATION SERVICE
U S Department of Commerce
Springfield VA 22151



AIR FORCE FLIGHT DYNAMICS LABORATORY
AIR FORCE SYSTEMS COMMAND
WRIGHT-PATTERSON AIR FORCE BASE, OHIO 45433

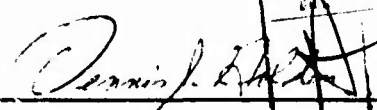
NOTICE

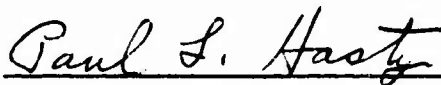
When Government drawings, specifications, or other data are used for any purpose other than in connection with a definitely related Government procurement operation, the United States Government thereby incurs no responsibility nor any obligation whatsoever; and the fact that the government may have formulated, furnished, or in any way supplied the said drawings, specifications, or other data, is not to be regarded by implication or otherwise as in any manner licensing the holder or any other person or corporation, or conveying any rights or permission to manufacture, use, or sell any patented invention that may in any way be related thereto.

This report has been reviewed and cleared for open publication and/or public release by the appropriate Office of Information (OI) in accordance with AFR 190-17 and DODD 5230.9. There is no objection to unlimited distribution of this report to the public at large or by DDC to the National Technical Information Service (NTIS).

This technical report has been reviewed and is approved for publication.

FOR THE COMMANDER


DENNIS J. GOLDEN, Major, USAF
Chief, Structural Integrity Branch
Structures Division
AF Flight Dynamics Laboratory


PAUL L. HASTY/GS-13
Project Engineer

Copies of this report should not be returned unless return is required by security considerations, contractual obligations, or notice on a specific document.

Unclassified

SECURITY CLASSIFICATION OF THIS PAGE (When Data Entered)

REPORT DOCUMENTATION PAGE		READ INSTRUCTIONS BEFORE COMPLETING FORM
1. REPORT NUMBER AFFDL-TR-74-151	2. GOVT ACCESSION NO.	3. RECIPIENT'S CATALOG NUMBER
4. TITLE (and Subtitle) Evaluation of 3-D Turbulence Techniques for Designing Aircraft		5. TYPE OF REPORT & PERIOD COVERED Final Report 10/1/73 to 4/15/75
		6. PERFORMING ORG. REPORT NUMBER
7. AUTHOR(s) Frederick D. Eichenbaum		8. CONTRACT OR GRANT NUMBER(s) F33615-74-C-3004
9. PERFORMING ORGANIZATION NAME AND ADDRESS Lockheed Aircraft Corporation Lockheed-Georgia Company Division 86 Cobb Drive Marietta, Georgia 30060		10. PROGRAM ELEMENT, PROJECT, TASK AREA & WORK UNIT NUMBERS 62201F/1367/02/26
11. CONTROLLING OFFICE NAME AND ADDRESS		12. REPORT DATE January 1975
		13. NUMBER OF PAGES 84
14. MONITORING AGENCY NAME & ADDRESS (if different from Controlling Office) Air Force Flight Dynamics Laboratory AFFDL/FBE, Air Force Systems Command Wright-Patterson AFB, Ohio 45433		15. SECURITY CLASS. (of this report) Unclassified
		15a. DECLASSIFICATION/DOWNGRADING SCHEDULE
16. DISTRIBUTION STATEMENT (of this Report) Approved for public release; distribution unlimited.		
17. DISTRIBUTION STATEMENT (of the abstract entered in Block 20, if different from Report)		
18. SUPPLEMENTARY NOTES		
19. KEY WORDS (Continue on reverse side if necessary and identify by block number) Three-Dimensional Turbulence Aircraft Structures Gust Loads Dynamic Response Analysis Power Spectra Transfer Functions		
20. ABSTRACT (Continue on reverse side if necessary and identify by block number) A recently developed multiple input power spectral technique is applied to predict the response of a C-5A aircraft to three-dimensional turbulence. Results are compared to the equivalent one-dimensional turbulence analysis, using corresponding C-5A dynamic response test data as a reference. Load variations attributable to the 3-d turbulence representation range from an increase of 3% to a decrease of 14% depending upon load component and location. Because the coherence properties of the turbulence field are fully accounted for in the 3-d gust		

Unclassified

SECURITY CLASSIFICATION OF THIS PAGE(When Data Entered)

20. ABSTRACT (Continued)

response analysis, theoretical results which depend upon the cross spectra between responses and probe-measured gust components tend to show a marked improvement over the 1-d case.

Computational procedures used to implement the theory are discussed, and two limiting cases are shown to be important to the turbulence formulation. The first limit corresponds to a large scale of turbulence and reduces the transverse gust coherences to functions of a single variable which is independent of the scale. The second limit corresponds to small transverse aircraft dimensions and reduces to the 1-d case. In fact, all of the restricted gust response formulations in current use may be deduced from the complete formulation by eliminating gust components and imposing appropriate restrictions on the aircraft geometry.

Unclassified

SECURITY CLASSIFICATION OF THIS PAGE(When Data Entered)

FOREWORD

This report was prepared by Lockheed-Georgia Company, Marietta, Georgia, under Air Force Contract F33615-74-C-3004. The contract was initiated under Project number 1367, "Structural Design Criteria", Task No. 136702, "Aerospace Vehicle Structural Loads Criteria". The work was administered under the direction of the Air Force Flight Dynamics Laboratory, Research and Technology Division, Air Force Systems Command, Wright-Patterson Air Force Base, Ohio, Mr. Paul L. Hasty (FBE-B), Project Engineer.

The work reported in this study was conducted by Lockheed-Georgia Company with Frederick D. Eichenbaum as principal investigator, and covers the period October 1973 to October 1974. The report was submitted by the author in December 1974.

TABLE OF CONTENTS

<u>Section</u>	<u>Title</u>	<u>Page</u>
I	INTRODUCTION	1
II	GUST VELOCITY CROSS SPECTRUM	4
	2.1 Cross Spectrum Tensor	4
	2.2 Closed Form Solution	6
	2.3 Large Scale Limit	8
	2.4 Planar and Nonplanar Coherences	12
	2.5 Small Aircraft Limit	13
	2.6 0-D, 1-D and 2-D Approximations	14
	2.7 Omission of Gust Components	15
	2.8 Anisotropic Turbulence	16
III	AIRCRAFT FREQUENCY RESPONSE FUNCTIONS	18
	3.1 Force Equilibrium	18
	3.2 Acceleration Response Functions	19
	3.3 Load Response Functions	20
IV	THREE-DIMENSIONAL GUST RESPONSE	22
	4.1 Lateral Symmetry	22
	4.2 Response Power Spectra	24
	4.3 Transfer Functions	25
	4.4 Response Parameters	26
	4.5 Response Cross Spectra	27
	4.6 Cross Transfer Functions	28
	4.7 Vertical and Lateral Gust	29
V	EVALUATION OF THE 3-D MODEL	33
	5.1 Aircraft Description	33
	5.2 Computational Model	33
	5.3 Computer Program	34
	5.4 1-D Versus 3-D Response Parameters	36
	5.5 Flight Test Comparison	39

TABLE OF CONTENTS (Continued)

<u>Section</u>	<u>Title</u>	<u>Page</u>
VI	CONCLUSIONS AND RECOMMENDATIONS	67
	REFERENCES	69

LIST OF ILLUSTRATIONS

<u>Figure</u>	<u>Title</u>	<u>Page</u>
1	Normalized Power Spectra of Longitudinal and Transverse Gust Velocity Components for the von Karman Case	9
2	Coherences of Longitudinal and Lateral Gust Components for the von Karman Case	10
3	Coherences of Vertical and Lateral Gust Components for the von Karman Case	11
4	Aerodynamic Configuration for the C-5A Analytical Model	35
5	Wing RMS Incremental Loads and Characteristic Frequencies in Turbulence	37
6	Horizontal Stabilizer RMS Incremental Loads and Characteristic Frequencies in Turbulence	38
7	Procedure for Evaluating Three-Dimensional Gust Response Analysis Methods	40

LIST OF SYMBOLS

Scalar and Tensor Quantities:

$C_j(\Omega)$	Response cross transfer function relative to a cartesian gust velocity component measured at the probe
\underline{e}_j	Cartesian unit vector in the aircraft coordinate system
g	Modal structural damping coefficient
$H_m(\Omega)$	Frequency response function relative to gust velocity normal to an aerodynamic reference panel. (The gust phase is taken at the origin of the aircraft coordinate system.)
$H_m^+(\Omega)$	Symmetry-restricted frequency response functions relative to gust velocities normal to a pair of aerodynamic reference panels. (The gust phase is taken at the origin of the aircraft coordinate system.)
i	$\sqrt{-1}$
$K_{1/6}, K_{5/6}$	Modified Bessel functions of the second kind of order 1/6 and 5/6, respectively
L	Effective longitudinal scale of turbulence
$\underline{m}, \underline{n}$	Unit vectors which may be normal to aerodynamic reference panels.
N	Number of aerodynamic reference panels on one side of the aircraft.

LIST OF SYMBOLS (Continued)

Scalar and Tensor Quantities:

N_o	Zero crossing rate
P	Transverse portion of the separation vector between gust measurements in the aircraft coordinate system
q	Dynamic pressure
\underline{r}	Separation vector between gust measurements in the aircraft coordinate system
$T^{\pm}(\Omega)$	Symmetry-restricted response transfer functions relative to vertical (+) and lateral (-) gust velocity
V	True airspeed
x, y, z	Relative or absolute longitudinal, lateral and vertical coordinates, respectively
γ	Dihedral angle of aerodynamic reference panel
$\gamma_j^2(\Omega)$	Response coherence function relative to a cartesian gust velocity component measured at the probe
Γ	Gamma function

LIST OF SYMBOLS (Continued)

Scalar and Tensor Quantities:

κ, μ	Parameters appearing in the analytical formulation of the gust velocity cross spectra
$\sigma, \sigma_w, \sigma_j$	RMS of response, gust velocity, and gust velocity component, respectively
$\Phi(\underline{m}, \underline{n}, \underline{r}, \Omega)$	Cross spectrum between gust velocity components measured along unit directional vectors
$\Phi_{jk}(p, \Omega)$	Cross spectrum between cartesian gust velocity components having a purely lateral separation
$\Phi_{jn}(\Omega)$	Cross spectrum between a cartesian gust velocity component measured at the probe and a gust velocity component normal to a reference plane. (The longitudinal separation between the gust components is ignored)
$\Phi_{mn}(\Omega)$	Cross spectrum between gust velocity components normal to two aerodynamic reference panels. (The longitudinal separation between the gust components is ignored)
$\Phi_{mn}^{\pm}(\Omega)$	Symmetry-restricted cross spectra between gust velocity components normal to two pairs of aerodynamic reference panels. (The longitudinal separation between the gust components is ignored)
$\Phi_j(\Omega)$	Power spectrum of a cartesian gust velocity component

LIST OF SYMBOLS (Continued)

Scalar and Tensor Quantities:

$\hat{\phi}, \tilde{\phi}$	Ordinary and infinite scale coherences, respectively, representing the normalized form of the corresponding cross spectra obtained by effectively dividing out the frequency distributions of the respective RMS gust velocity components
ϕ_P, ϕ_N	Planar and nonplanar gust velocity cross spectra, respectively
$\phi(\Omega), \phi^{\pm}(\Omega)$	Total and symmetry-restricted response power spectra, respectively
$\bar{\omega}, \omega, \Omega$	Eigenfrequency, radial frequency and reduced frequency, respectively

Subscripts and Superscripts:

j, k	Cartesian components
m, n	Aerodynamic panels, or panel pairs whose members are reflected through the plan of symmetry
o	Gust probe
\pm	Restricted to responses that are either symmetric (+) or antisymmetric (-) about the plane of symmetry

LIST OF SYMBOLS (Continued)

Subscripts and Superscripts:

$()'$ Reflected through the plane of symmetry

$*$ Complex conjugate

Matrix Notation:

$\{ \}$ Column matrix

$[]$ Rectangular matrix

$[\downarrow]$ Diagonal matrix

$[]^{-1}$ Inverted matrix

$[\bar{}]$ Dependent (row) quantity is generalized (expressed in modal coordinates)

Matrix Root Symbols:

A Aerodynamic load coefficient relative to generalized displacement

\bar{B} Ratio of generalized gust force to generalized displacement

C Aerodynamic load coefficient relative to control surface angle of attack

E Ratio of elastic load to generalized displacement

LIST OF SYMBOLS (Continued)

Matrix Root Symbols:

F	Ratio of control surface angle of attack to sensor response
G	Aerodynamic load coefficient relative to gust angle of attack at an aerodynamic reference panel
H	Frequency response function for load or acceleration response to gust velocity normal to an aerodynamic reference panel (The gust phase is taken at the origin of the aircraft coordinate system)
M	Inertia load coefficient relative to generalized displacement (It is also referred to as the generalized mass if the overbar is affixed as described under Matrix Notation)
R, S	Ratios of accelerometer and sensor displacement, respectively, to generalized displacement
W	Gust velocity normal to an aerodynamic reference panel (The gust phase is taken at the origin of the aircraft coordinate system)
ξ	Generalized displacement

SECTION I

INTRODUCTION

Dramatic increases in the size and flexibility of new aircraft have induced a greater reliance upon power spectral methods in gust design. Corresponding structural representations of the aircraft are typically of the lumped mass variety, and three-dimensional lifting surface aerodynamics is routinely employed. However, in certain important respects, the current atmospheric turbulence description has not kept pace with these developments.

Since gust velocity varies in magnitude and direction along the path of an airplane, it is obvious that a similar variation must exist along any line perpendicular to the path. It has long been recognized that the latter gust variation may be sufficient over the transverse dimensions of a large aircraft to justify its inclusion in the analytical turbulence description. However, because of the extremely cumbersome mathematics required to generate the necessary turbulence description, the most common procedure has consisted of retaining only the vertical gust component and ignoring gust variations which depend upon vertical position. This results in a single-component, two-dimensional turbulence model. The earlier and more common one-dimensional model completely ignores transverse variations in gust and treats vertical and lateral gust responses as separate calculations.

An exact, but simple three-dimensional gust model consistent with current structural and aerodynamic computational procedures is presented in References 1 through 4. The original development is contained in References 1 and 2, and consists of the following essential steps: (1) a unique rotational transformation is applied to reduce from nine to four, the number of independent components required to specify the gust velocity cross spectrum tensor. (2) Closed form solutions of the cross spectrum tensor are derived for both the Dryden and von Karman spectral models. (3) The computational redundancies which arise when the analytical

representation of the aircraft is introduced are eliminated by invoking the appropriate symmetry properties of the cross spectrum tensor.

This procedure results in a concise, unified multiple input formulation that describes the dynamic response of a bilaterally symmetric, flexible aircraft traversing a random, isotropic field of atmospheric turbulence. The new method incorporates in its present form the following significant features: (1) The formulation is fully three-dimensional, so that even if the aircraft is assumed to be unresponsive to one or two of the three components of turbulence, the result still differs from the 1-d or 2-d case. (2) The computation is efficient; i.e., all three components of turbulence may be included in a single calculation, and the cost per case of performing a 3-d gust response analysis of a flexible airplane is essentially the same as the corresponding 1-d calculation. (3) The correlation properties of the 3-d turbulence field are conveniently described in terms of only two functions of a single variable. These are designated as the planar and nonplanar gust coherences and are furnished in tabular form. (4) Since the formulation separates the amplitude properties of the turbulence field from its correlation properties, the same analytical or empirical gust spectra may be employed as in the conventional 1-d analysis. (5) If the scale of turbulence is much larger than the transverse dimensions of the aircraft, then the formulation becomes independent of the scale except in specifying the analytical gust spectra. (6) If the transverse dimensions of the aircraft are ignored, then the method reduces to the conventional 1-d analysis. (7) If the vertical dimensions of the aircraft are ignored and the calculation is confined to vertical gust only, then the method reduces to the current 2-d analysis. (8) The method is compatible with current turbulence design criteria procedures, so that only a possible adjustment of existing parameter values would be required. (9) Anisotropic turbulence can be introduced by a simple procedure which preserves isotropy at small wavelengths.

The theory encompasses two types of response analysis: power spectral and cross spectral. The power spectral approach may be used to furnish data

for gust design, including fatigue, design loads, stability and control. Cross spectral methods are primarily employed to relate structural responses to gust inputs as measured by a probe attached to the aircraft. By comparing cross spectral data with actual flight measurements, a direct verification of the analytical model may be achieved. Power spectral data may also be used for this purpose. The work described herein covers both methods, and the objective is to demonstrate and evaluate the effect of three-dimensional turbulence models in comparison to one-dimensional models by means of dynamic response test data from the C-5A aircraft.

This effort represents part of a long range plan which is programmed to achieve four interrelated objectives: (1) implementation of three-dimensional gust response methods, (2) validation of these methods by comparison with dynamic response test results, (3) incorporation of these methods into current design procedures, (4) development of new methods and applications, including treatment of aircraft response to turbulence conditions which depart from current ideal assumptions. This report is intended to achieve objective (2), to demonstrate and evaluate the effect of three-dimensional turbulence by means of available aircraft dynamic response data.

SECTION II

GUST VELOCITY CROSS SPECTRUM

The turbulence description required for a 3-d gust response analysis of an aircraft is provided by the gust velocity cross spectrum tensor as measured by traversing a statistically stationary, random, isotropic field of atmospheric turbulence. The cross spectrum tensor is used to compute the gust velocity cross spectrum between gusts impinging upon any two points of the aircraft. The analytical representation of the gust velocity cross spectrum tensor for the von Karman turbulence model was originally derived in Reference 2 (See also References 3 and 4). A derivation of the cross spectrum tensor for the Dryden model originally appeared in Reference 1, but it is considered to be less representative of atmospheric turbulence under most flight conditions.

2.1 CROSS SPECTRUM TENSOR

A unique rotational transformation was also employed in References 1 through 4 to reduce the required number of distinct cross spectrum components to four. Moreover, the transverse separation in the original frame becomes the lateral separation in the rotated frame, so that explicit dependence upon the vertical separation variable is eliminated. It was also shown that under Taylor's "frozen turbulence" hypothesis, the dependence of the cross spectrum tensor upon the longitudinal separation reduces to the conventional phase factor for gust penetration. As such, the latter quantity may be transferred to the frequency response function of the aircraft. The four distinct cross spectrum components are thus reduced to functions of the reduced frequency $\Omega = \omega/V$ and the transverse separation $p = \sqrt{y^2 + z^2}$.

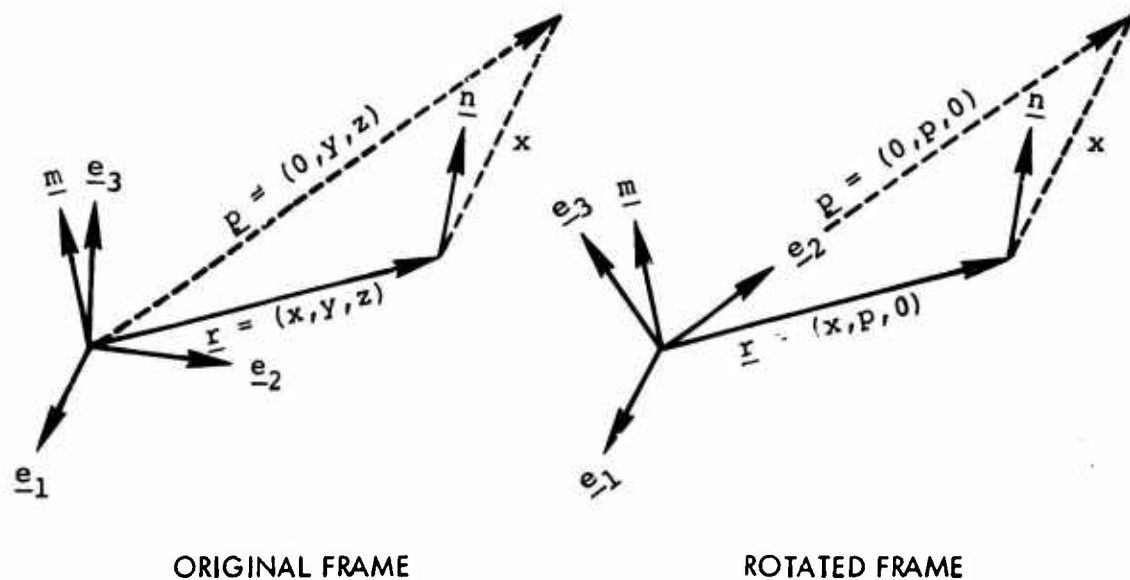
The cross spectrum between gust velocity components measured along the respective unit directional vectors $\underline{m} = (m_1, m_2, m_3)$ and $\underline{n} = (n_1, n_2, n_3)$ which are separated by the vector $\underline{r} = (x, y, z)$ whose transverse component is $\underline{p} = (0, y, z)$, then becomes

$$\begin{aligned}
\phi(\underline{m}, \underline{n}, \underline{r}, \Omega) = e^{-i\Omega x} \bigg\{ & \phi_{11}(p, \Omega) m_1 n_1 + \\
& \phi_{12}(p, \Omega) (m_1 (y n_2 + z n_3) + n_1 (y m_2 + z m_3)) / p + \\
& (\phi_{22}(p, \Omega) - \phi_{33}(p, \Omega)) (y n_2 + z n_3) (y m_2 + z m_3) / p^2 + \\
& \phi_{33}(p, \Omega) (m_2 n_2 + m_3 n_3) \bigg\} \quad (2.1)
\end{aligned}$$

(3-D TURBULENCE)

where $\phi_{jk}(p, \Omega) \equiv \phi(\underline{e}_j, \underline{e}_k, p \underline{e}_2, \Omega)$ (2.2)

is the cross spectrum between cartesian gust velocity components having a purely lateral separation. The cartesian unit vector is denoted by \underline{e}_j . The vector configuration is illustrated by the following sketch.



2.2 CLOSED FORM SOLUTION

For evaluation and analysis, it is convenient to separate the correlation and amplitude properties of the four distinct cross spectrum components of the tensor by factoring them into the general form

$$\Phi_{jk}(p, \Omega) = \hat{\Phi}_{jk}(p, \Omega) \sqrt{\Phi_j(\Omega) \Phi_k(\Omega)} \quad (2.3)$$

where
$$\hat{\Phi}_{jk}(p, \Omega) \equiv \Phi_{jk}(p, \Omega) / \sqrt{\Phi_j(\Omega) \Phi_k(\Omega)} \quad (2.4)$$

and
$$\Phi_j(\Omega) \equiv \Phi_{jj}(0, \Omega) \quad (2.5)$$

Equation (2.5) defines the power spectrum of a gust velocity (the auto spectrum of a velocity component). It is a real function representing the frequency distribution of the mean square amplitude of a cartesian velocity component.

Equation (2.4) defines the gust coherence. It represents the normalized form of the corresponding gust velocity cross spectrum of equation (2.3), and is obtained by effectively dividing out the frequency distributions of the respective RMS gust velocity components. What remains is a complex function whose modulus and phase angle correspond to the frequency distributions of the correlation coefficient and phase difference, respectively, between the gust components.

References 2 through 5 give the following closed form solution for the von Karman power spectra and gust coherences required in equation (2.3) to compute the four cross spectrum components of equation (2.1).

$$\phi_j(\Omega) \equiv \phi_{jj}(0, \Omega) = \begin{cases} 2L\sigma_W^2/\pi(1 + \kappa^2)^{5/6} & (j = 1) \\ L\sigma_W^2(1 + 8\kappa^2/3)/\pi(1 + \kappa^2)^{11/6} & (j = 2, 3) \end{cases} \quad (2.6)$$

where $\kappa \equiv 1.339L\Omega$, $\Omega = \omega/V$

and $1.339 \approx \Gamma(1/3)/\Gamma(1/2)\Gamma(5/6)$

$$\begin{aligned} \text{Also, } \hat{\phi}_{11}(p, \Omega) &= 0.9944(\mu^{5/6} K_{5/6}(\mu) - \mu^{11/6} K_{1/6}(\mu)/2) \\ -i\hat{\phi}_{12}(p, \Omega) &= 0.9944\mu^{11/6} K_{5/6}(\mu)\kappa/2^{1/2}\sqrt{1 + 8\kappa^2/3} \end{aligned} \quad (2.7)$$

$$\hat{\phi}_{22}(p, \Omega) - \hat{\phi}_{33}(p, \Omega) = 0.9944\mu^{11/6} K_{1/6}(\mu)(1 + \kappa^2)/(1 + 8\kappa^2/3)$$

$$\hat{\phi}_{33}(p, \Omega) = 0.9944(\mu^{5/6} K_{5/6}(\mu) - \mu^{11/6} K_{1/6}(\mu)/(1 + 8\kappa^2/3))$$

where $\mu \equiv (p/1.339L)\sqrt{1 + \kappa^2}$

and $0.9944 \approx 2^{1/6} \Gamma(5/6)$

Γ and K denote the gamma function and the modified Bessel function of the second kind, respectively. Notice that the scale of turbulence L , which is a measure of average eddy size, emerges as a parameter in the closed form solution. Since the coherence between longitudinal and lateral gust is a positive imaginary quantity, it is multiplied by $-i$ to yield a positive real quantity. Similarly, the coherence between lateral components is replaced by a difference for computational convenience.

Figure 1 contains the longitudinal and transverse (lateral and vertical) power spectra. They are normalized and plotted versus nondimensional reduced frequency ΩL , by taking the RMS gust velocity component and the scale of turbulence to be of unit magnitude.

Figures 2 and 3 show the four gust coherences plotted versus $p\Omega$, the lateral separation in radians. Each coherence appears as a family of curves with p/L , the lateral separation in scale lengths, as parameter. All of coherences are monotonic with respect to the parameter except for the family of curves at the top of Figure 3. There, for values of the parameter greater than are shown, the curves fall back onto the horizontal axis.

The fact that $\hat{\phi}_{12}(p,\Omega)$ is imaginary indicates that a $\pi/2$ phase difference exists between the coherent portions of the longitudinal and lateral gust velocity components. Similarly, $\hat{\phi}_{11}(p,\Omega)$ drops below the zero axis and exhibits small negative values at all subsequent lateral separations. Therefore, coherent vertical gust components have a phase difference of π under these conditions. Reference to equation (2.1) shows that introducing a longitudinal separation merely imposes a further difference in phase due to gust penetration, and has no effect upon the modulus of the coherence. Moreover, since the modulus corresponds to a correlation coefficient, its value cannot exceed unity.

Reference 4 shows that although the power spectra for the Dryden and von Karman spectral models are quite dissimilar, the numerical values of their gust coherences are almost identical. This suggests that the gust coherences of equation (2.7) may be used in equation (2.3) with empirical power spectra that need not conform to the von Karman model.

2.3 LARGE SCALE LIMIT

If the scale of turbulence is large compared to the transverse dimensions of the aircraft, then the gust coherences of equations (2.7) lose their dependence upon the scale and reduce to the following single-variable functions of the lateral separation in radians:

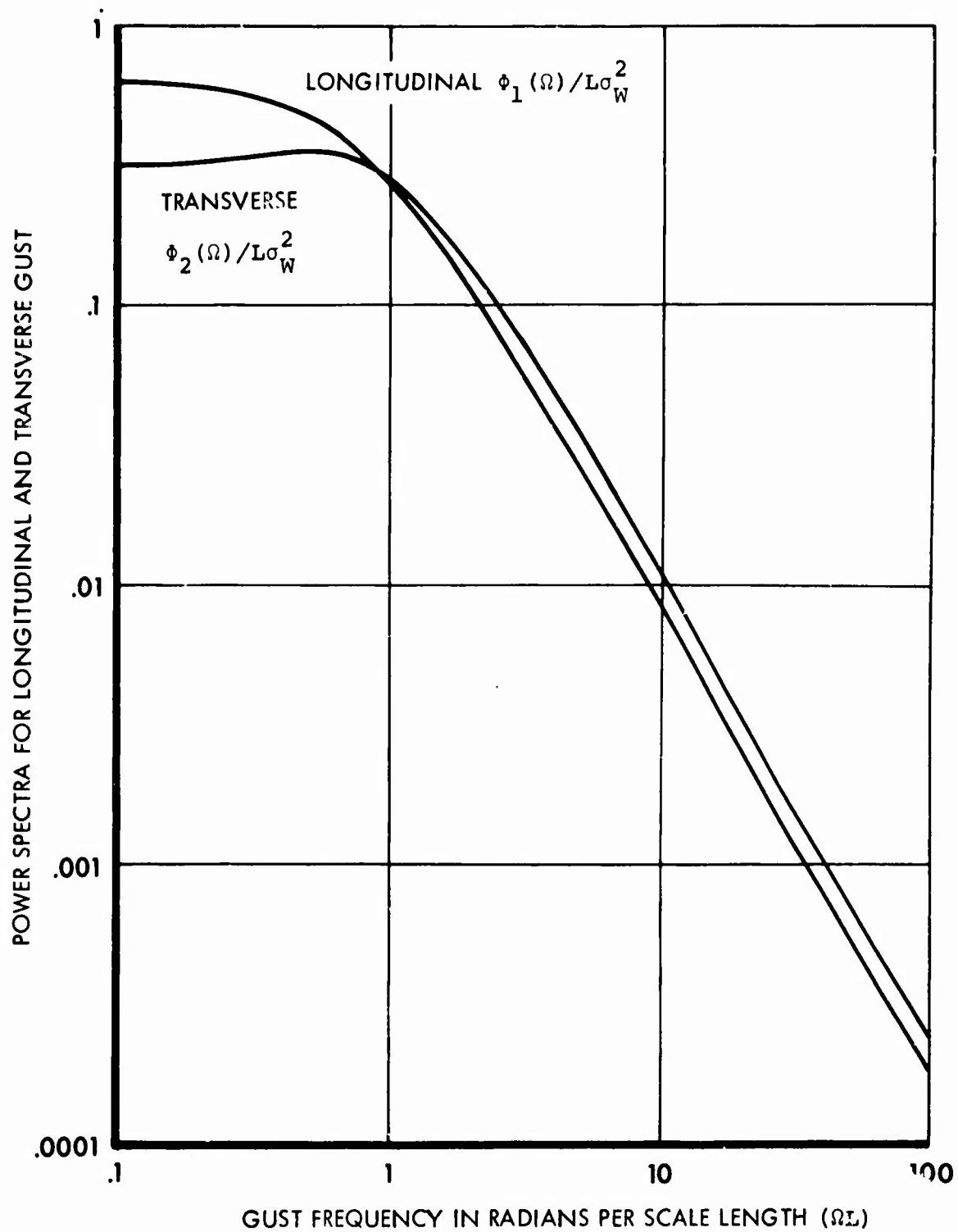


Figure 1. Normalized Power Spectra of Longitudinal and Transverse Gust Velocity Components for the von Karman Case

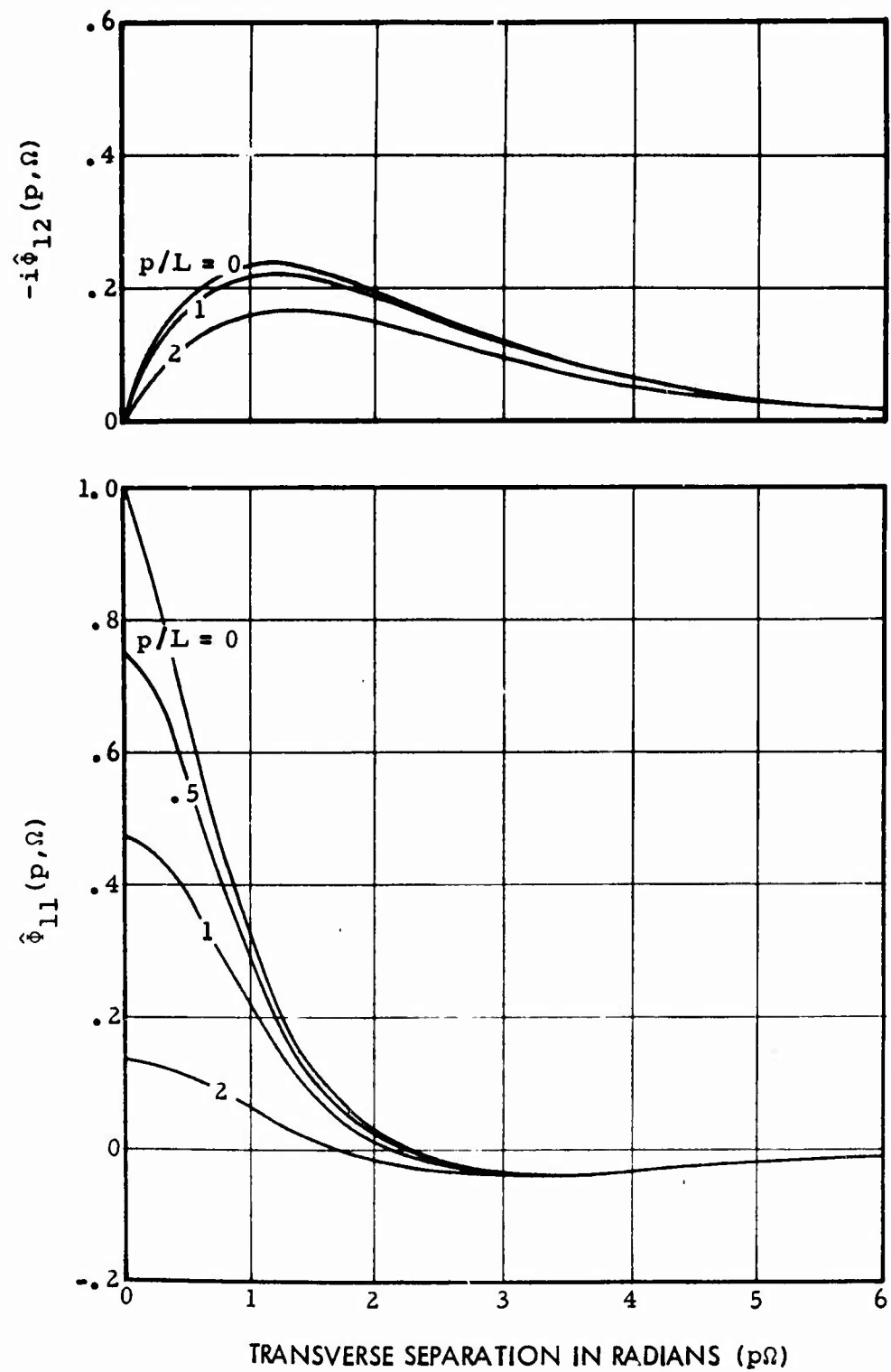


Figure 2. Coherences of Longitudinal and Lateral Gust Components for the von Karman Case

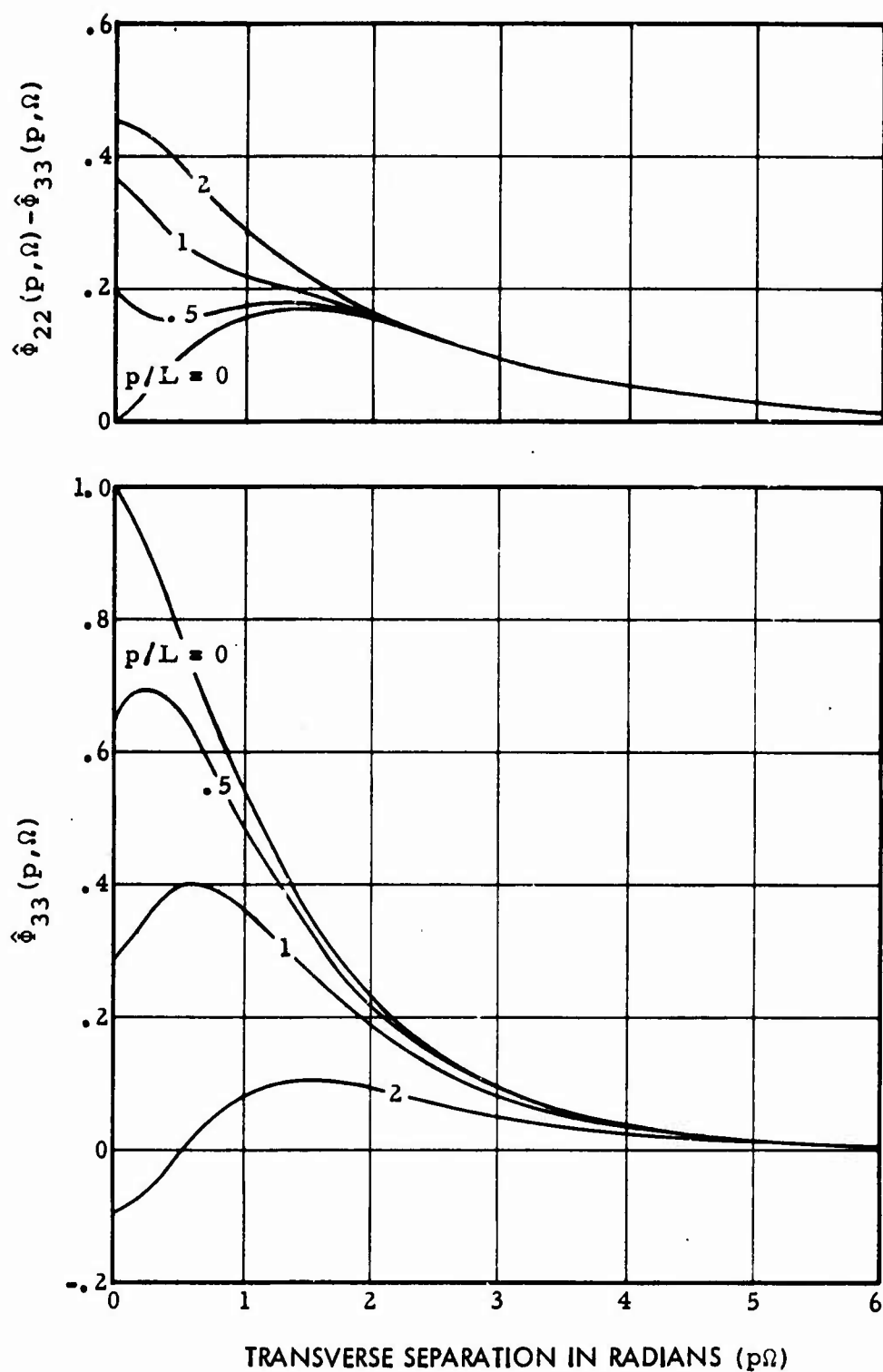


Figure 3. Coherences of Vertical and Lateral Gust Components for the von Karman Case

$$\begin{aligned}
\tilde{\phi}_{11}(p\Omega) &= 0.9944 \left((p\Omega)^{5/6} \kappa_{5/6}(p\Omega) - (p\Omega)^{11/6} \kappa_{1/6}(p\Omega)/2 \right) \\
-i\tilde{\phi}_{12}(p\Omega) &= 0.9944 (\sqrt{3}/4) (p\Omega)^{11/6} \kappa_{5/6}(p\Omega) \\
\tilde{\phi}_{22}(p\Omega) - \tilde{\phi}_{33}(p\Omega) &= 0.9944 (3/8) (p\Omega)^{11/6} \kappa_{1/6}(p\Omega) \\
\tilde{\phi}_{33}(p\Omega) &= 0.9944 (p\Omega)^{5/6} \kappa_{5/6}(p\Omega)
\end{aligned} \tag{2.8}$$

$$\text{where } \tilde{\phi}_{jk}(p\Omega) \equiv \lim_{p/L \rightarrow 0} \hat{\phi}_{jk}(p, \Omega) = \lim_{L \rightarrow \infty} \hat{\phi}_{jk}(p, \Omega) \tag{2.9}$$

Notice that the same result may be derived from the more restrictive assumption of infinite scale. It is therefore referred to as the large scale limit.

2.4 PLANAR AND NONPLANAR COHERENCES

Examination of the four terms in the cross spectrum formulation given by equation (2.1) shows that if longitudinal gust is ignored, the first two terms may be omitted. Furthermore, when the resulting gusts are measured normal to a plane, the fourth term assumes its maximum value, and the third term vanishes. We will therefore designate the corresponding cross spectra as the planar and nonplanar, respectively, denoted by ϕ_P and ϕ_N . According to equations (2.8) and (2.9), the corresponding planar and nonplanar coherences in the large scale limit may be written

$$\begin{aligned}
\tilde{\phi}_P(p\Omega) &\equiv \tilde{\phi}_{33}(p\Omega) = 0.9944 (p\Omega)^{5/6} \kappa_{5/6}(p\Omega) \\
\tilde{\phi}_N(p\Omega) &\equiv \tilde{\phi}_{22}(p\Omega) - \tilde{\phi}_{33}(p\Omega) = 0.9944 (3/8) (p\Omega)^{11/6} \kappa_{1/6}(p\Omega)
\end{aligned} \tag{2.10}$$

The asymptotic coherences defined by equations (2.10) may be substituted back into equations (2.7) by changing the variable from $p\Omega$ to μ and matching up similar terms. All four coherences are thereby expressed in terms of the asymptotic planar and nonplanar coherences. The result is

$$\begin{aligned}
 \hat{\phi}_{11}(p, \Omega) &= \tilde{\phi}_P(\mu) - (4/3)\tilde{\phi}_N(\mu) \\
 -i\hat{\phi}_{12}(p, \Omega) &= \tilde{\phi}_P(\mu) \mu \kappa / 2^{1/2} \sqrt{1 + 8\kappa^2/3} \\
 \hat{\phi}_{22}(p, \Omega) - \hat{\phi}_{33}(p, \Omega) &= \tilde{\phi}_N(\mu) (1 + \kappa^2) / (3/8 + \kappa^2) \\
 \hat{\phi}_{33}(p, \Omega) &= \tilde{\phi}_P(\mu) - \tilde{\phi}_N(\mu) / (3/8 + \kappa^2)
 \end{aligned} \tag{2.11}$$

Notice that $\tilde{\phi}_P(p\Omega)$ and $\tilde{\phi}_N(p\Omega)$ correspond to the $p/L = 0$ curves in Figure 3. As single-variable functions, they may be conveniently tabulated for use in the above expressions. Furthermore, if p/L is sufficiently small, then the gust coherences may be obtained directly from equations (2.8).

2.5 SMALL AIRCRAFT LIMIT

If the large scale limit described in Paragraph 2.3 is satisfied, and if the transverse separation in radians is sufficiently small, then

$$\lim_{\substack{p/L \rightarrow 0 \\ p\Omega \rightarrow 0}} \hat{\phi}_{jk}(p, \Omega) = \lim_{p \rightarrow 0} \hat{\phi}_{jk}(p, \Omega) = \tilde{\phi}_{jk}(0) = \begin{cases} 1 & j = k \\ 0 & j \neq k \end{cases} \tag{2.12}$$

Notice that the same result may be derived from the more restrictive assumption of zero transverse separation. It is therefore referred to as the small aircraft limit, although the restriction applies only to the transverse dimensions of the aircraft and not to its length. Since $\Omega = \omega/V$, the limit $p\Omega = 0$ is also approached when the radial frequency is small or the airspeed is large.

2.6 0-D, 1-D AND 2-D APPROXIMATIONS

The zero-dimensional approximation for the gust velocity cross spectrum corresponds to the assumption of a point aircraft and is valid if gust variations are negligible within the spatial boundaries of the aircraft. Setting $\underline{r} = \underline{0}$ in equation (2.1) and applying equation (2.3) and (2.12) yields

$$\phi(\underline{m}, \underline{n}, \underline{0}, \Omega) = \sum_{j=1}^3 \phi_j(\Omega) m_j n_j \quad (2.13)$$

(0-D TURBULENCE)

The conventional 1-d turbulence approximation corresponds to the assumption of a linear aircraft and is valid if gust variations are negligible except across the longitudinal dimension of the aircraft. This condition is identical to the small aircraft limit discussed in Paragraph 2.5. Setting $\underline{r} = x\underline{e}_1$ in equation (2.1) and proceeding as before, we obtain

$$\phi(\underline{m}, \underline{n}, x\underline{e}_1, \Omega) = e^{-i\Omega x} \sum_{j=1}^3 \phi_j(\Omega) m_j n_j \quad (2.14)$$

(1-D TURBULENCE)

This result differs from the 0-d turbulence case only in that the phase factor for gust penetration is now included.

The conventional 2-d turbulence approximation corresponds to a planar aircraft and is valid if gust variations across the vertical dimension of the aircraft are small enough to be ignored. Setting $\underline{r} = x\underline{e}_1 + y\underline{e}_2$ in equation (2.1) yields

$$\begin{aligned} \phi(\underline{m}, \underline{n}, x\underline{e}_1 + y\underline{e}_2, \Omega) = e^{-i\Omega x} & (\phi_{11}(y, \Omega) m_1 n_1 + \phi_{12}(y, \Omega) (m_1 n_1 + m_2 n_2) + \\ & \phi_{22}(y, \Omega) m_2 n_2 + \phi_{33}(y, \Omega) m_3 n_3) \end{aligned} \quad (2.15)$$

(2-D TURBULENCE)

A comparison of equations (2.1) and (2.13-2.15) shows that the 0-d and 1-d cases require only the gust power spectra, whereas the 2-d and 3-d cases also require the gust coherences according to equation (2.3).

2.7 OMISSION OF GUST COMPONENTS

The aerodynamic representation of the aircraft to which the gust velocity cross spectrum is applied may exclude response to a given cartesian gust velocity component. In that case the corresponding components of the directional vectors \underline{m} and \underline{n} in the cross spectrum expression are simply set to zero. This may result in the elimination of various terms in equations (2.1) and (2.13-2.15). For example, in Reference 5 the 2-d approximation is applied to the Concord aircraft, but longitudinal and lateral gust responses are omitted. In that case equation (2.15) reduces to

$$\phi(\underline{m}, \underline{n}, x\underline{e}_1 + y\underline{e}_2, \Omega) = e^{-i\Omega x} \phi(y, \Omega) m_3 n_3 \quad (2.16)$$

(2-D VERTICAL GUST)

The response to lateral gust may be included in a separate 1-d calculation. In that case equation (2.14) reduces to

$$\phi(\underline{m}, \underline{n}, x_{e1}, \Omega) = e^{-i\Omega x} \phi_2(\Omega) m_2 n_2 \quad (2.17)$$

(1-D LATERAL GUST)

2.8 ANISOTROPIC TURBULENCE

Both the scale of turbulence and the RMS value of a gust velocity component may depend upon direction if the turbulence field is anisotropic. In that case the following substitutions may be made in the von Karman power spectra for isotropic turbulence given by equations (2.6).

$$\sigma_W \rightarrow \sigma_j, \quad L \rightarrow L_j \quad (2.18)$$

(ANISOTROPIC TURBULENCE)

Constraints upon the values of these parameters may be derived from the condition that anisotropic turbulence approaches isotropy in the high frequency range (Reference 6). Therefore, the gust spectra for anisotropic turbulence must assume the same asymptotic form as equations (2.6) in the limit of large Ω , thereby yielding

$$L_j \propto \sigma_j^3 \quad (2.19)$$

Moreover, if horizontal isotropy is present, then the further restriction that $L_1 = L_2$ may be imposed. These constraints may be invoked when applying an analytical fit to simultaneously measured gust spectra. They are also

useful for establishing gust criteria for analytical gust spectrum formulations and are reflected in current military design criteria specifications (References 7 and 8).

Figures 2 and 3 show the gust coherences to be quite insensitive to the assumed scale of turbulence for the small values of p/L that typically prevail. It is then permissible to assume the isotropic turbulence relation $L = L_3$ in computing the gust coherences for anisotropic turbulence. Anisotropy in gust amplitude may be accounted for by multiplying each directional vector component m_j and n_j by the corresponding power spectrum amplitude $\sqrt{\phi_j(\Omega)}$ and in compensation, replacing each cross spectrum $\phi_{jk}(p, \Omega)$ by its coherence $\hat{\phi}_{jk}(p, \Omega)$.

SECTION III

AIRCRAFT FREQUENCY RESPONSE FUNCTIONS

The aircraft structural and aerodynamic description used in the analysis of flight in turbulence is contained in the conventional frequency response function which relates a given structural response to the gust impinging upon an aerodynamic reference panel. This function is independent of the turbulence description and is therefore applicable to all of the turbulence cases discussed in Section II. The necessary frequency response functions for loads and accelerations are derived in the following paragraphs from the principle of balanced forces. Matrix notation is used throughout the development.

3.1 FORCE EQUILIBRIUM

The aerodynamic surfaces of the aircraft are assumed to be represented by reference panels with respect to which there exists a normal gust velocity distribution $\{W\}$ that is furnished independently by the turbulence description. The resulting generalized displacements $\{\xi\}$ are assigned to the modal shapes derived from a free-free modal analysis of the aircraft structure. The force balance principle for the aircraft may be expressed in terms of either the generalized forces,

$$(q/V) [\bar{G}] e^{-i\Omega x} \{W\} +$$

$$(\omega^2 [\bar{M}] - [\bar{M}] \bar{\omega}^2 (1 + ig)) + q[\bar{A}] + q[\bar{C}][F][S]) \{\xi\} = \{0\} \quad (3.1)$$

or the response loads

$$(q/V) [G] e^{-i\Omega x} \{W\} +$$

$$(\omega^2 [M] - [M] \bar{\omega}^2 (1 + ig)) + q[A] + q[C][F][S]) \{\xi\} = \{0\} \quad (3.2)$$

The first term of each equation represents the applied gust forces, whereas the second term contains the forces resulting from the displacement of the structure. These are obtained by multiplying the generalized displacements by the respective inertia, elastic, structural damping, aerodynamic and control surface load coefficients. Notice that the load coefficients which furnish the generalized forces are indicated by an overbar in equation (3.1) to distinguish them from those which yield the response loads in equation (3.2). Notice also that a diagonal matrix of gust penetration factors has been inserted to shift the phase of $\{W\}$ from the origin of the aircraft coordinate system to the aerodynamic reference panels.

3.2 ACCELERATIONS

Equation (3.1) may be solved for the generalized displacements by matrix inversion. Thus,

$$\{\xi\} = (q/V) [\bar{B}]^{-1} [\bar{G}] [e^{-i\Omega x}] \{W\} \quad (3.3)$$

where $[\bar{B}] \equiv -[\bar{M}] (\omega^2 - [\bar{\omega}^2 (1 + ig)]) - q[\bar{A}] - q[\bar{C}] [F] [S]$

The matrix $[\bar{B}]^{-1}$ is seen to contain the ratios of generalized displacement to generalized gust force.

Let $[R]$ represent the ratios of accelerometer displacement to generalized displacement. Then with the aid of equation (3.3), the acceleration responses may be written

$$-\omega^2 [R] \{\xi\} = -\omega^2 (q/V) [R] [\bar{B}]^{-1} [\bar{G}] [e^{-i\Omega x}] \{W\} \quad (3.4)$$

The matrix coefficient of $\{W\}$ in the above equation contains the influence coefficients for acceleration response due to unit gust velocity normal to each aerodynamic reference panel, with the gust phase taken at the origin. It is

therefore recognized as the matrix of frequency response functions for acceleration,

$$[H] = -\omega^2 (q/V) [R] [\bar{B}]^{-1} [\bar{G}] [e^{-i\Omega x}] \quad (3.5)$$

(ACCELERATION RESPONSE FUNCTIONS)

3.3 ELASTIC LOADS

Solving for the elastic loads $[M] [\bar{\omega}^2] \{\xi\}$ in equation (3.2) and substituting equation (3.3) for $\{\xi\}$ yields

$$(q/V) [M] [\bar{\omega}^2] [\bar{B}]^{-1} [\bar{G}] [e^{-i\Omega x}] \{W\} = (q/V) ([G] + [E] [\bar{B}]^{-1} [\bar{G}]) [e^{-i\Omega x}] \{W\} \quad (3.6)$$

where $[E] \equiv [M] (\omega^2 - [ig\bar{\omega}^2]) + q[A] + q[C] [F] [S]$

The matrix coefficients of $\{W\}$ on each side of equation (3.6) contain the influence coefficients for elastic load response due to unit gust velocity normal to each aerodynamic reference panel, with the gust phase taken at the origin. They represent alternative forms of the frequency response function for elastic loads and correspond to the mode displacement and mode acceleration methods, respectively (Reference 9). Accordingly,

$$[H] = (q/V) [M] [\bar{\omega}^2] [\bar{B}]^{-1} [\bar{G}] [e^{-i\Omega x}] \quad (3.7)$$

(MODE DISPLACEMENT METHOD)

$$[H] = (q/V) ([G] + [E] [\bar{B}]^{-1} [\bar{G}]) [e^{-i\Omega x}] \quad (3.8)$$

(MODE ACCELERATION METHOD)

The mode displacement method is sometimes preferred because it requires only the generalized form of the aerodynamic load coefficients, whereas the mode acceleration method requires both forms. However, $\bar{\omega} = 0$ for the rigid body degrees of freedom, so that according to equation (3.7), the mode displacement method yields no loads at all until flexible modes are included. Since the mode acceleration method has a head start, it tends to be closer to convergence for a given number of included modes. The two methods ultimately approach the same limit, however.

SECTION IV

THREE-DIMENSIONAL GUST RESPONSE

The gust velocity cross spectra and frequency response functions developed in Sections II and III, respectively, may be combined to yield the various dynamic response quantities required for gust response analysis. These include the response power spectra, from which are derived the transfer functions, RMS responses and zero crossing rates. Response cross spectra with respect to the three probe-measured cartesian gust components may also be computed from the analytical model if corresponding cross transfer functions and coherence functions are required. These are useful for verifying the analytical model when equivalent dynamic response flight test data is available for comparison. The aircraft is assumed to have lateral symmetry to allow the symmetric and antisymmetric responses to be computed separately and superimposed. A discussion of 3-d vertical and lateral gust response procedure is specifically included, since it corresponds to the case treated by the computer program described in Paragraph 5.3. This case is also shown to reduce to the conventional 1-d gust response formulation in the small aircraft limit of Paragraph 2.5.

4.1 LATERAL SYMMETRY

If the aircraft has lateral symmetry, then the symmetric and antisymmetric responses may be computed separately and superimposed. Quantities pertaining to the symmetric and antisymmetric response calculations will be distinguished by affixing + and - superscripts, respectively.

In particular, each row of the matrix $[H]$ in Section III corresponds to a given response and contains the elements $H_m(\Omega)$, where $m = 1, \dots, 2N$, and N is the number of aerodynamic reference panels on one side of the aircraft. In the symmetry-restricted case, however, the matrices of the symmetric and antisymmetric frequency response functions are written $[H]^\pm$, and a row of elements is given by

$$H_m^\pm(\Omega) = H_m(\Omega) \pm H_{m'}(\Omega) \quad (m = 1, \dots, N; m' = m + N) \quad (4.1)$$

Here, each column corresponds to panel pair m , consisting of aerodynamic reference panel m and its image $m' = m + N$ reflected in the plane of symmetry.

The single panel frequency response functions may be recovered by alternately adding and subtracting the two equations (4.1) to yield

$$H_m(\Omega) = (H_m^+(\Omega) + H_m^-(\Omega))/2 \quad (4.2)$$

$$H_{m'}(\Omega) = (H_m^+(\Omega) - H_m^-(\Omega))/2$$

Since the gust phase of each frequency response function is taken at the origin, the longitudinal separation may be removed from the corresponding gust velocity cross spectra. Accordingly, let

$$\phi_{mn}(\Omega) \equiv \phi(\underline{n}_m, \underline{n}_n, \underline{p}_{mn}, \Omega) \quad (m = 1, \dots, 2N; n = 1, \dots, 2N) \quad (4.3)$$

This expression defines the cross spectrum between gust velocity components normal to panels m and n . Longitudinal separation between the panels is ignored by the use of $\underline{p}_{mn} = y_{mn}\underline{e}_2 + z_{mn}\underline{e}_3$. The removal of the longitudinal separation has no effect upon the original cross spectrum except to eliminate the phase factor $e^{-i\Omega x_{mn}}$, where $x_{mn} \equiv x_n - x_m$.

Symmetry-restricted cross spectra between panel pairs corresponding to the frequency response functions defined by equation (4.1) are given by

$$\Phi_{mn}^{\pm}(\Omega) = (\Phi_{mn}(\Omega) \pm \Phi_{m',n}(\Omega))/2 \quad (4.4)$$

$$(m = 1, \dots, N; n = 1, \dots, N; m' = m + N)$$

The gust velocity cross spectra between single panels on the same side and opposite sides of the aircraft, respectively, are recovered from the sum and difference of equations (4.4). Thus,

$$\Phi_{mn}(\Omega) = \Phi_{mn}^{+}(\Omega) + \Phi_{mn}^{-}(\Omega) \quad (4.5)$$

$$\Phi_{m',n}(\Omega) = \Phi_{mn}^{+}(\Omega) - \Phi_{mn}^{-}(\Omega)$$

Symmetry considerations also imply that

$$\Phi_{mn}(\Omega) = \Phi_{m',n}(\Omega), \quad \Phi_{m',n}(\Omega) = \Phi_{mn}(\Omega), \quad \Phi_{nm}(\Omega) = \Phi_{mn}^{*}(\Omega) \quad (4.6)$$

4.2 RESPONSE POWER SPECTRA

The power spectral density of an aircraft response to gust is given by the quadratic form (References 1-4),

$$\begin{aligned} \phi(\Omega) &= \sum_{m=1}^{2N} \sum_{n=1}^{2N} H_n^{*}(\Omega) \Phi_{mn}(\Omega) H_n(\Omega) \\ &= \sum_{m=1}^N \sum_{n=1}^N (H_m^{*} \Phi_{mn} H_n + H_m^{*} \Phi_{mn} H_{n'} + H_m^{*} \Phi_{m',n} H_n + H_m^{*} \Phi_{m',n} H_{n'}) \end{aligned} \quad (4.7)$$

where the reduced frequency argument is suppressed for brevity, and the single term is expanded into four by using a primed subscript to denote the image panel. Substitution of equations (4.2), (4.5) and (4.6) into (4.7) yields after some manipulation,

$$\phi(\Omega) = \phi^+(\Omega) + \phi^-(\Omega) \quad (4.8)$$

$$\begin{aligned} \text{where} \quad \phi^{\pm}(\Omega) &= \sum_{m=1}^N \sum_{n=1}^N H_m^{\pm*}(\Omega) \phi_{mn}^{\pm}(\Omega) H_n^{\pm}(\Omega) \\ &= \sum_{m=1}^N \left(|H_m^{\pm}|^2 \phi_{mm}^{\pm} + \sum_{n=1}^{m-1} (H_m^{\pm*} \phi_{mn}^{\pm} H_n^{\pm} + H_n^{\pm*} \phi_{nn}^{\pm}) \right) \\ &= \sum_{m=1}^N \left\{ |H_m^{\pm}|^2 \phi_{mm}^{\pm} + 2 \sum_{n=1}^{m-1} \left(\operatorname{Re}(H_m^{\pm*} H_n^{\pm}) \operatorname{Re}(\phi_{mn}^{\pm}) - \operatorname{Im}(H_m^{\pm*} H_n^{\pm}) \operatorname{Im}(\phi_{mn}^{\pm}) \right) \right\} \end{aligned}$$

Notice that the power spectra $\phi^{\pm}(\Omega)$ of the symmetric and antisymmetric responses are computed separately and summed to obtain the total power spectrum $\phi(\Omega)$.

The computational effort required to generate the $N(N+1)$ gust velocity cross spectra required in the two response expressions is usually negligible compared to the rest of the calculation. Furthermore, gust input panels having the same transverse coordinates and spatial orientation may be combined by summing the frequency response functions which are referenced to them. This can result in a significant reduction in the effective number of panels. For example, a fuselage whose constituent panels are lined up in a longitudinal strip may be treated as a single panel.

4.3 TRANSFER FUNCTIONS

Since symmetric and antisymmetric responses are predominantly caused by vertical and lateral gust, respectively, it is appropriate to define corresponding transfer functions

$$T^+(\Omega) = \sqrt{\phi_1^+(\Omega) / \phi_3(\Omega)}$$

$$T^-(\Omega) = \sqrt{\phi_1^-(\Omega) / \phi_2(\Omega)}$$
(4.9)

This allows equation (4.8) to be cast into the alternative form

$$\phi(\Omega) = T^{2+}(\Omega) \phi_3(\Omega) + T^{2-}(\Omega) \phi_2(\Omega)$$
(4.10)

The response transfer functions are usually quite insensitive to the turbulence field parameters, particularly if the scale of turbulence is much larger than the transverse dimensions of the aircraft. This suggests that the analytical transfer functions may be used with measured gust power spectra in equation (4.10). Thus, if the aircraft is equipped to measure both gust component and response time histories, response power spectra may be extracted from dynamic response flight test data for direct comparison with corresponding analytical power spectra, thereby providing a means of substantiating the analytical model. This procedure is followed in the comparison study described in Section V.

4.4 RESPONSE PARAMETERS

The RMS load amplitude σ , and the characteristic frequency (or zero-crossing rate) N_0 represent the significant dynamic response parameters applicable to fatigue design and limit load calculations. These quantities may be obtained directly from the corresponding response power spectra by the following expressions.

$$\sigma = \left(\int_0^\infty \phi(\Omega) d\Omega \right)^{1/2}$$

$$N_0 = \frac{V}{2\pi\sigma} \left(\int_0^\infty \phi(\Omega) \Omega^2 d\Omega \right)^{1/2}$$
(4.11)

When calculating RMS load amplitudes, it is customary to employ a finite upper limit on the integral, since the power spectrum of a typical gust load tends to diminish rapidly with frequency. However, the integral used to calculate the zero crossing rate is usually quite sensitive to cutoff frequency because of the squared frequency factor present in the integrand. As a result, the high frequency tail of the response power spectrum may significantly affect the zero crossing rate, even though its contribution to the RMS amplitude is negligible. To eliminate this high frequency, low amplitude influence, the upper limit of the zero crossing rate integral is typically set to a frequency corresponding to 0.99σ (Reference 10).

4.5 RESPONSE CROSS SPECTRA

If a gust probe is mounted on the aircraft at point (x_o, y_o, z_o) , then in analogy with equation (4.3), let

$$\Phi_{jn}(\Omega) \equiv \Phi(\underline{e}_j, \underline{n}_n, \underline{p}_{on}, \Omega) \quad (j = 1, 2, 3; n = 1, \dots, 2N) \quad (4.12)$$

This expression defines the cross spectrum between cartesian gust velocity component j measured at the probe and the gust velocity component normal to panel n . Longitudinal separation between the probe and the panel is ignored by the use of $\underline{p}_{on} = y_{on}\underline{e}_2 + z_{on}\underline{e}_3$.

If the probe is mounted in the plane of symmetry ($y_o = 0$), then the first of equations (4.6) and further symmetry considerations yield

$$\Phi_{jn'}(\Omega) = \Phi_{j'n}(\Omega) = \begin{cases} \Phi_{jn}(\Omega) & (j = 1, 3) \\ -\Phi_{jn}(\Omega) & (j = 2) \end{cases} \quad (4.13)$$

The cross spectrum between a probe-measured gust velocity component and an aircraft response is then given by (References 1-4)

$$\begin{aligned}\phi_j(\Omega) &= e^{i\Omega x_0} \sum_{n=1}^{2N} \phi_{jn}(\Omega) H_n(\Omega) \\ &= e^{i\Omega x_0} \sum_{n=1}^N (\phi_{jn} H_n + \phi_{jn'} H_{n'})\end{aligned}\quad (4.14)$$

The above cross spectrum expression may be compared with equation (4.7) for the response power spectrum. Notice that the summation is single, and that a phase factor is required to shift the gust phase of the probe measurement to the origin of the aircraft coordinate system. Substitution of equations (4.2) and (4.13) reduces (4.14) to

$$\phi_j(\Omega) = e^{i\Omega x_0} \sum_{n=1}^N \phi_{jn}(\Omega) \times \begin{cases} H_n^+(\Omega) & (j = 1, 3) \\ H_n^-(\Omega) & (j = 2) \end{cases} \quad (4.15)$$

4.6 CROSS TRANSFER FUNCTIONS

Rather than to compare corresponding response cross spectra obtained from dynamic response test and analysis, it is somewhat more meaningful to compare the corresponding cross transfer functions, given by

$$C_j(\Omega) = \phi_j(\Omega) / \phi_j(\Omega) \quad (4.16)$$

Physically, this function represents the complex amplitude ratio between the statistically correlated portion of the response and the corresponding gust velocity component j measured at the probe.

Another useful function for comparison purposes is the fraction of the mean square response amplitude that is statistically correlated with gust velocity component j measured at the probe. This quantity is known as the coherence function and is written

$$\gamma_j^2(\Omega) = |\phi_j(\Omega)|^2 / \phi(\Omega) \phi_j(\Omega) \quad (4.17)$$

4.7 VERTICAL AND LATERAL GUST

The vertical and lateral gust response case is of particular interest because response to longitudinal gust is usually omitted from the analytical representation of the aircraft. This case will be considered in detail, since it is the formulation used in the computer program and flight test comparison described in Section V, and it provides a convenient recapitulation of the preceding development.

If longitudinal gust is ignored, then by the procedure described in Paragraph 2.7, the gust velocity cross spectrum given by equation (2.1) reduces to a real function except for the phase factor for gust penetration. Consequently, if this result is substituted into equation (4.8), the term which contains the imaginary part of the gust velocity cross spectrum vanishes. If this expression is in turn substituted into equations (4.9) and the definition of the gust coherence given by equation (2.4) is applied, then the squared transfer functions become

$$T^{2\pm}(\Omega) = \sum_{m=1}^N (|H_m^\pm|^2 \hat{\phi}_{mm}^\pm + 2 \sum_{n=1}^{m-1} \text{Re}(H_m^{\pm*} H_n^\pm) \text{Re}(\hat{\phi}_{mn}^\pm)) \quad (4.18)$$

where
$$\hat{\phi}_{mn}^\pm(\Omega) = (\hat{\phi}_{mn}(\Omega) \pm \hat{\phi}_{m'n}(\Omega))/2$$

and
$$\hat{\phi}_{mn}(\Omega) = \hat{\phi}_P(p_{mn}, \Omega) (n_{m2} n_{n2} + n_{m3} n_{n3}) +$$

$$\hat{\phi}_N(p_{mn}, \Omega) (y_{mn} n_{m2} + z_{mn} n_{m3}) (y_{mn} n_{n2} + z_{mn} n_{n3}) / p_{mn}^2$$

$$y_{mn} = y_n - y_m, \quad z_{mn} = z_n - z_m, \quad p_{mn} = \sqrt{y_{mn}^2 + z_{mn}^2}$$

$$y_{m'} = -y_m, \quad z_{m'} = z_m, \quad n_{m'2} = -n_{m2}, \quad n_{m'3} = n_{m3}$$

$$n_{m2} = -\sin \gamma_m, \quad n_{m3} = \cos \gamma_m$$

(3-D VERTICAL AND LATERAL GUST)

Notice that the vertical and lateral components of the unit normal vector are expressed in terms of the dihedral angle of the reference panel.

The cross transfer functions of equation (4.16) become by a similar procedure,

$$c_j(\Omega) = e^{i\Omega x_0} \sum_{n=1}^N \hat{\phi}_{jn}(\Omega) \times \begin{cases} H_n^+(\Omega) & (j = 3) \\ H_n^-(\Omega) & (j = 2) \end{cases} \quad (4.19)$$

where

$$\hat{\phi}_{jn}(\Omega) = \hat{\phi}_P(p_{on}, \Omega) n_{nj} + \hat{\phi}_N(p_{on}, \Omega) (y_n n_{n2} + z_{on} n_{n3}) \times \begin{cases} z_{on}/p_{on}^2 & (j = 3) \\ y_n/p_{on}^2 & (j = 2) \end{cases}$$

(3-D VERTICAL AND LATERAL GUST)

Reference to Paragraph 2.4 shows that the planar and nonplanar coherences in equations (4.18) and (4.19) may be written in terms of their large scale limit forms.

$$\hat{\phi}_P(p, \Omega) = \tilde{\phi}_P(\mu) - \tilde{\phi}_N(\mu) / (3/8 + \kappa^2) \quad (4.20)$$

$$\hat{\phi}_N(p, \Omega) = \tilde{\phi}_N(\mu) (1 + \kappa^2) / (3/8 + \kappa^2)$$

where $\tilde{\phi}_P(\mu) = 0.9944 \mu^{5/6} K_{5/6}(\mu)$

$$\tilde{\phi}_N(\mu) = 0.9944 (3/8) \mu^{11/6} K_{11/6}(\mu)$$

and $\kappa = 1.339 L \Omega, \quad \mu = (p / 1.339 L) \sqrt{1 + \kappa^2}$

Anisotropic turbulence as discussed in Paragraph 2.8 is introduced by setting

$$L = L_3 \quad (4.21)$$

and by multiplying:

$$\begin{cases} n_{m2} \text{ and } n_{n2} \text{ by } \sqrt{\Phi_2(\Omega) / \Phi_3(\Omega)} & \text{in the symmetric case} \\ n_{m3} \text{ and } n_{n3} \text{ by } \sqrt{\Phi_3(\Omega) / \Phi_2(\Omega)} & \text{in the antisymmetric case} \end{cases}$$

(ANISOTROPIC TURBULENCE)

If L_2 and L_3 are arbitrarily set to very large values, the result will correspond to the large scale limit of Paragraph 2.3 in which the scale of turbulence disappears as a parameter, and equations (4.20) are replaced by

$$\begin{aligned}\hat{\phi}_P(p, \Omega) &= \tilde{\phi}_P(p, \Omega) \\ &\text{(LARGE SCALE LIMIT)} \\ \hat{\phi}_N(p, \Omega) &= \tilde{\phi}_N(p, \Omega)\end{aligned}\tag{4.22}$$

If the lateral and vertical coordinates of the gust probe and the aerodynamic reference panels are arbitrarily set to zero, the result will correspond to the small aircraft limit of Paragraph 2.4 in which the scale of turbulence again disappears as a parameter, and equations (4.20) are reduced to

$$\begin{aligned}\hat{\phi}_P(p, \Omega) &= 1 \\ &\text{(SMALL AIRCRAFT LIMIT)} \\ \hat{\phi}_N(p, \Omega) &= 0\end{aligned}\tag{4.23}$$

This is identical to the 1-d turbulence case discussed in Paragraph 2.6. Substituting this result into equations (4.18) and (4.19) yields the conventional 1-d vertical and lateral gust formulation,

$$\begin{aligned}T^+(\Omega) &= |C_3(\Omega)| \\ &\text{(1-D VERTICAL AND LATERAL GUST)}\end{aligned}\tag{4.24}$$

$$T^-(\Omega) = |C_2(\Omega)|$$

where

$$C_j(\Omega) = e^{i\Omega x_0} \sum_{n=1}^N n_{nj} \times \begin{cases} H_n^+(\Omega) & (j = 3) \\ H_n^-(\Omega) & (j = 2) \end{cases}$$

SECTION V

EVALUATION OF THE 3-D MODEL

The three-dimensional gust response methods described in the preceding sections were incorporated into a dynamic response computer program which was utilized to obtain a comparison between 1-D and 3-D analytical results. These results were substantiated by further comparison with flight-measured data from the C-5A aircraft. Because of its size, configuration, and subsonic speed, this aircraft provides a unique opportunity to demonstrate and evaluate the effects of three-dimensional turbulence.

5.1 AIRCRAFT DESCRIPTION

The C-5A is a land based cargo transport with a four turbofan jet engine, high-wing monoplane configuration. The empennage is a cantilever Tee arrangement of a vertical stabilizer and a variable incidence horizontal stabilizer.

The total wing span is 2630 inches; the basic fuselage length is 2767 inches; and the horizontal stabilizer span is 812 inches. The four engines are attached to wing pylons and are located two on a side at wing butt lines 476 and 743. Sweep at the local quarter chord is 25.0° for the wing, 25.5° for the horizontal stabilizer, and 34.9° for the vertical stabilizer. Equipped weight empty of the aircraft is 323,904 pounds.

5.2 COMPUTATIONAL MODEL

The flight test event used in the comparison is characterized by a set of conditions which are incorporated into the corresponding theoretical case. These consist of altitude, gross weight, fuel weight, cargo weight, Mach number and airspeed.

The theoretical model represents the aircraft structure by the use of six rigid body and the first fifteen symmetric and fifteen antisymmetric flexible modes of vibration, based on a system of 68 lumped masses connected by flexible shafts having the elastic and geometric properties of the intervening structure.

The analytical aerodynamic configuration of the C-5A analytical model is shown in Figure 4. It is constructed from a series of plane trapezoidal surfaces which are divided into span and chord segments to define subpanels. Doublet lattice methods (References 11 and 12) are applied to the resulting subpanel distribution to furnish aerodynamic influence coefficients at uniformly spaced frequencies, using the Mach number associated with the flight test event.

The resulting mass distribution, modal characteristics and aerodynamic data are employed to generate the inertial and aerodynamic load coefficients. The inertial load coefficients are taken with respect to the lumped masses, whereas the aerodynamic load coefficients are computed relative to specified aerodynamic reference panels, each composed of one or more of the doublet lattice subpanels. The model employed in this study contains 43 subpanels, which are combined to furnish 29 reference panels.

5.3 COMPUTER PROGRAM

The computer program developed for the theoretical gust response calculation accounts for simultaneous three-dimensional vertical and lateral gust under anisotropic turbulence conditions. The asymptotic planar and nonplanar coherences, stored in tabular form, are used to compute the required gust coherences by correcting for nonzero p/L according to equations (4.20). Frequency response functions for acceleration are obtained by equation (3.5). Frequency response functions for loads may be calculated by either the mode acceleration or the mode displacement methods, corresponding to equations (3.7) and (3.8), respectively. In the latter case only the generalized aerodynamic load coefficients are required. If a one-dimen-

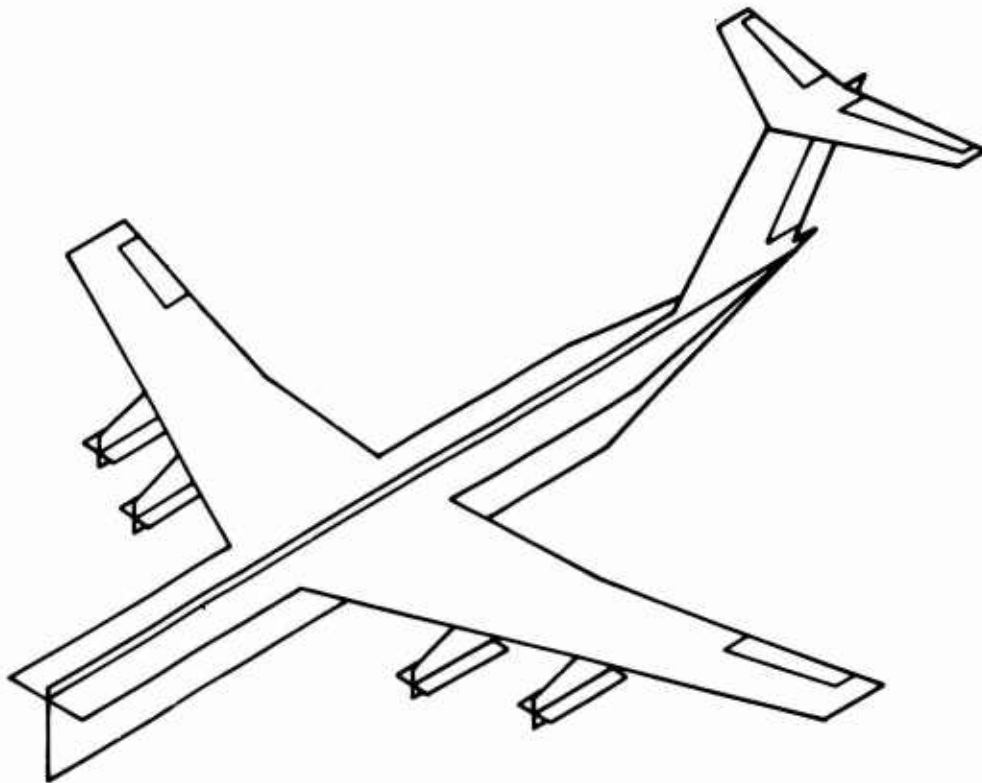


Figure 4. Aerodynamic Configuration for the C-5A
Analytical Model

sional turbulence field is requested, the program furnishes it by setting to zero the vertical coordinate of the probe and the vertical and lateral coordinates of the reference panels.

The initial output data consists of response transfer functions and cross transfer functions, given by equations (4.18) and (4.19) respectively. Response power spectra, response parameters and coherence functions are then calculated according to equations (4.10 - 4.11) and (4.16 - 4.17), respectively, using either measured gust input spectra or the vertical and lateral analytical spectra given by equations (2.6) and (2.18).

The only significant computational effort required by the 3-d gust response analysis beyond that of the conventional 1-d calculation is attributable to the generation of the gust coherences. This amounts to approximately 3 seconds for a typical run on the UNIVAC 1106.

5.4 1-D VERSUS 3-D RESPONSE PARAMETERS

Calculated spanwise distributions of RMS loads and characteristic frequencies for the wing and horizontal stabilizer are shown in Figures 5 and 6, respectively. The general reduction in wing loads which occurs under the 3-d turbulence assumption is attributable to spanwise averaging effects, which are omitted in the 1-d model. This interpretation is supported by the fact that the fractional reduction in loads increases with span, and the bending moment, which gives the greatest weight to the most outboard load sources, shows the greatest overall decline. Such a result is expected, since the outboard load sources tend to be most susceptible to spanwise averaging. The reduction in wing vertical bending in the 3-d case ranges from about 7% at the wing root to about 13% further outboard. Reduction in vertical shear ranges from 3% inboard to 14% outboard, and torsion from 1% to 5%.

The 3-d calculation yields a totally different result for horizontal stabilizer loads. Here, there is an increase instead of a decrease in vertical bending, and the fractional change is a nearly uniform 2% to 3%

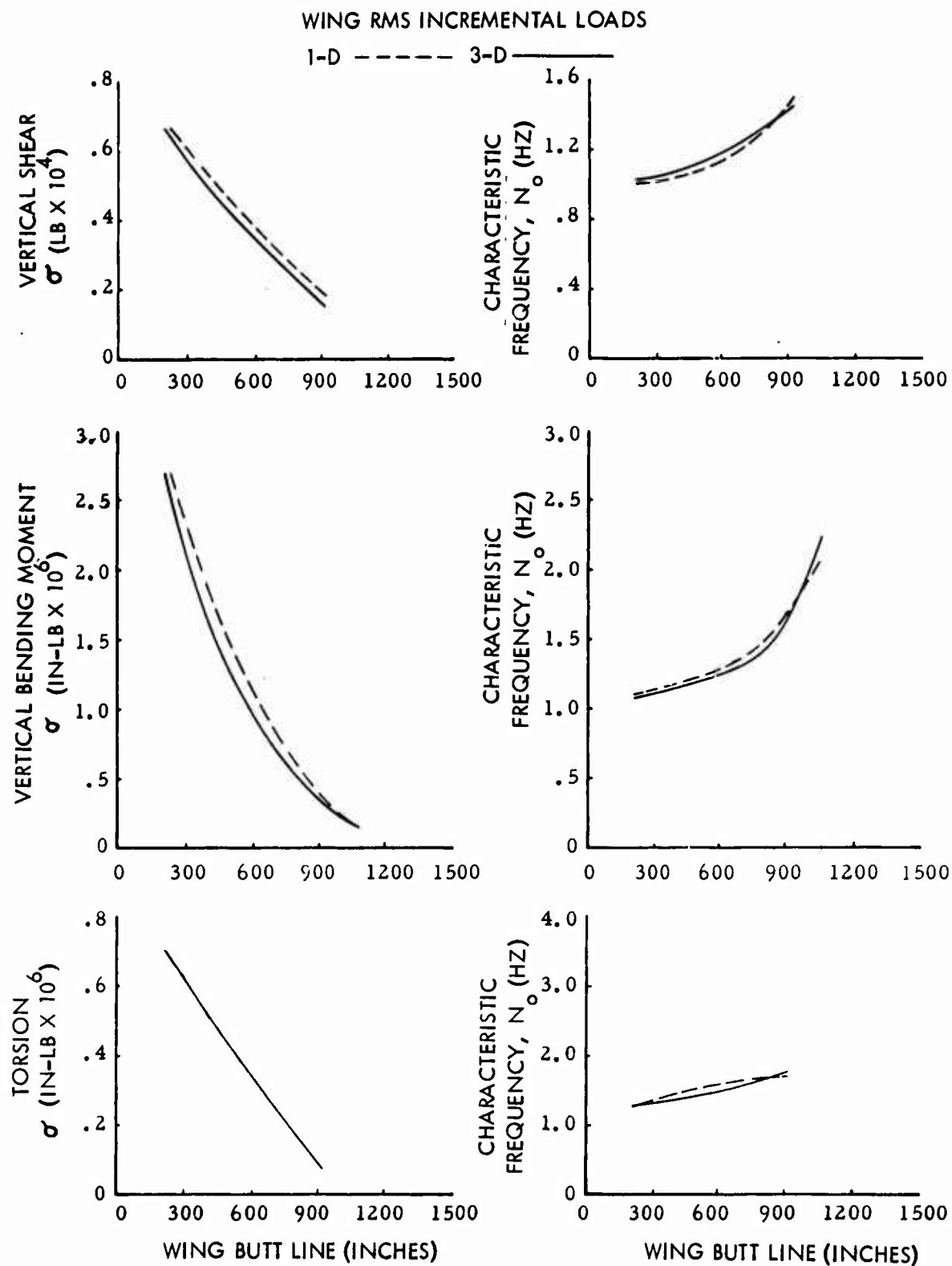


Figure 5. Wing RMS Incremental Loads and Characteristic Frequencies in Turbulence

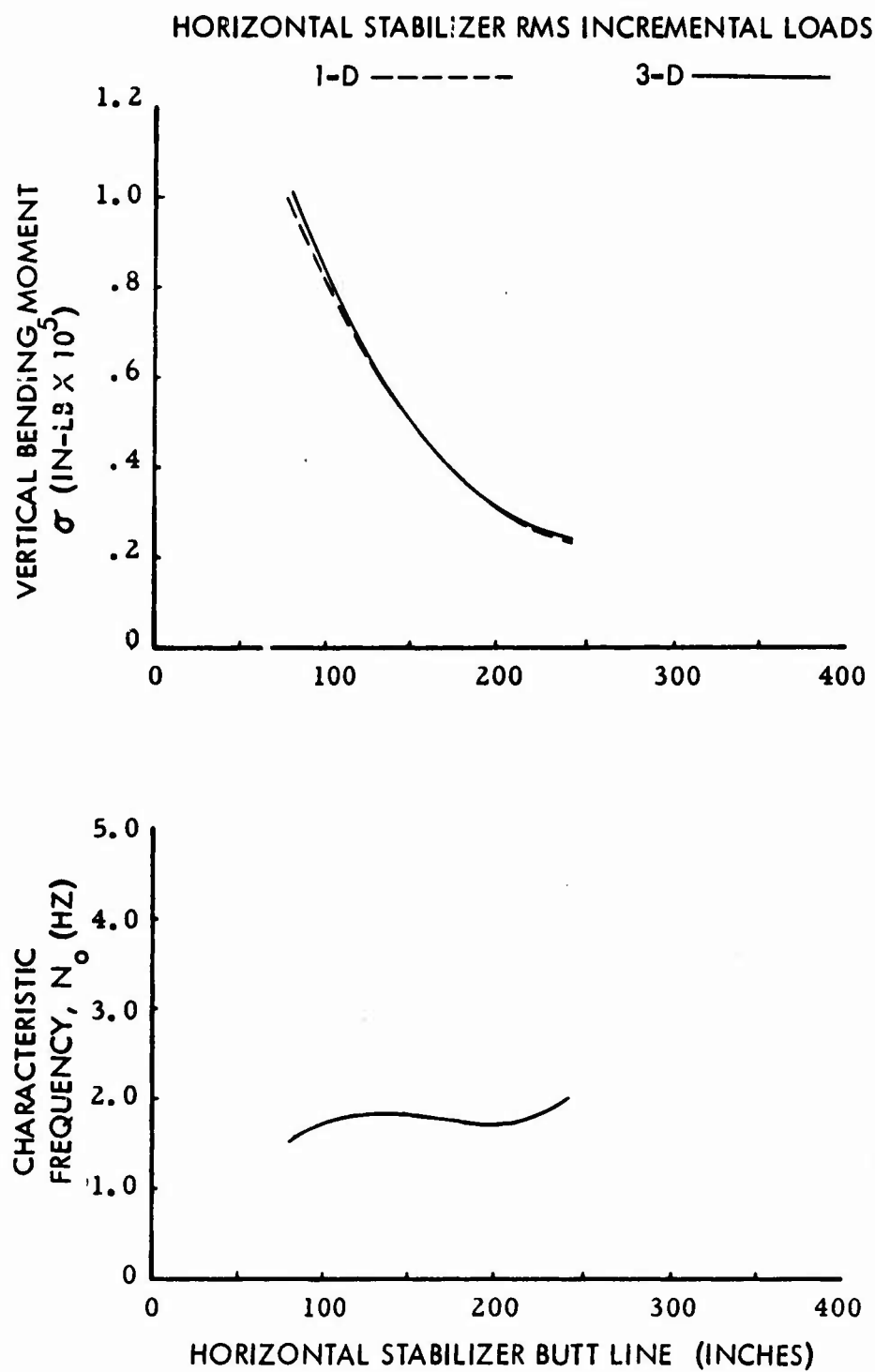


Figure 6. Horizontal Stabilizer RMS Incremental Loads and Characteristic Frequencies in Turbulence

all across the span. This is probably attributable to increased antisymmetric modal excitation caused by 3-d antisymmetric vertical gust impinging upon the wing.

The RMS incremental vertical and lateral acceleration results at the aircraft center of gravity (fuselage station 1333) are summarized below:

	C.G. RMS INCREMENTAL ACCELERATION					
	(G's)			N _o (HZ)		
	1-D	3-D	Change	1-D	3-D	Change
VERTICAL	.0314	.0293	-7%	.885	.818	-8%
LATERAL	.0112	.0118	5%	1.574	1.615	3%

5.5 FLIGHT TEST COMPARISON

The flight test instrumentation and data reduction procedures used to obtain dynamic response gust flight data for comparison with the corresponding theoretical analysis are described in Reference 10. Digital spectral analysis procedures are employed to obtain flight-measured power spectra and cross spectra from which all of the necessary flight test data may be computed. Both test and theoretical procedures are briefly illustrated in Figure 7.

The spectral method gives results based upon the total output spectra, without regard to input source. The cross-spectral method gives data based upon that part of the output that is statistically coherent with the input, and thus eliminates noise in the output, regardless of source. In this case the noise is primarily a combination of trend removal errors, uncorrelated pilot inputs and longitudinal gust. Since these are primarily low frequency phenomena, they appear in the form of spurious low frequency increments to the measured response power spectra. Because the coherence properties of the turbulence field are accounted for in the 3-d gust response analysis, theoretical results which depend directly upon the cross spectrum tend to show a marked improvement over the 1-d case. These include cross transfer functions and coherence functions.

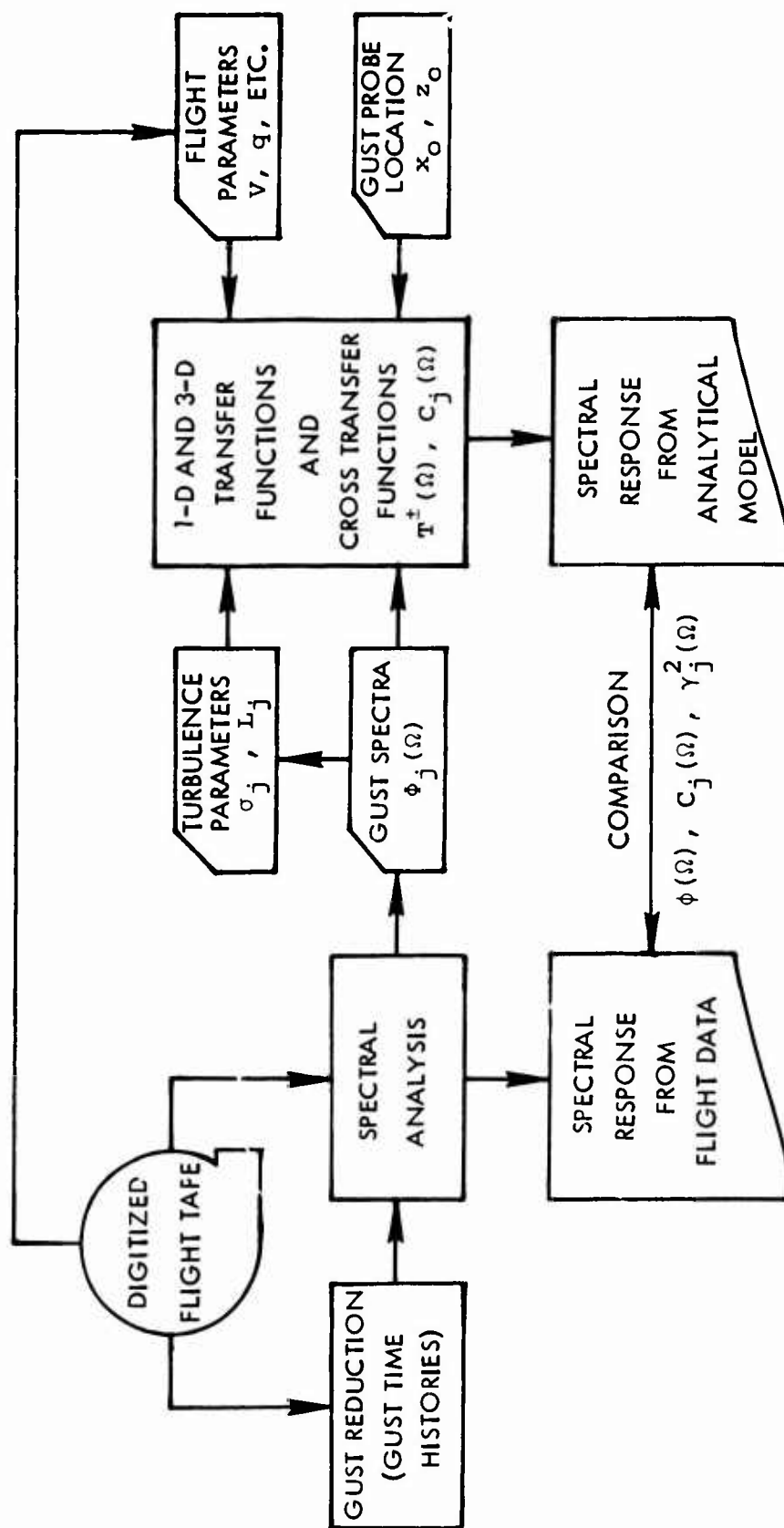


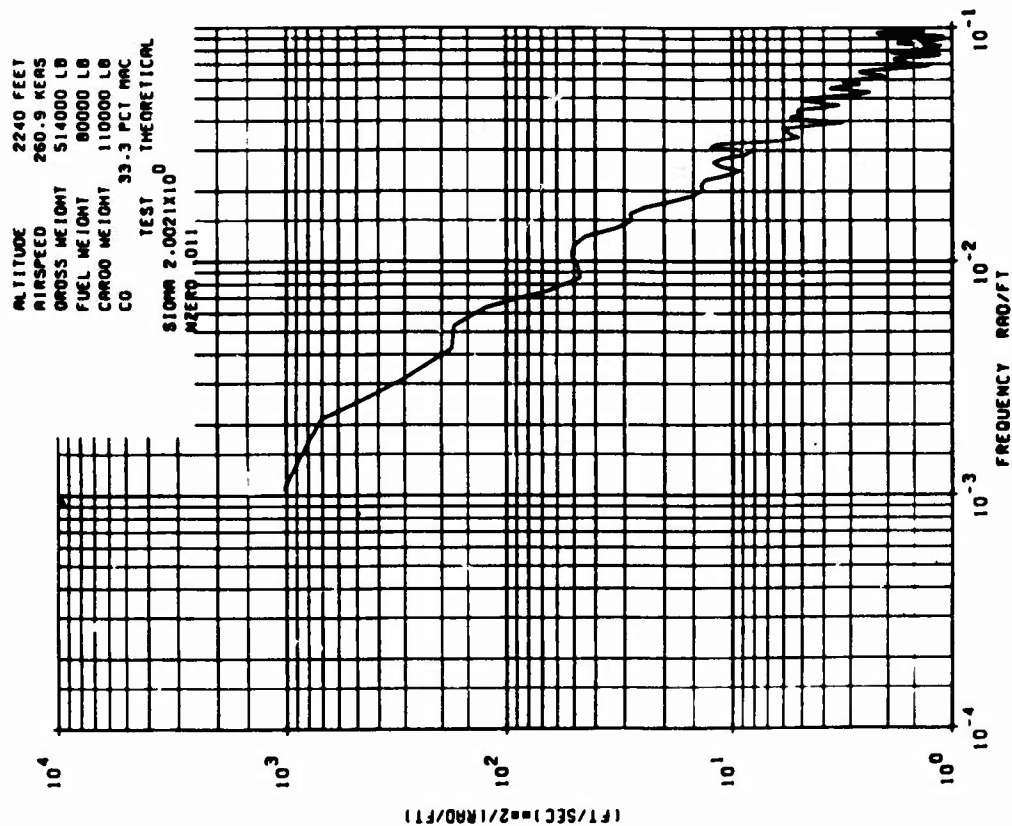
Figure 7. Procedure for Evaluating Three-Dimensional Gust Response Analysis Methods

Response power spectra, cross transfer functions and coherence functions obtained from gust flight measurements are compared on the following pages with the corresponding theoretical 1-d and 3-d gust response analyses. The plots include the vertical and lateral gust velocity power spectra, vertical and lateral accelerations at the center of gravity, and loads on the wing and horizontal stabilizer. The theoretical loads were computed by the mode acceleration method.

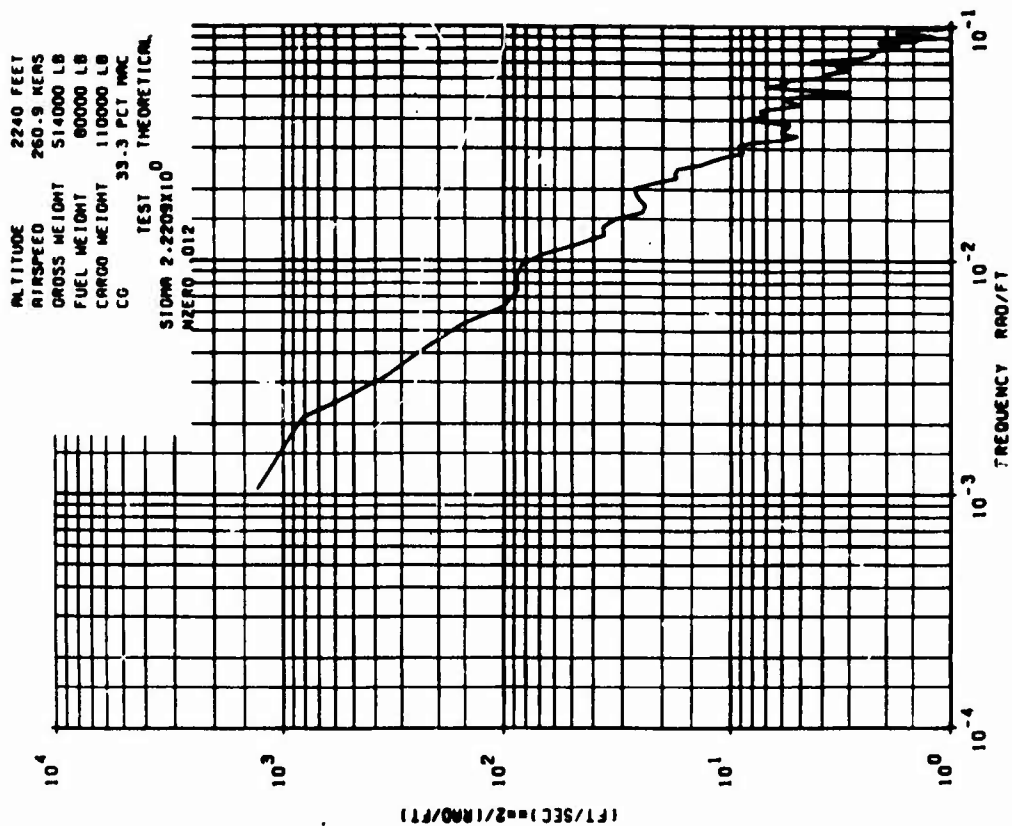
Approximately 3.7 minutes of recorded data (8925 time history points at 40 points per second) were used to compute the test spectra at 65 equally spaced frequencies over a range of 0-5 Hz. The flight test was conducted with automatic flight control systems inactive, and pilot input at a minimum. Theoretical and experimental flight parameters are summarized below.

Altitude	=	2,240 ft.
Gross Weight	=	514,000 lb
Fuel Weight	=	80,000 lb
Cargo Weight	=	110,000 lb
Mach Number	=	.411
Equivalent Airspeed	=	260.9 kts
True Airspeed	=	462 ft/sec
RMS Vertical Gust Velocity	=	2.2435 ft/sec
RMS Lateral Gust Velocity	=	2.0196 ft/sec
Vertical Scale of Turbulence (Fitted)	=	700 ft
Lateral Scale of Turbulence (Fitted)	=	960 ft

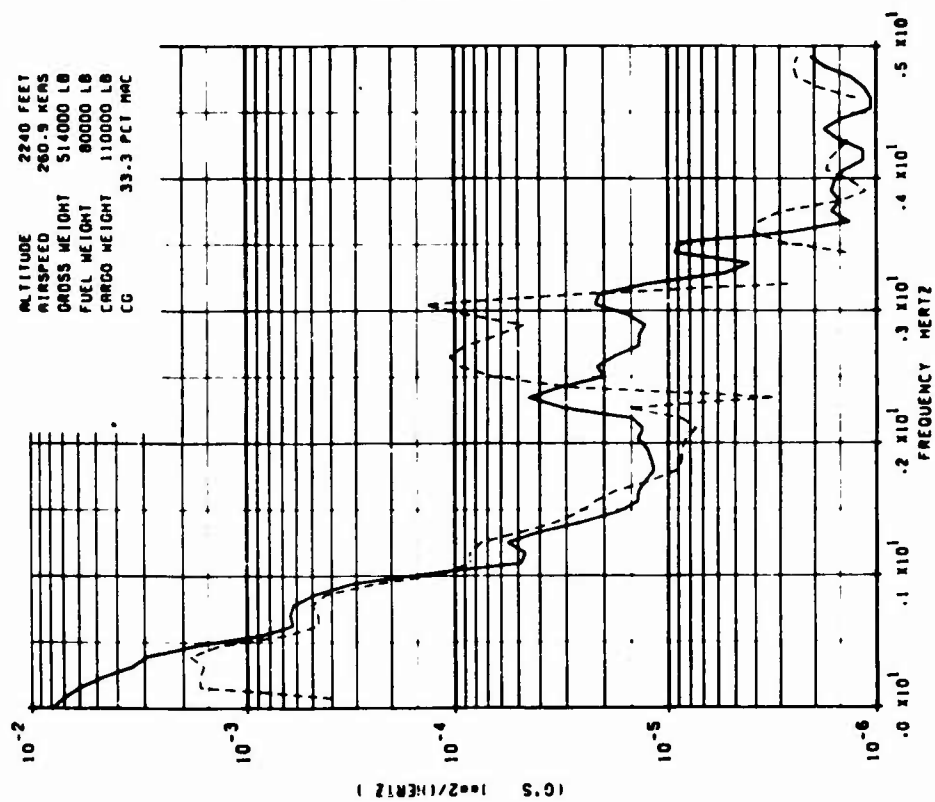
1-D GUST RESPONSE COMPARISON FOR C-5A AIRCRAFT
POWER SPECTRUM
VERTICAL GUST VELOCITY



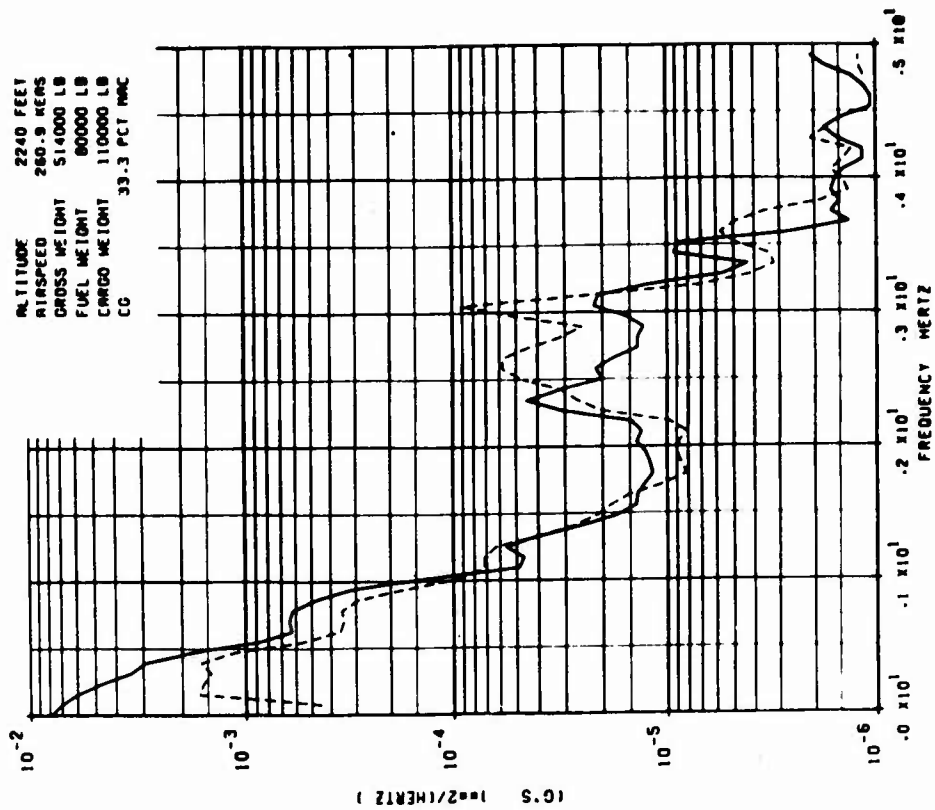
1-D GUST RESPONSE COMPARISON FOR C-5A AIRCRAFT
POWER SPECTRUM
LATERAL GUST VELOCITY



1-0 GUST RESPONSE COMPARISON FOR C-5A AIRCRAFT
POWER SPECTRUM
AIRCRAFT CG ACCELERATION (HZ) AT FS 1333
TEST — THEORETICAL —



3-0 GUST RESPONSE COMPARISON FOR C-5A AIRCRAFT
POWER SPECTRUM
AIRCRAFT CG ACCELERATION (HZ) AT FS 1333
TEST — THEORETICAL —



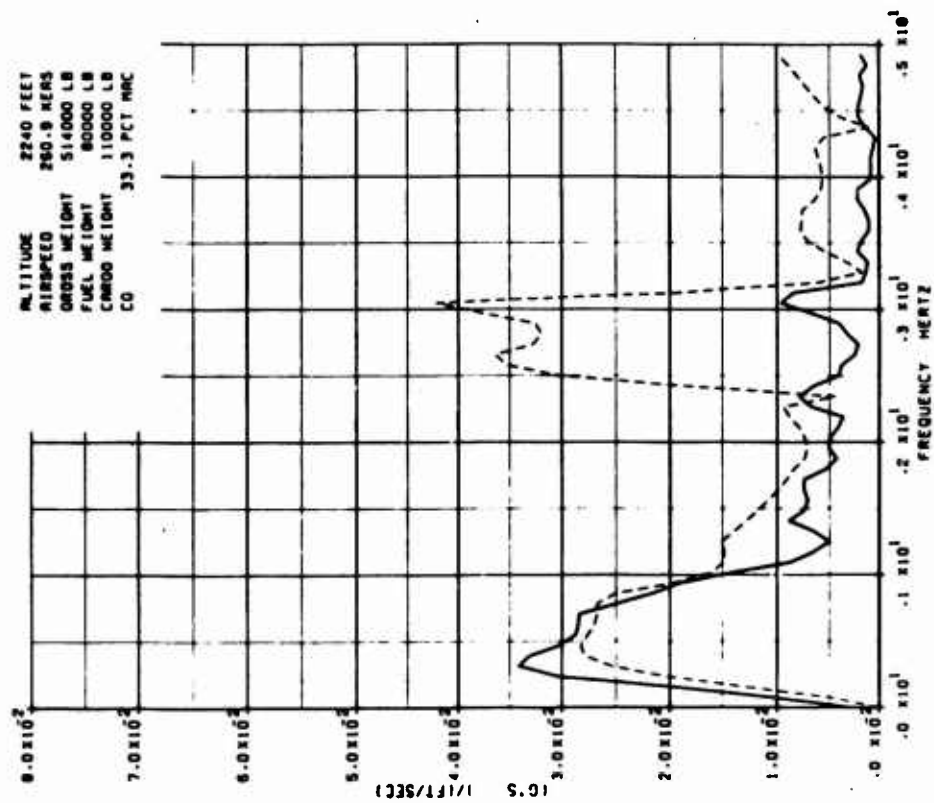
1-D GUST RESPONSE COMPARISON FOR C-5A AIRCRAFT

CROSS TRANSFER FUNCTION

OUTPUT- AIRCRAFT CG ACCELERATION (IN2) AT FS 1333

INPUT- VERTICAL GUST VELOCITY

TEST --- THEORETICAL



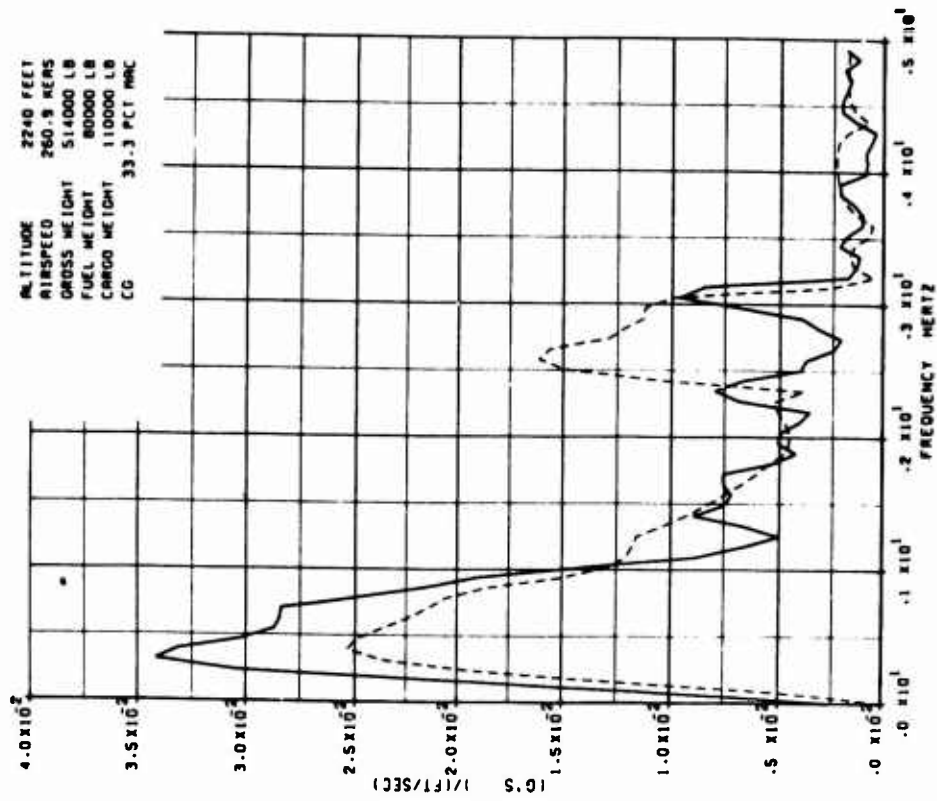
3-D GUST RESPONSE COMPARISON FOR C-5A AIRCRAFT

CROSS TRANSFER FUNCTION

OUTPUT- AIRCRAFT CG ACCELERATION (IN2) AT FS 1333

INPUT- VERTICAL GUST VELOCITY

TEST --- THEORETICAL



1-D QUST RESPONSE COMPARISON FOR C-5A AIRCRAFT

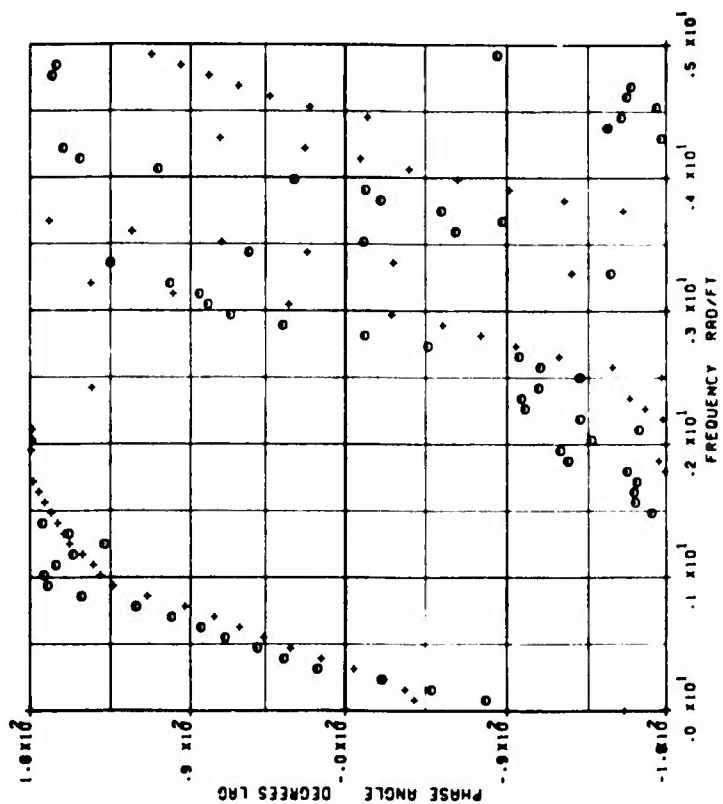
PHASE ANGLE

OUTPUT- AIRCRAFT CG ACCELERATION (INZ) AT FS 1333

INPUT- VERTICAL QUST VELOCITY

TEST O THEORETICAL +

ALTITUDE 2240 FEET
AIRSPEED 260.9 KEAS
GROSS WEIGHT 514000 LB
FUEL WEIGHT 80000 LB
CARGO WEIGHT 110000 LB
CG 33.3 PCT MAC



3-D QUST RESPONSE COMPARISON FOR L-5A AIRCRAFT

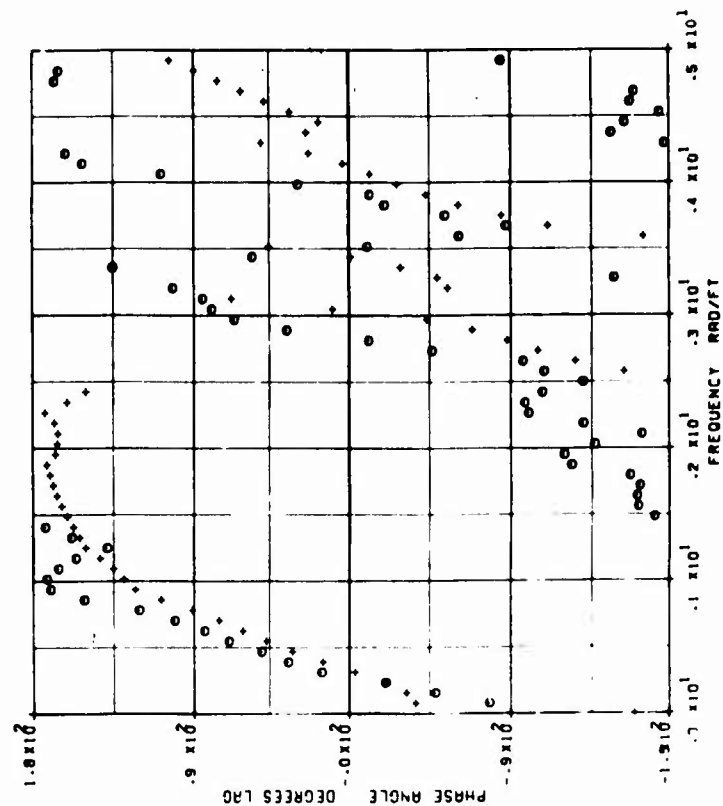
PHASE ANGLE

OUTPUT- AIRCRAFT CG ACCELERATION (INZ) AT FS 1333

INPUT- VERTICAL QUST VELOCITY

TEST O THEORETICAL +

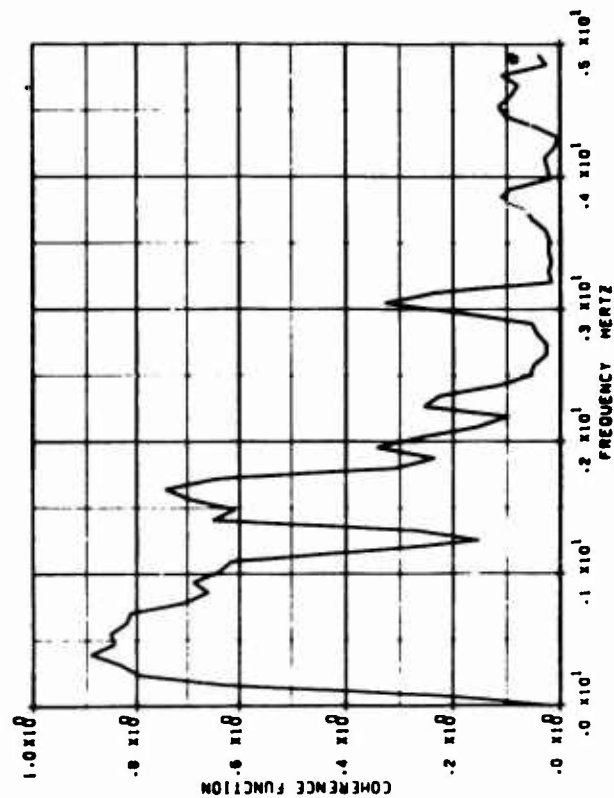
ALTITUDE 2240 FEET
AIRSPEED 260.9 KEAS
GROSS WEIGHT 514000 LB
FUEL WEIGHT 80000 LB
CARGO WEIGHT 110000 LB
CG 33.3 PCT MAC



1-D QUST RESPONSE COMPARISON FOR C-SA AIRCRAFT

OUTPUT- AIRCRAFT CO ACCELERATION (IN2) AT FS 1333
 INPUT- VERTICAL QUST VELOCITY
 TEST --- THEORETICAL ---

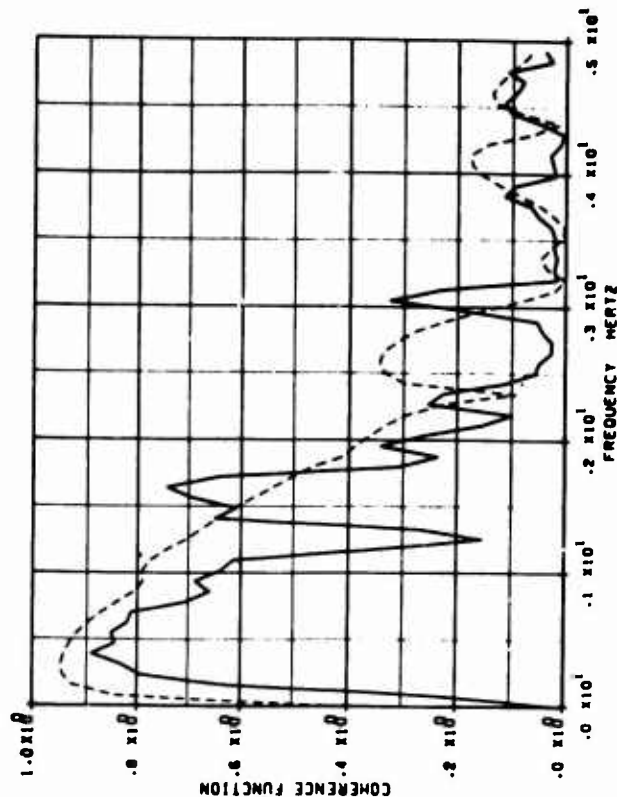
ALTITUDE 2240 FEET
 AIRSPEED 260.9 KERS
 GROSS WEIGHT 514000 LB
 FUEL WEIGHT 80000 LB
 CARGO WEIGHT 110000 LB
 CO 33.3 PCT MAC



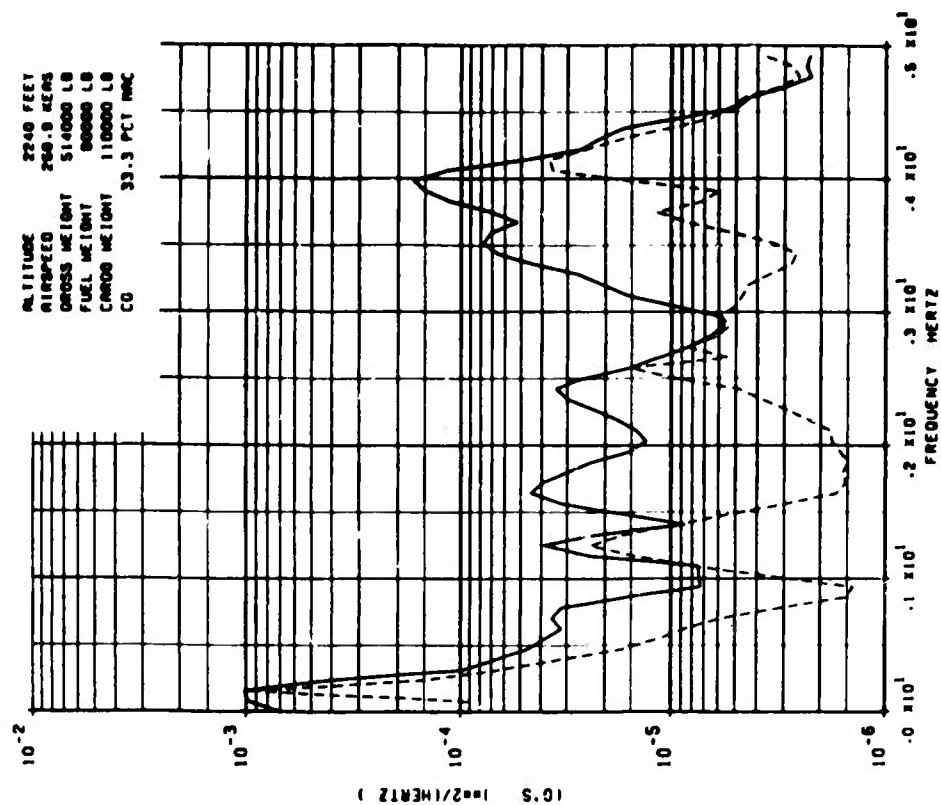
3-D QUST RESPONSE COMPARISON FOR C-SA AIRCRAFT

OUTPUT- AIRCRAFT CO ACCELERATION (IN2) AT FS 1333
 INPUT- VERTICAL QUST VELOCITY
 TEST --- THEORETICAL ---

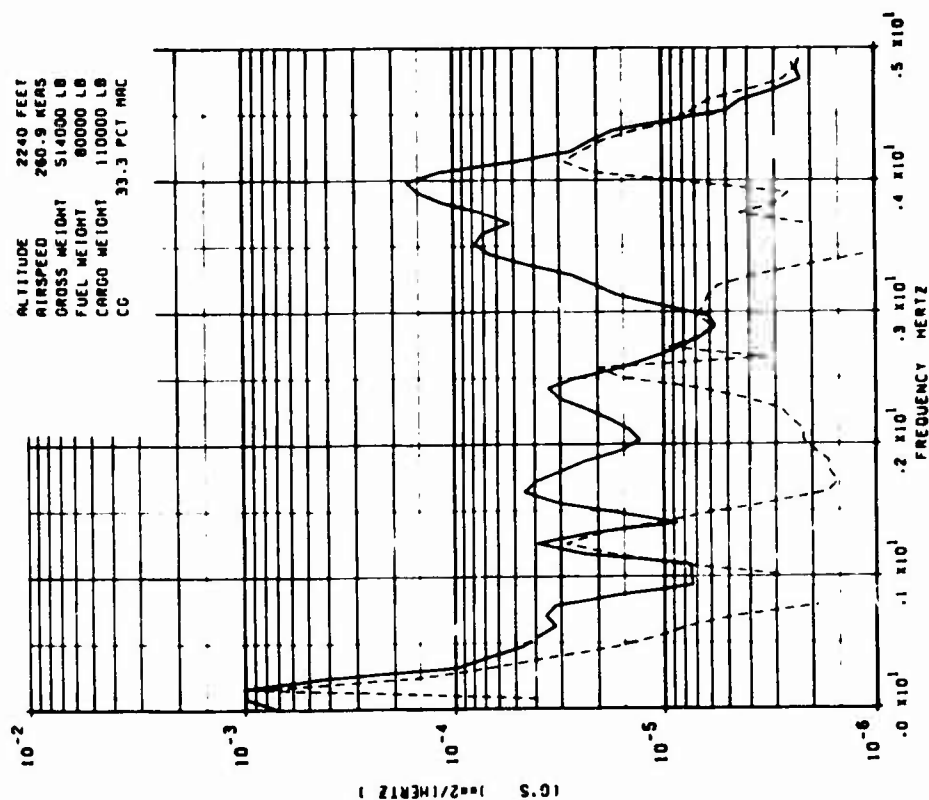
ALTITUDE 2240 FEET
 AIRSPEED 260.9 KERS
 GROSS WEIGHT 514000 LB
 FUEL WEIGHT 80000 LB
 CARGO WEIGHT 110000 LB
 CO 33.3 PCT MAC



3-D GUST RESPONSE COMPARISON FOR C-5A AIRCRAFT
 POWER SPECTRUM
 AIRCRAFT CG ACCELERATION INT) AT FS 1333
 TEST — THEORETICAL —

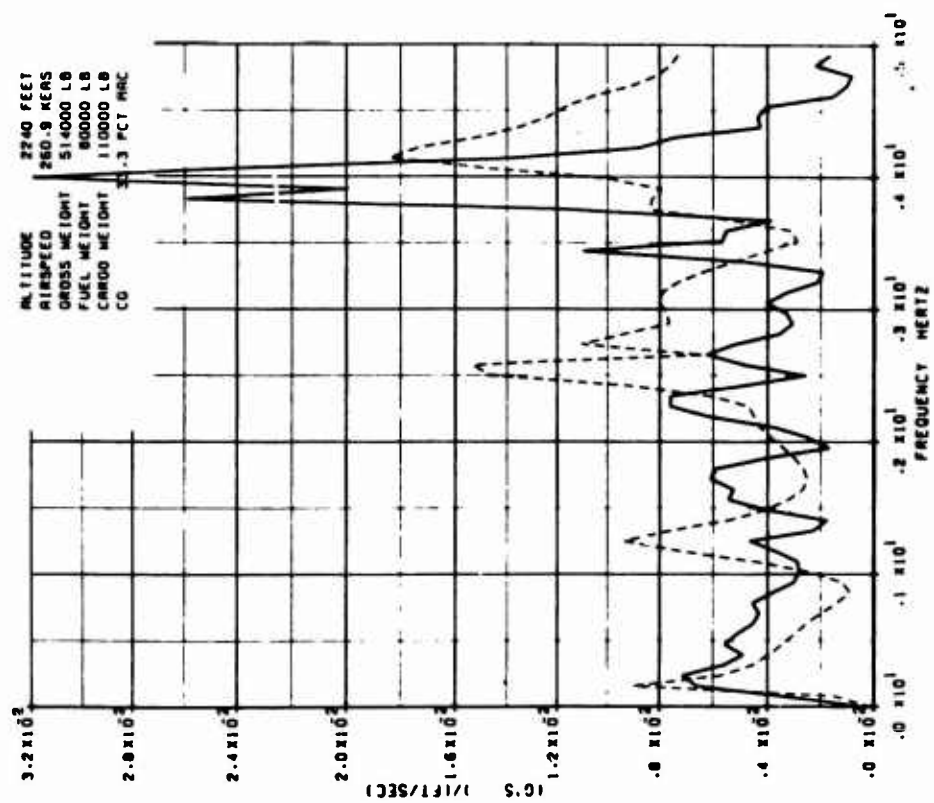


1-D GUST RESPONSE COMPARISON FOR C-5A AIRCRAFT
 POWER SPECTRUM
 AIRCRAFT CG ACCELERATION INT) AT FS 1333
 TEST — THEORETICAL —



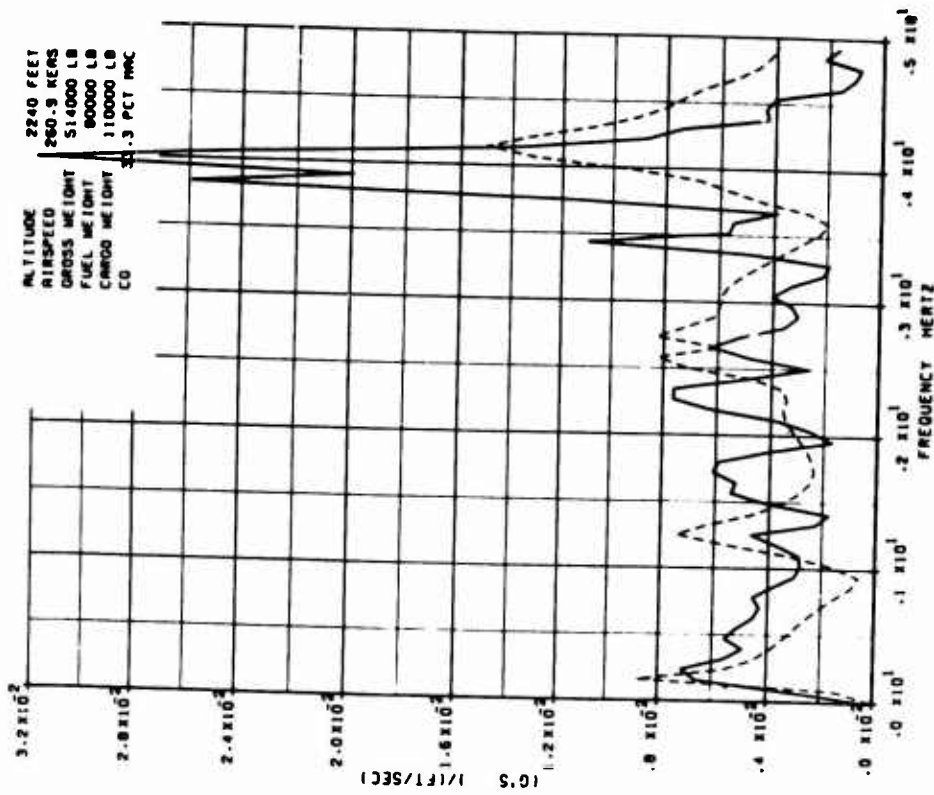
1-0 GUST RESPONSE COMPARISON FOR C-SA AIRCRAFT

CROSS TRANSFER FUNCTION
 OUTPUT- AIRCRAFT CG ACCELERATION (NY) AT FS 1333
 INPUT- LATERAL GUST VELOCITY
 TEST --- THEORETICAL --



3-0 GUST RESPONSE COMPARISON FOR C-SA AIRCRAFT

CROSS TRANSFER FUNCTION
 OUTPUT- AIRCRAFT CG ACCELERATION (NY) AT FS 1333
 INPUT- LATERAL GUST VELOCITY
 TEST --- THEORETICAL --



1-D GUST RESPONSE COMPARISON FOR C-5A AIRCRAFT

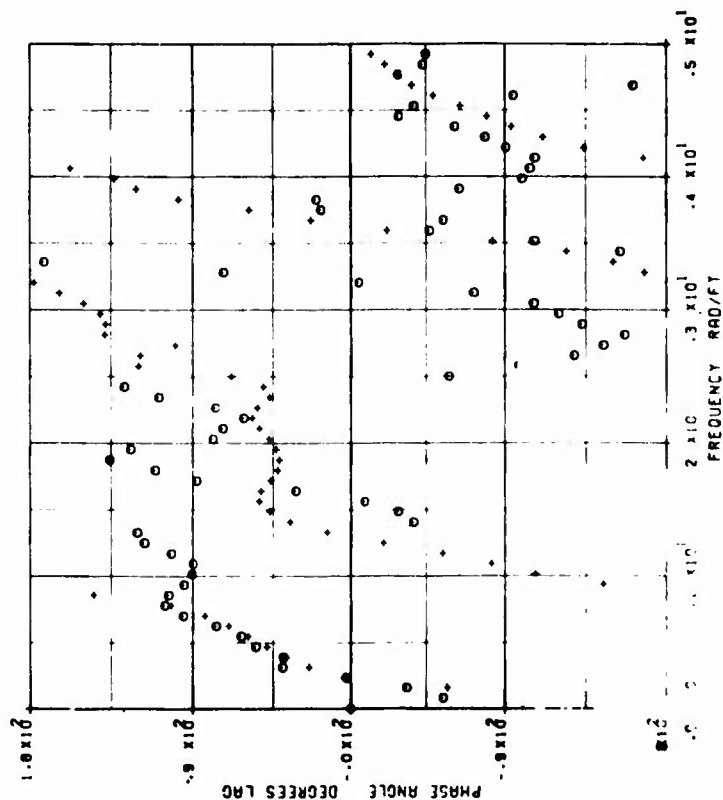
PHASE ANGLE

OUTPUT- AIRCRAFT CG ACCELERATION (NY) AT FS 1333

INPUT- LATERAL GUST VELOCITY

TEST O THEORETICAL +

ALTITUDE 2240 FEET
AIRSPEED 260.9 KNOTS
GROSS WEIGHT 514000 LB
FUEL WEIGHT 80000 LB
CARGO WEIGHT 110000 LB
CG 33.3 PCT MAC



3-D GUST RESPONSE COMPARISON FOR C-5A AIRCRAFT

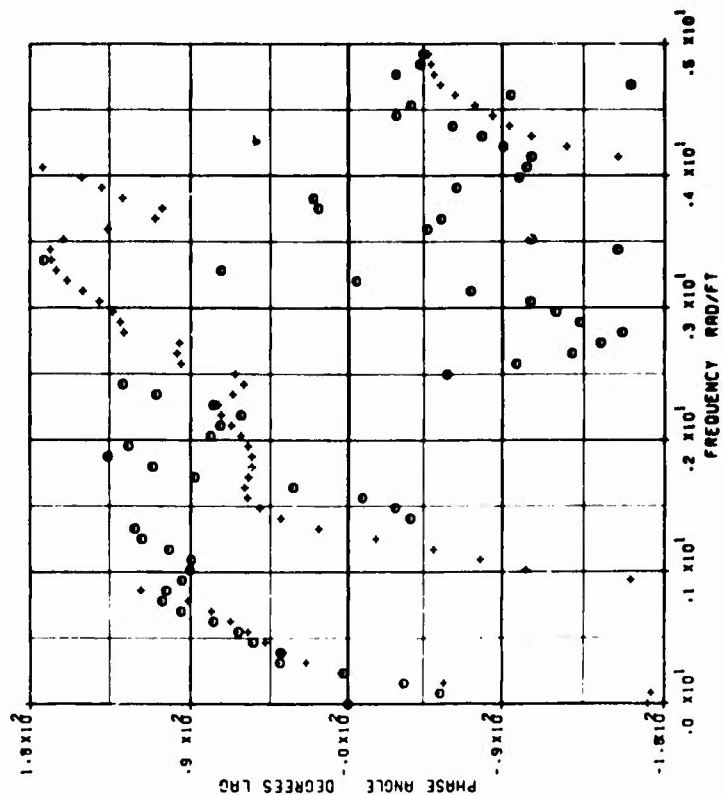
PHASE ANGLE

OUTPUT- AIRCRAFT CG ACCELERATION (NY) AT FS 1333

INPUT- LATERAL GUST VELOCITY

TEST O THEORETICAL +

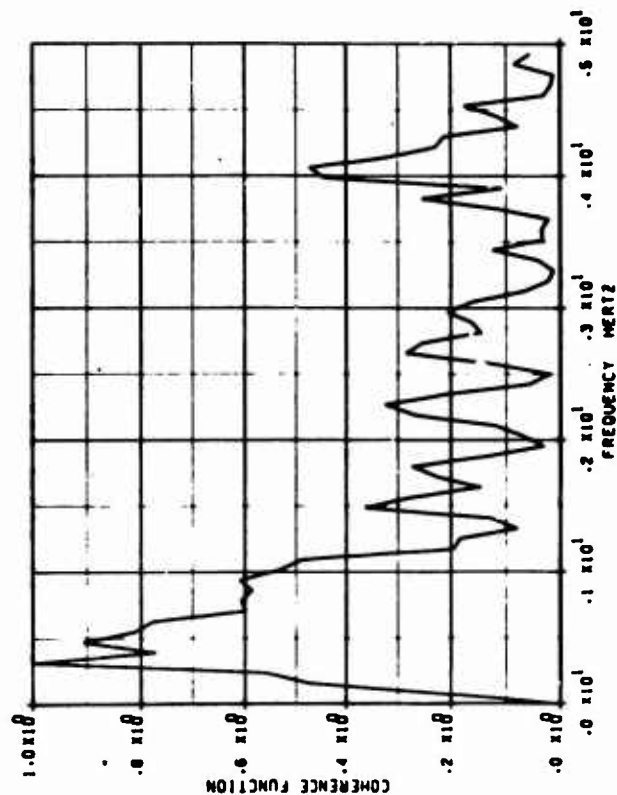
ALTITUDE 2240 FEET
AIRSPEED 260.9 KNOTS
GROSS WEIGHT 514000 LB
FUEL WEIGHT 80000 LB
CARGO WEIGHT 110000 LB
CG 33.3 PCT MAC



1 -0 DUST RESPONSE COMPARISON FOR C-SA AIRCRAFT

CONCRETE FUNCTION
 OUTPUT- AIRCRAFT CO ACCELERATION (INT) AT FS 1333
 INPUT- LATERAL DUST VELOCITY
 TEST --- THEORETICAL ---

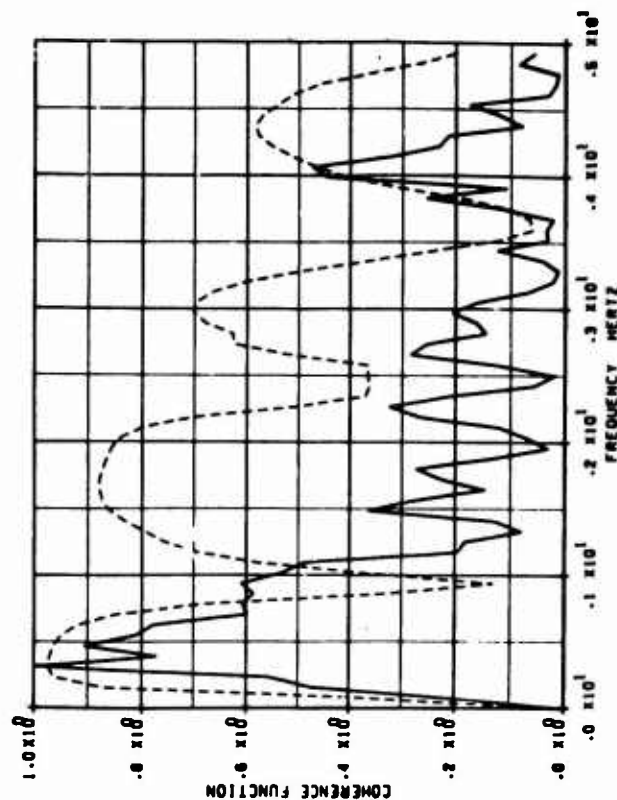
ALTITUDE 2240 FEET
 AIRSPEED 260.9 KNOTS
 GROSS WEIGHT 514000 LB
 FUEL WEIGHT 90000 LB
 CARGO WEIGHT 110000 LB
 CO 33.3 PCT MAC



3 -0 DUST RESPONSE COMPARISON FOR C-SA AIRCRAFT

CONCRETE FUNCTION
 OUTPUT- AIRCRAFT CO ACCELERATION (INT) AT FS 1333
 INPUT- LATERAL DUST VELOCITY
 TEST --- THEORETICAL ---

ALTITUDE 2240 FEET
 AIRSPEED 260.9 KNOTS
 GROSS WEIGHT 514000 LB
 FUEL WEIGHT 90000 LB
 CARGO WEIGHT 110000 LB
 CO 33.3 PCT MAC



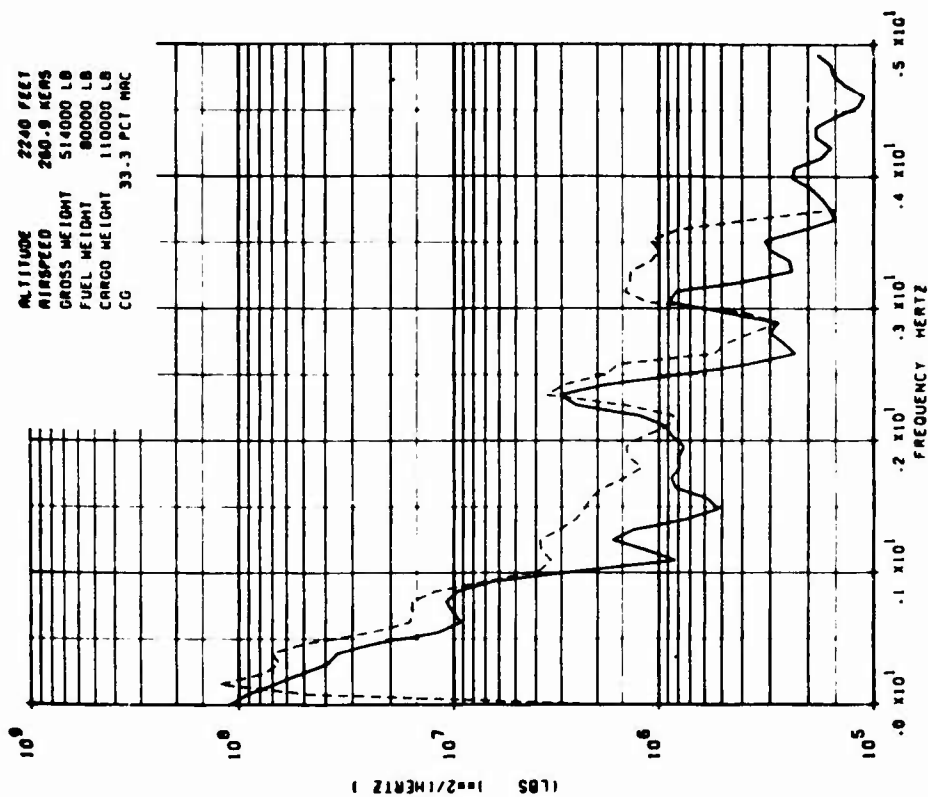
1-0 QUST RESPONSE COMPARISON FOR C-5A AIRCRAFT

POWER SPECTRUM

WIND SHEAR (SZP) AT WS 190R

TEST — THEORETICAL —

ALTITUDE 2240 FEET
AIRSPEED 260.8 KNOTS
GROSS WEIGHT 514000 LB
FUEL WEIGHT 80000 LB
CARGO WEIGHT 110000 LB
CG 33.3 PCT MAC



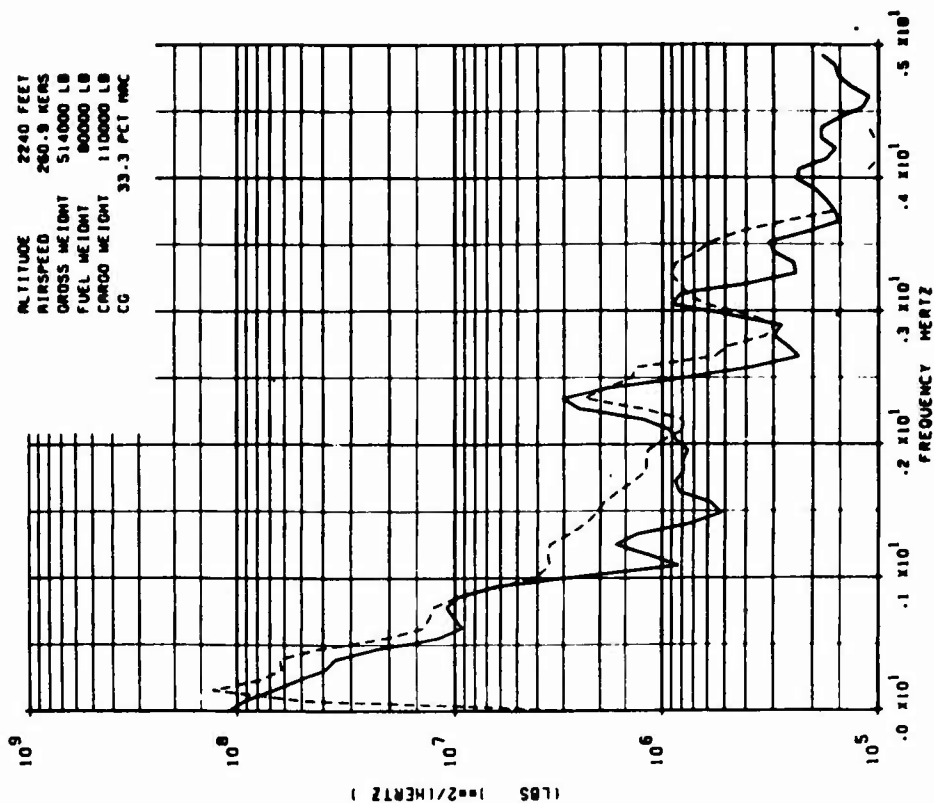
3-0 QUST RESPONSE COMPARISON FOR C-5A AIRCRAFT

POWER SPECTRUM

WIND SHEAR (SZP) AT WS 190R

TEST — THEORETICAL —

ALTITUDE 2240 FEET
AIRSPEED 260.8 KNOTS
GROSS WEIGHT 514000 LB
FUEL WEIGHT 80000 LB
CARGO WEIGHT 110000 LB
CG 33.3 PCT MAC



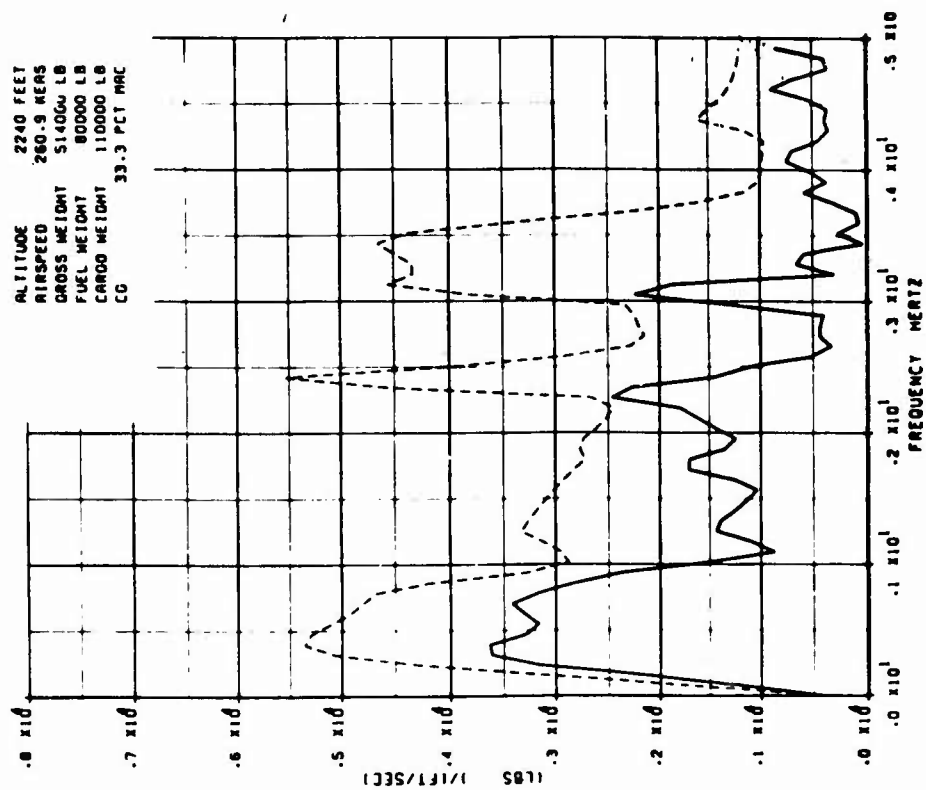
1-0 GUST RESPONSE COMPARISON FOR C-SA AIRCRAFT

CROSS TRANSFER FUNCTION

OUTPUT- WING SHEAR (SZP) AT WS 198R

INPUT- VERTICAL GUST VELOCITY

TEST --- THEORETICAL ---



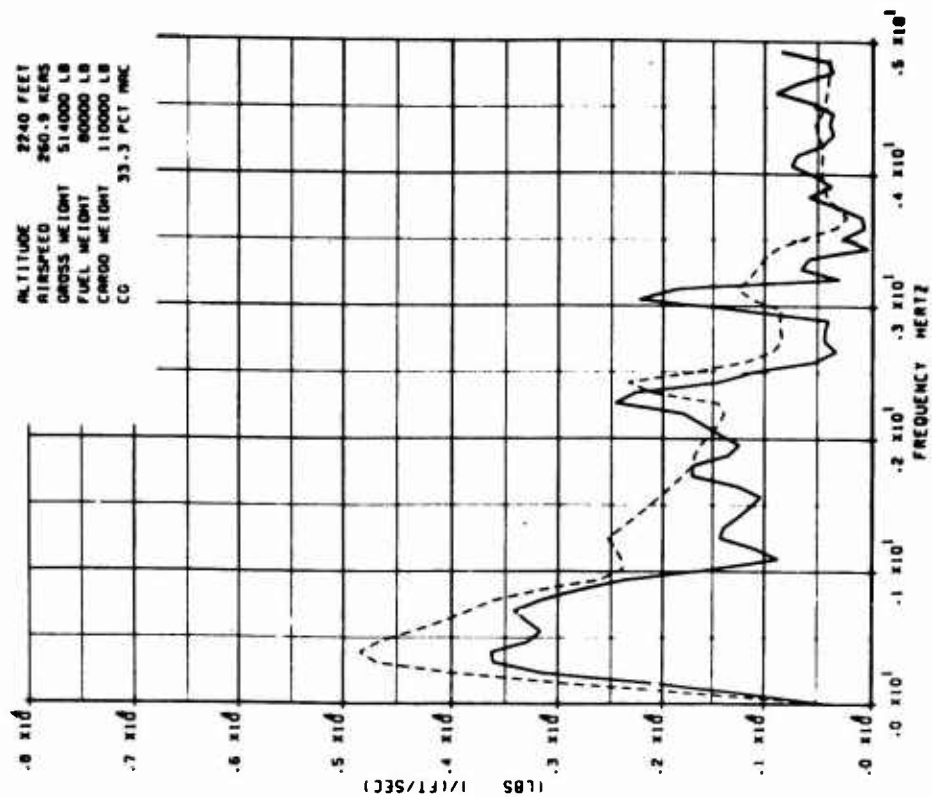
3-0 GUST RESPONSE COMPARISON FOR C-SA AIRCRAFT

CROSS TRANSFER FUNCTION

OUTPUT- WING SHEAR (SZP) AT WS 198R

INPUT- VERTICAL GUST VELOCITY

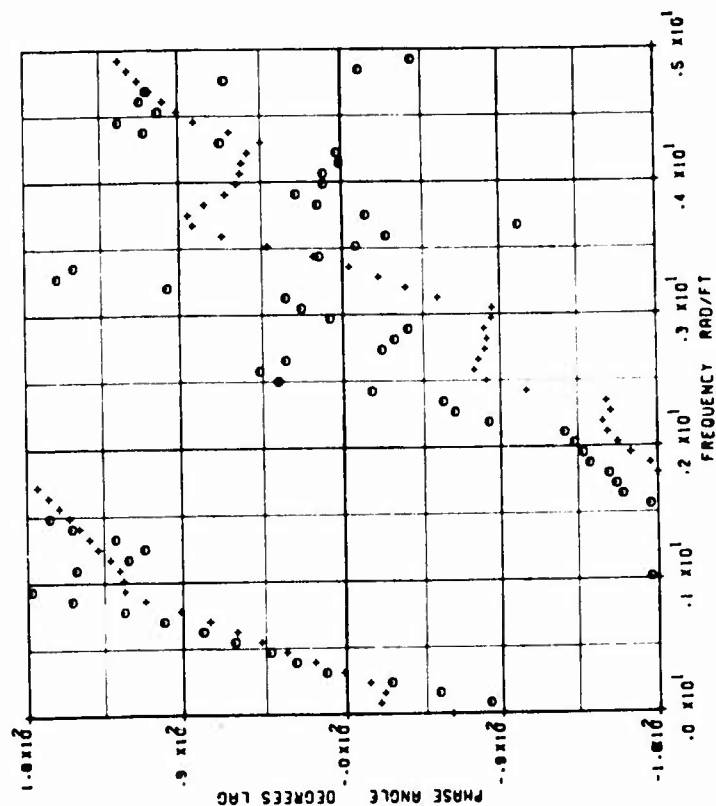
TEST --- THEORETICAL ---



1-D GUST RESPONSE COMPARISON FOR C-5A AIRCRAFT

PHASE ANGLE
 OUTPUT- WING SHEAR (SZP) AT WS 198R
 INPUT- VERTICAL GUST VELOCITY
 TEST O THEORETICAL +

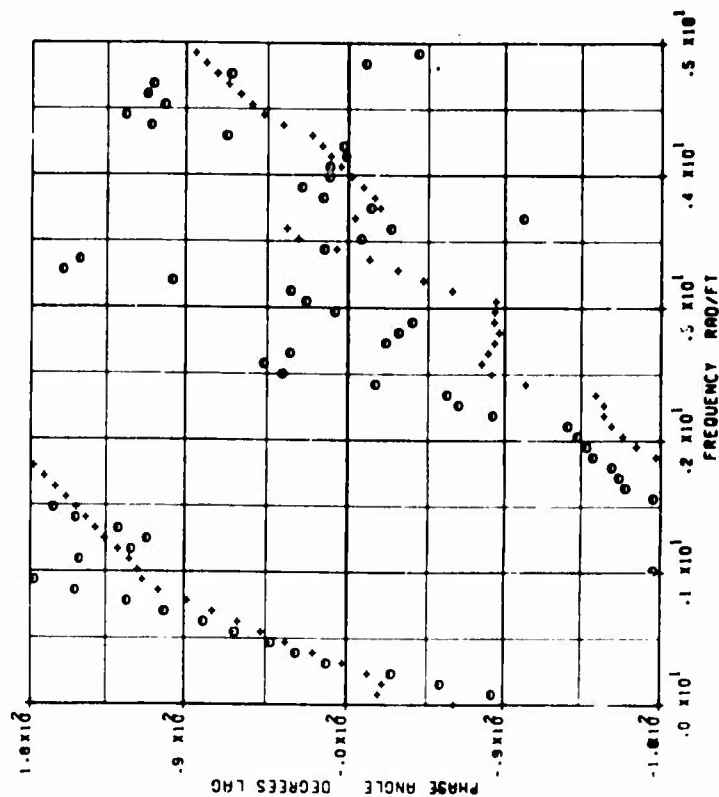
ALTITUDE 2240 FEET
 AIRSPEED 260.9 KIAS
 GROSS WEIGHT 514000 LB
 FUEL WEIGHT 80000 LB
 CARGO WEIGHT 110000 LB
 CG 33.3 PCT MAC



3-D GUST RESPONSE COMPARISON FOR C-5A AIRCRAFT

PHASE ANGLE
 OUTPUT- WING SHEAR (SZP) AT WS 197R
 INPUT- VERTICAL GUST VELOCITY
 TEST O THEORETICAL +

ALTITUDE 2240 FEET
 AIRSPEED 260.9 KIAS
 GROSS WEIGHT 514000 LB
 FUEL WEIGHT 80000 LB
 CARGO WEIGHT 110000 LB
 CL 33.3 PCT MAC



1-0 QUST RESPONSE COMPARISON FOR C-SA AIRCRAFT

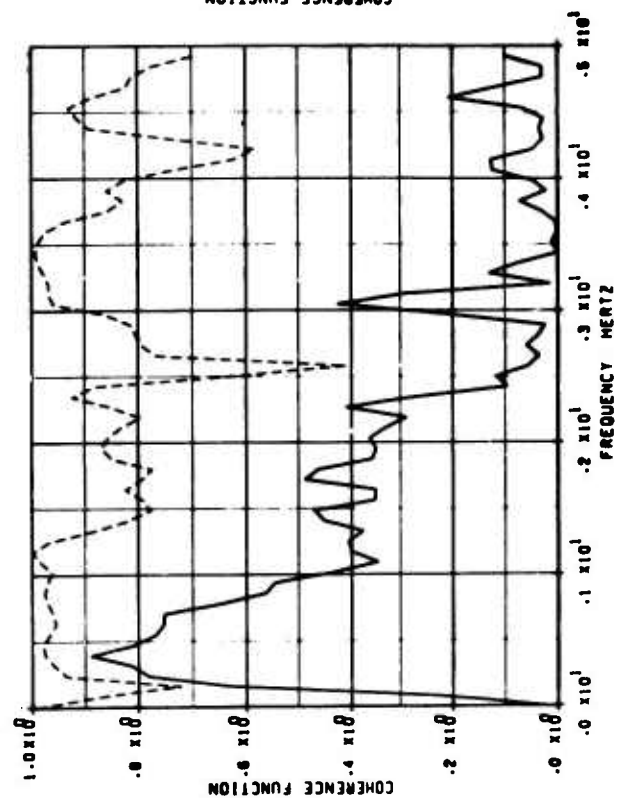
CONFERENCE FUNCTION

OUTPUT- WIND SHEAR (SEP) AT MS 198R

INPUT- VERTICAL QUST VELOCITY

TEST --- THEORETICAL ---

ALTITUDE 2240 FEET
AIRSPEED 280.9 KERS
GROSS WEIGHT 514000 LB
FUEL WEIGHT 80000 LB
CARGO WEIGHT 110000 LB
CO 33.3 PCT MAC



3-0 QUST RESPONSE COMPARISON FOR C-SA AIRCRAFT

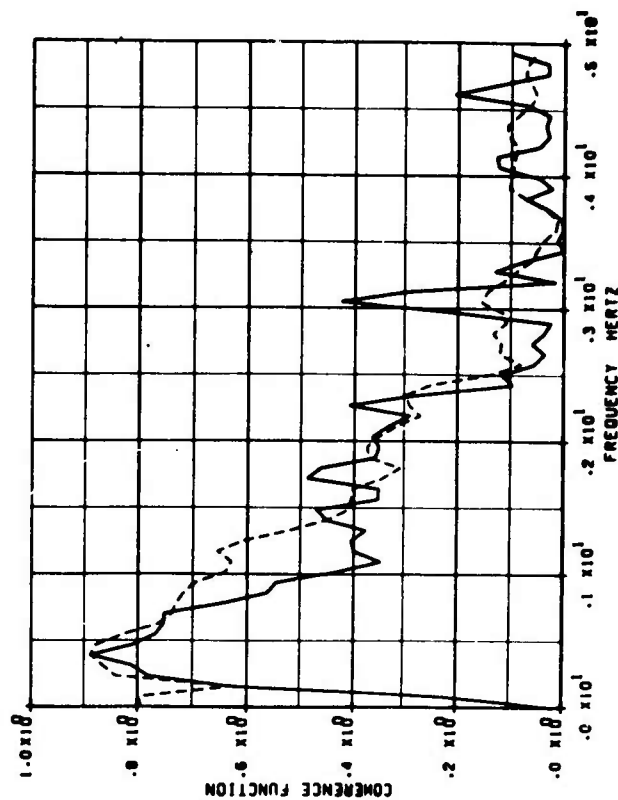
CONFERENCE FUNCTION

OUTPUT- WIND SHEAR (SEP) AT MS 198R

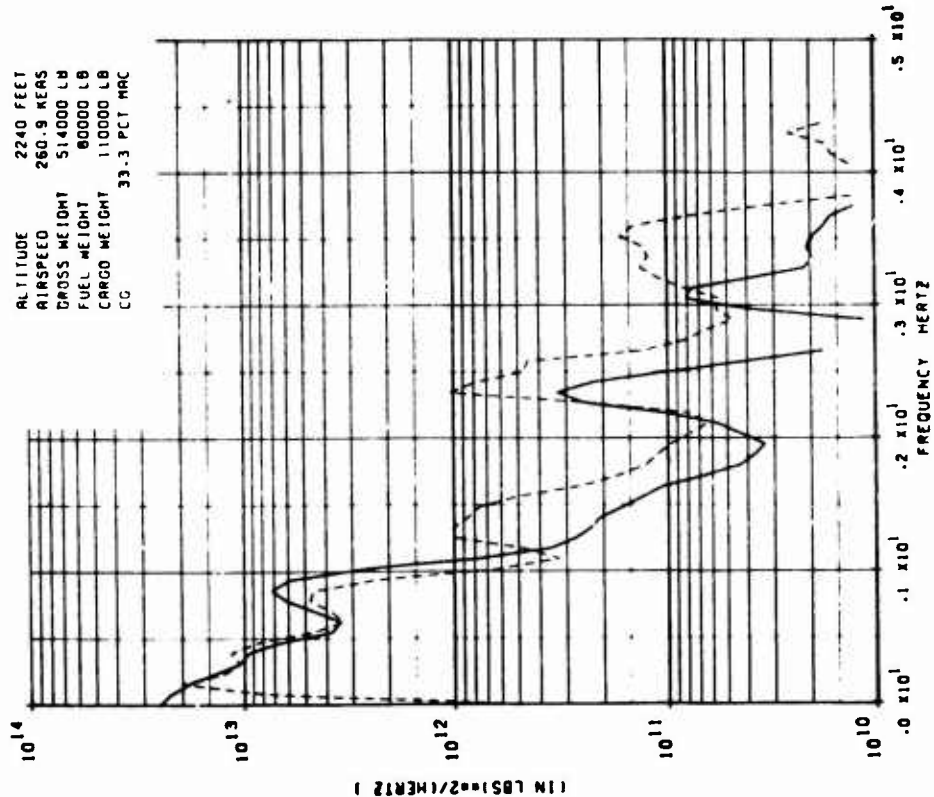
INPUT- VERTICAL QUST VELOCITY

TEST --- THEORETICAL ---

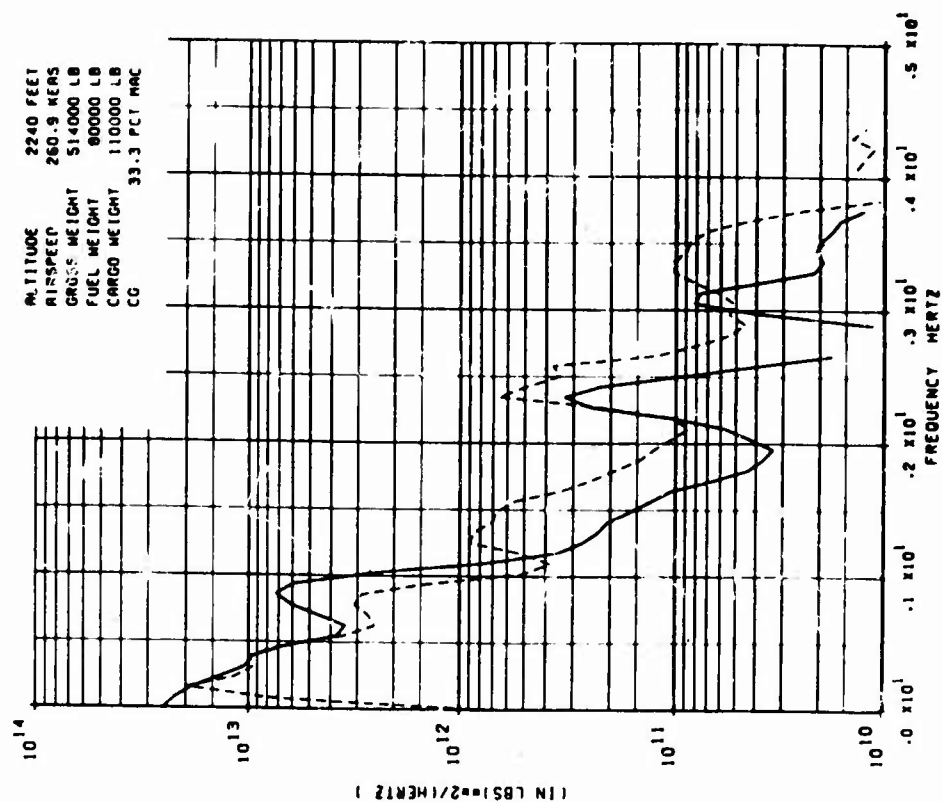
ALTITUDE 2240 FEET
AIRSPEED 280.9 KERS
GROSS WEIGHT 514000 LB
FUEL WEIGHT 80000 LB
CARGO WEIGHT 110000 LB
CO 33.3 PCT MAC



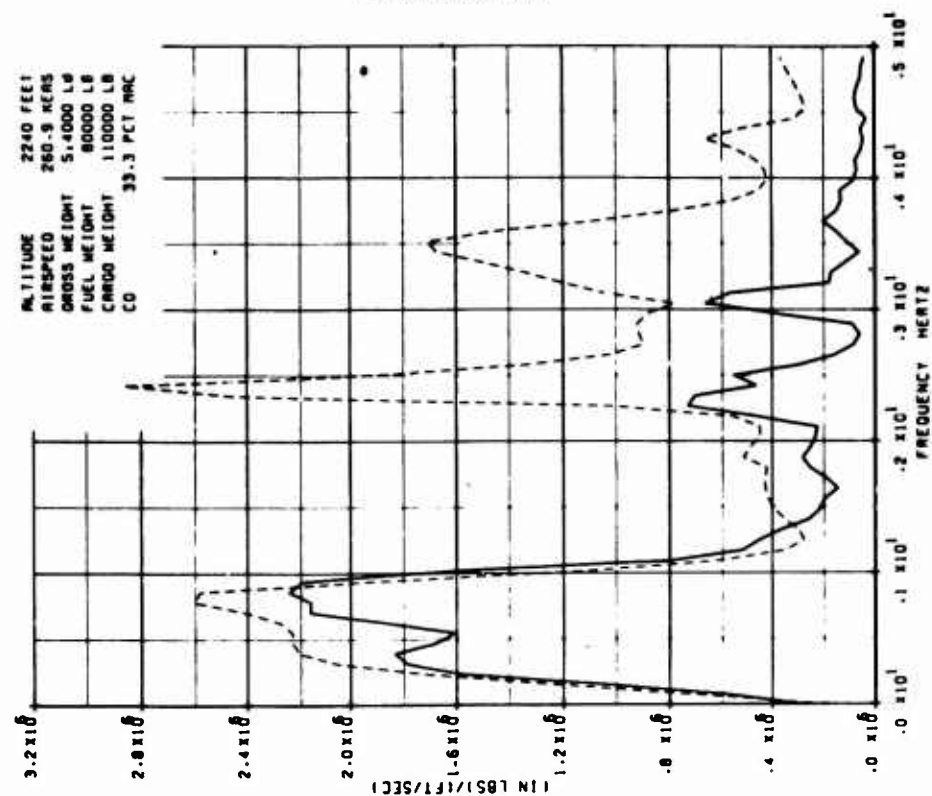
1-0 GUST RESPONSE COMPARISON FOR C-5A AIRCRAFT
 POWER SPECTRUM
 WIND BENDING (INXPI) AT WS 198
 TEST — THEORETICAL — —



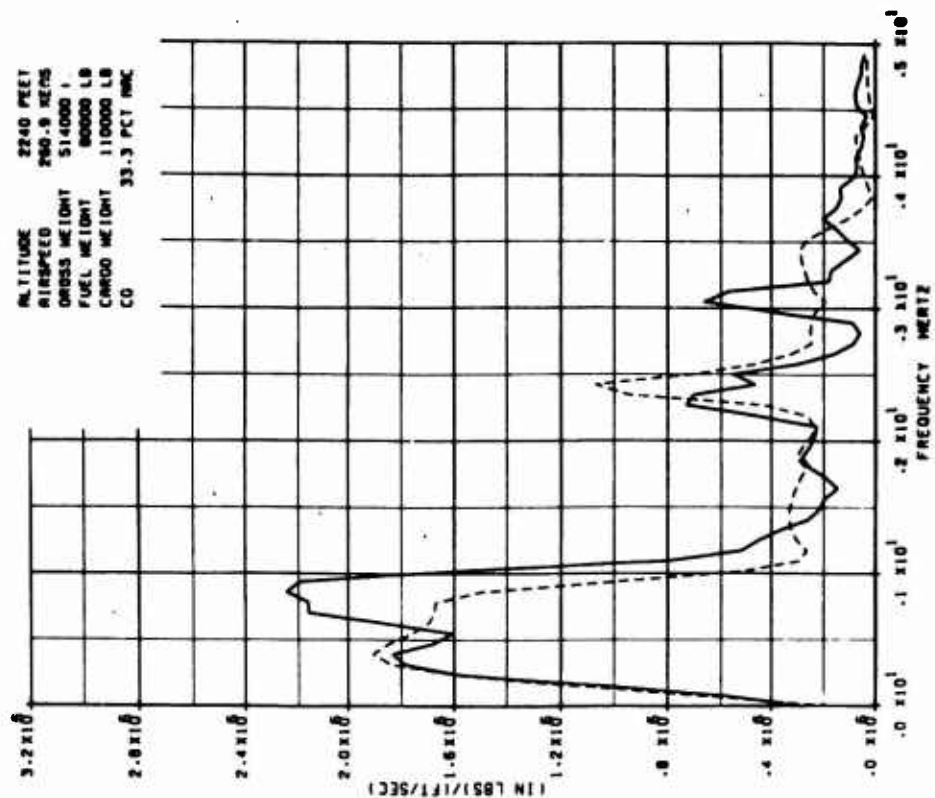
3-0 GUST RESPONSE COMPARISON FOR L-5A AIRCRAFT
 POWER SPECTRUM
 WIND BENDING (INXPI) AT WS 198
 TEST — THEORETICAL — —



1-D GUST RESPONSE COMPARISON FOR C-SA AIRCRAFT
CROSS TRANSFER FUNCTION
OUTPUT- WING BENDING (INP) AT HS 190
INPUT- VERTICAL GUST VELOCITY
TEST: — THEORETICAL —



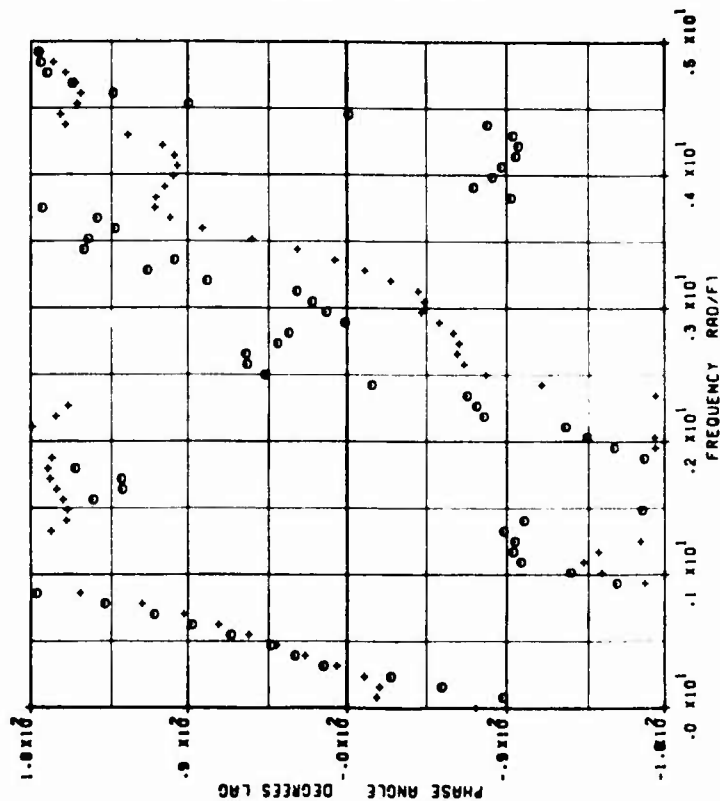
3-D GUST RESPONSE COMPARISON FOR C-SA AIRCRAFT
CROSS TRANSFER FUNCTION
OUTPUT- WING BENDING (INP) AT HS 190
INPUT- VERTICAL GUST VELOCITY
TEST: — THEORETICAL —



1-D GUST RESPONSE COMPARISON FOR C-SA AIRCRAFT

PHASE ANGLE
 OUTPUT- WING BENDING (INCH) AT WS 198
 INPUT- VERTICAL GUST VELOCITY
 TEST O THEORETICAL +

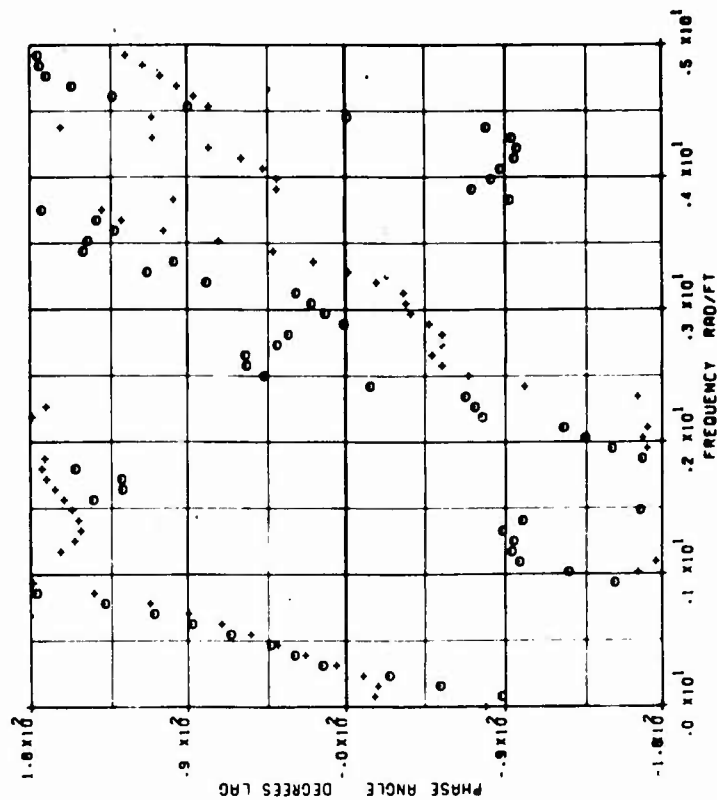
ALTITUDE 2240 FEET
 AIRSPEED 260.9 KIAS
 GROSS WEIGHT 514000 LB
 FUEL WEIGHT 80000 LB
 CARGO WEIGHT 110000 LB
 CG 33.3 PCT MAC



3-D GUST RESPONSE COMPARISON FOR C-SA AIRCRAFT

PHASE ANGLE
 OUTPUT- WING BENDING (INCH) AT WS 198
 INPUT- VERTICAL GUST VELOCITY
 TEST O THEORETICAL +

ALTITUDE 2240 FEET
 AIRSPEED 260.9 KIAS
 GROSS WEIGHT 514000 LB
 FUEL WEIGHT 80000 LB
 CARGO WEIGHT 110000 LB
 CG 33.3 PCT MAC



1-0 GUST RESPONSE COMPARISON FOR C-5A AIRCRAFT

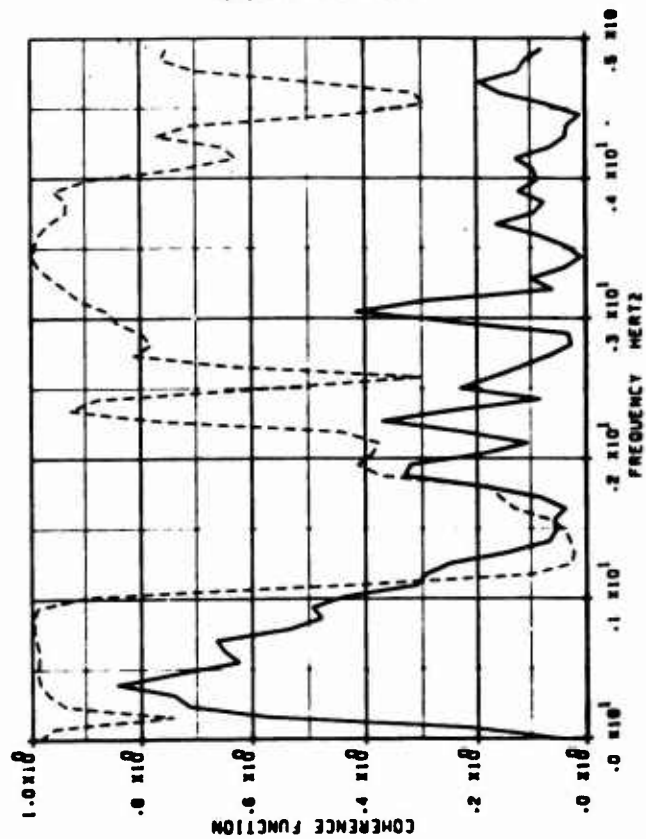
COHERENCE FUNCTION

OUTPUT- WING BENDING (MYP) AT WS 190

INPUT- VERTICAL GUST VELOCITY

TEST --- THEORETICAL --

ALTITUDE 2240 FEET
AIRSPEED 260.9 KIAS
GROSS WEIGHT 514000 LB
FUEL WEIGHT 80000 LB
CARGO WEIGHT 110000 LB
CG 33.3 PCT MAC



3-0 GUST RESPONSE COMPARISON FOR C-5A AIRCRAFT

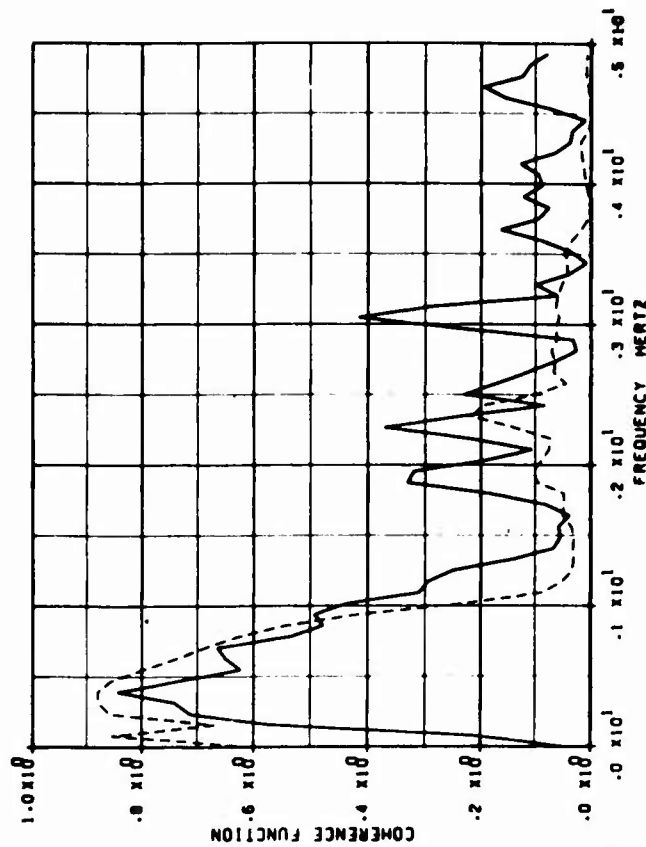
COHERENCE FUNCTION

OUTPUT- WING BENDING (MYP) AT WS 190

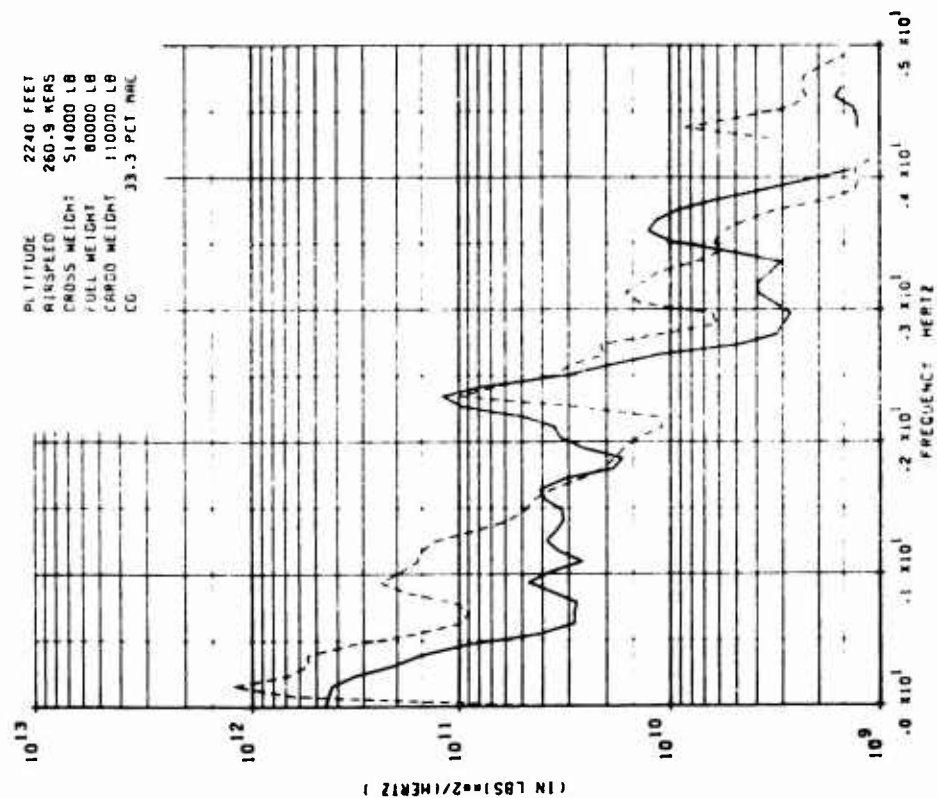
INPUT- VERTICAL GUST VELOCITY

TEST --- THEORETICAL --

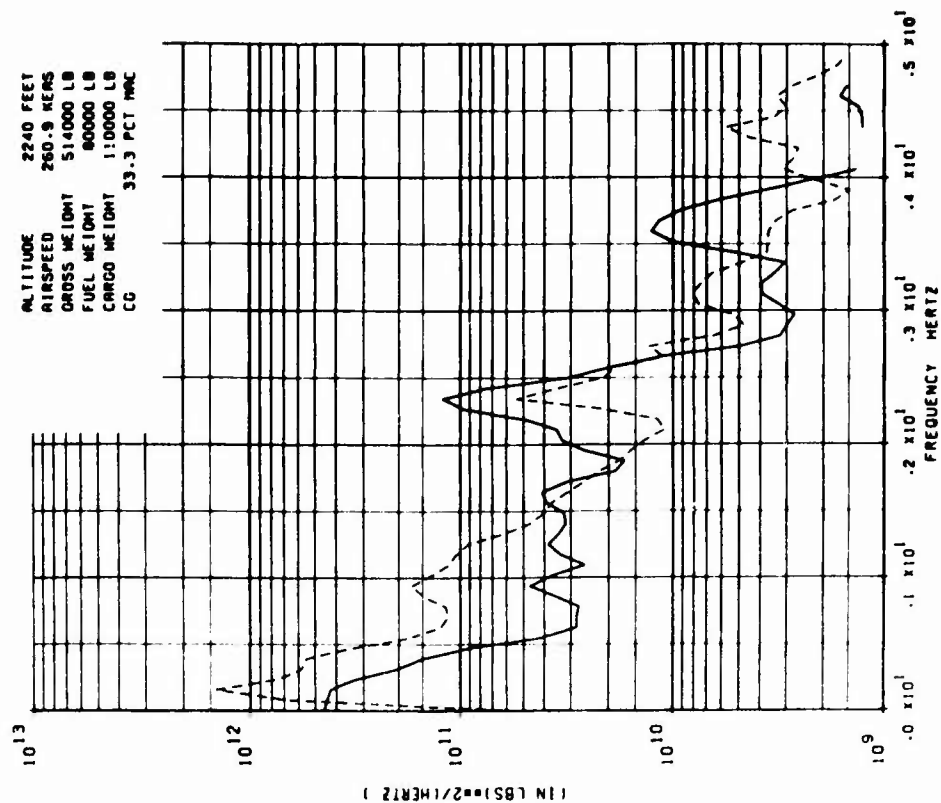
ALTITUDE 2240 FEET
AIRSPEED 260.9 KIAS
GROSS WEIGHT 514000 LB
FUEL WEIGHT 80000 LB
CARGO WEIGHT 110000 LB
CG 33.3 PCT MAC



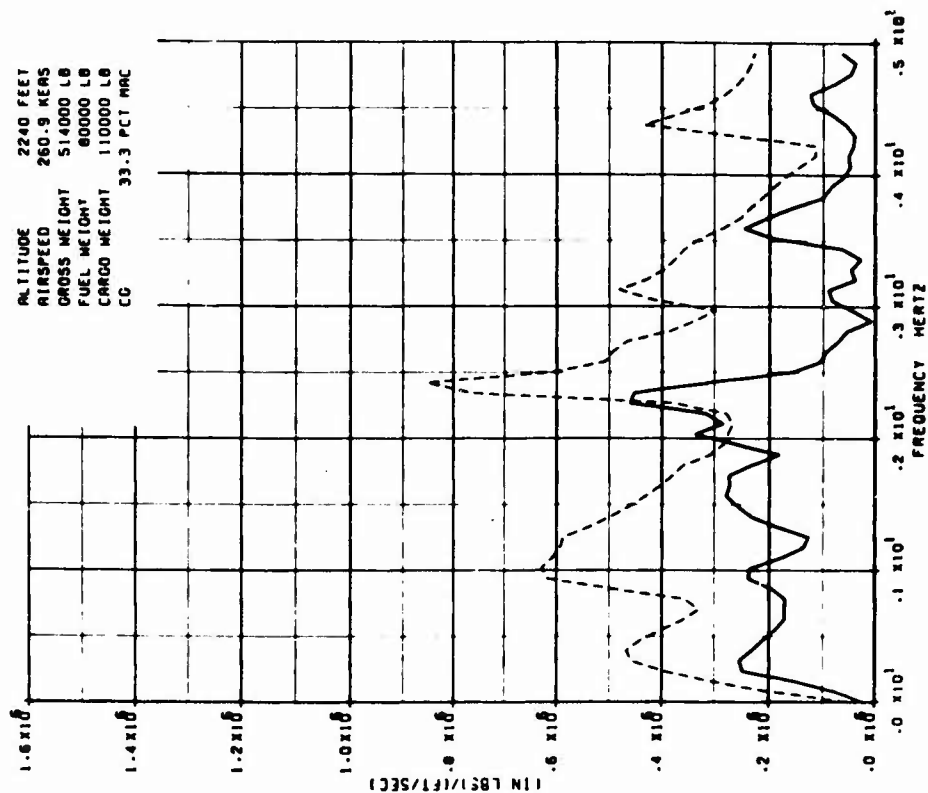
1-0 GUST RESPONSE COMPARISON FOR C-5A AIRCRAFT
 POWER SPECTRUM
 WING TORSION (NYP) AT WS 198
 TEST — THEORETICAL —



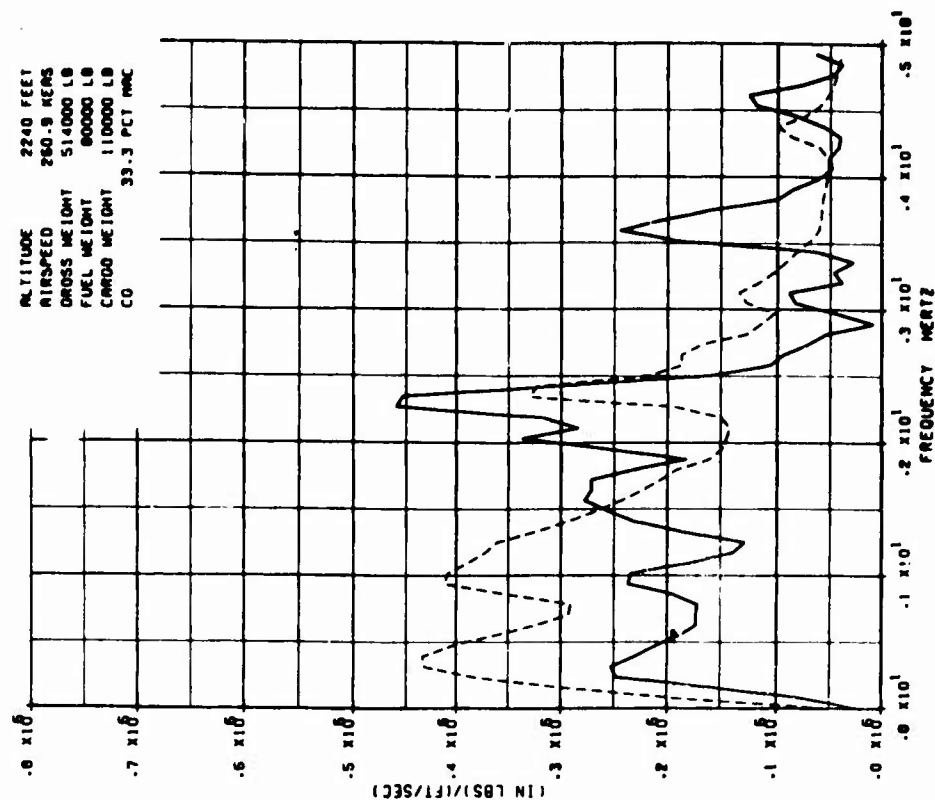
3-0 GUST RESPONSE COMPARISON FOR C-5A AIRCRAFT
 POWER SPECTRUM
 WING TORSION (NYP) AT WS 198
 TEST — THEORETICAL —



1-D GUST RESPONSE COMPARISON FOR C-SA AIRCRAFT
CROSS TRANSFER FUNCTION
OUTPUT- WING TORSION (MPL) AT WS 198
INPUT- VERTICAL GUST VELOCITY
TEST --- THEORETICAL --



3-D GUST RESPONSE COMPARISON FOR C-SA AIRCRAFT
CROSS TRANSFER FUNCTION
OUTPUT- WING TORSION (MPL) AT WS 198
INPUT- VERTICAL GUST VELOCITY
TEST --- THEORETICAL --



1-0 GUST RESPONSE COMPARISON FOR C-5A AIRCRAFT

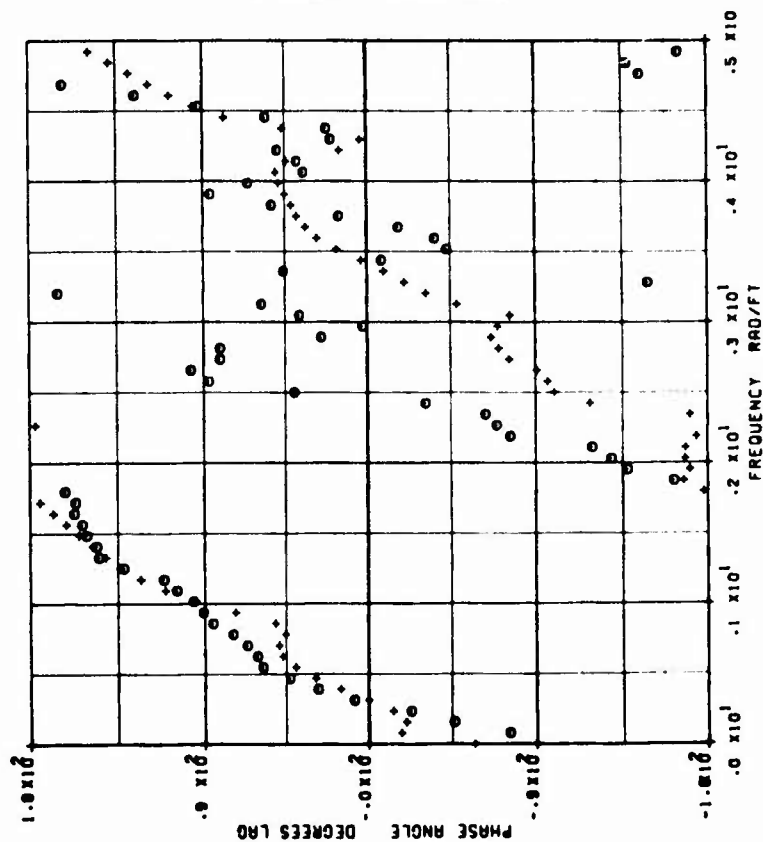
PHASE ANGLE

OUTPUT- MIMO TORSION (MYP) AT WS 198

INPUT- VERTICAL GUST VELOCITY

TEST O THEORETICAL +

ALTITUDE 2240 FEET
AIRSPEED 260.9 KEAS
GROSS WEIGHT 514000 LB
FUEL WEIGHT 80000 LB
CARGO WEIGHT 110000 LB
CG 33.3 PCT MAC



3-0 GUST RESPONSE COMPARISON FOR C-5A AIRCRAFT

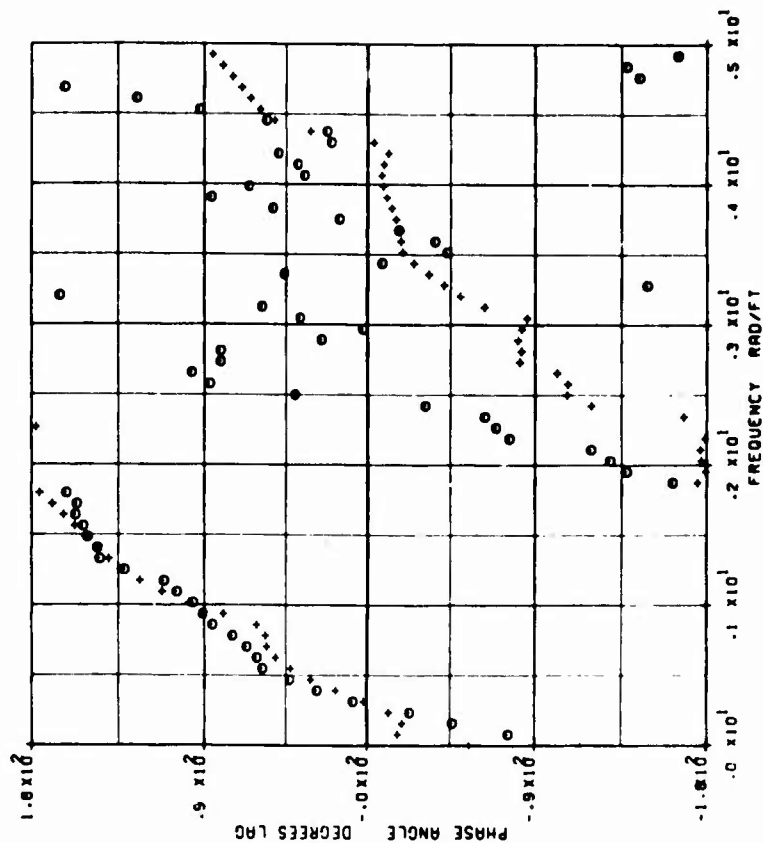
PHASE ANGLE

OUTPUT- MIMO TORSION (MYP) AT WS 198

INPUT- VERTICAL GUST VELOCITY

TEST O THEORETICAL +

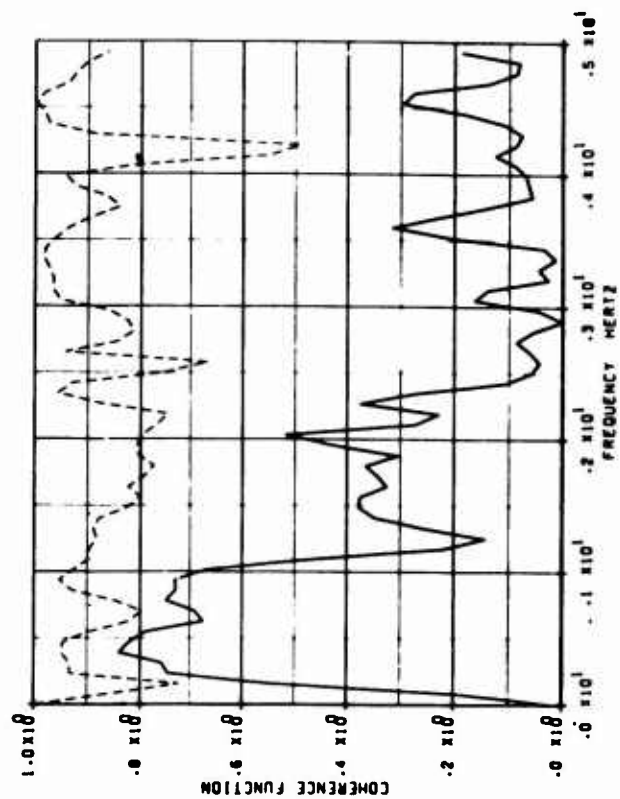
ALTITUDE 2240 FEET
AIRSPEED 260.9 KEAS
GROSS WEIGHT 514000 LB
FUEL WEIGHT 80000 LB
CARGO WEIGHT 110000 LB
CG 33.3 PCT MAC



1-D GUST RESPONSE COMPARISON FOR C-5A AIRCRAFT

COMPREHENSIVE FUNCTION
 OUTPUT- WING TORSION (NTP) AT WS 190
 INPUT- VERTICAL GUST VELOCITY
 TEST --- THEORETICAL ---

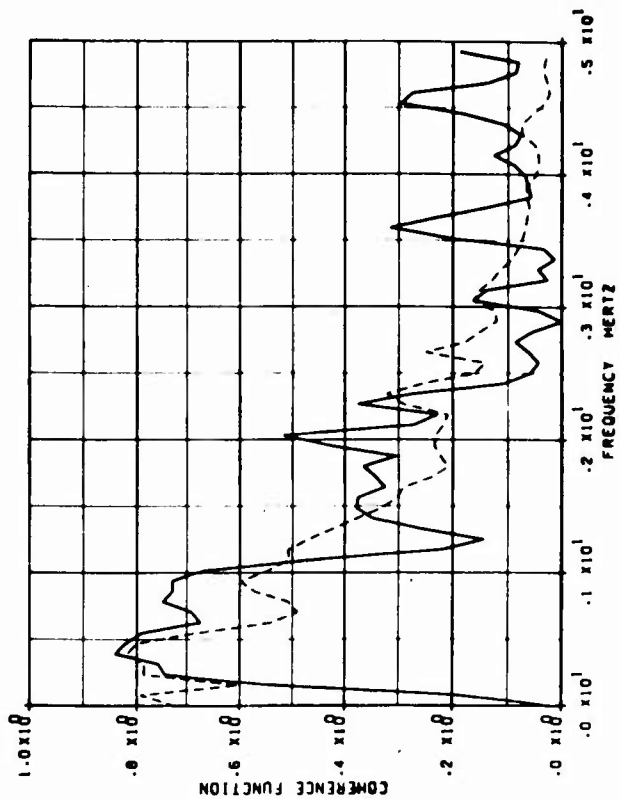
ALTITUDE 2240 FEET
 AIRSPEED 260.9 KNOTS
 GROSS WEIGHT 514000 LB
 FUEL WEIGHT 80000 LB
 CARGO WEIGHT 110000 LB
 CG 33.3 PCT MAC



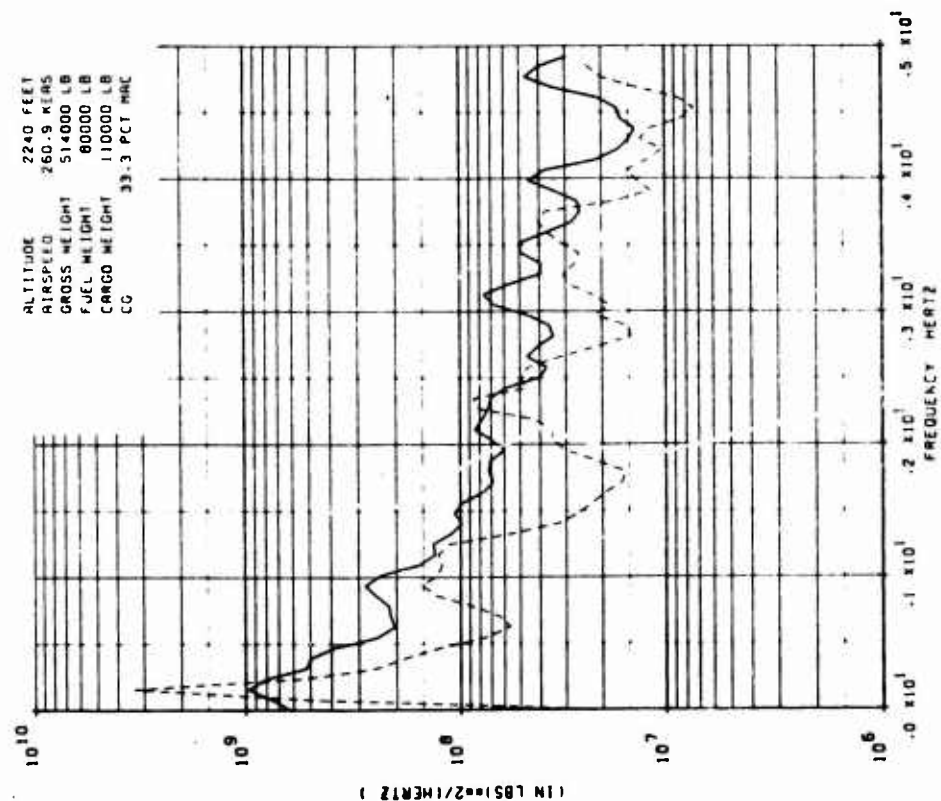
3-D GUST RESPONSE COMPARISON FOR C-5A AIRCRAFT

COMPREHENSIVE FUNCTION
 OUTPUT- WING TORSION (NTP) AT WS 190
 INPUT- VERTICAL GUST VELOCITY
 TEST --- THEORETICAL ---

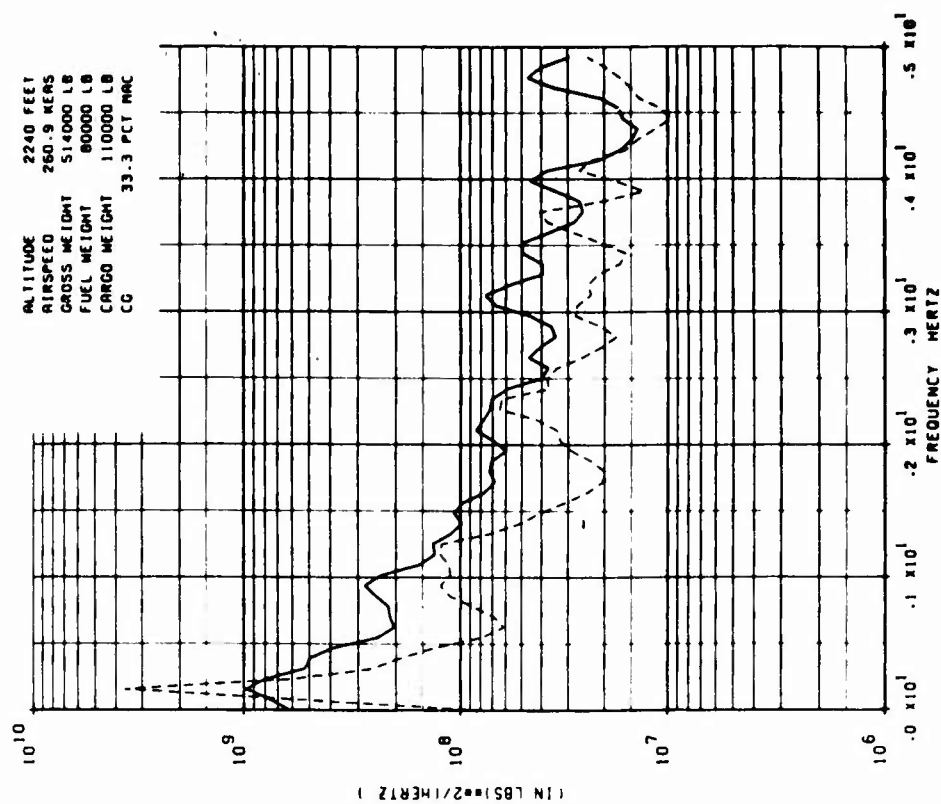
ALTITUDE 2240 FEET
 AIRSPEED 260.9 KNOTS
 GROSS WEIGHT 514000 LB
 FUEL WEIGHT 80000 LB
 CARGO WEIGHT 110000 LB
 CG 33.3 PCT MAC



1-0 GUST RESPONSE COMPARISON FOR C-5A AIRCRAFT
 POWER SPECTRUM
 HORIZONTAL STABILIZER BENDING (INP) AT HSS 232
 TEST — THEORETICAL —



3-0 GUST RESPONSE COMPARISON FOR C-5A AIRCRAFT
 POWER SPECTRUM
 HORIZONTAL STABILIZER BENDING (INP) AT HSS 232
 TEST — THEORETICAL —



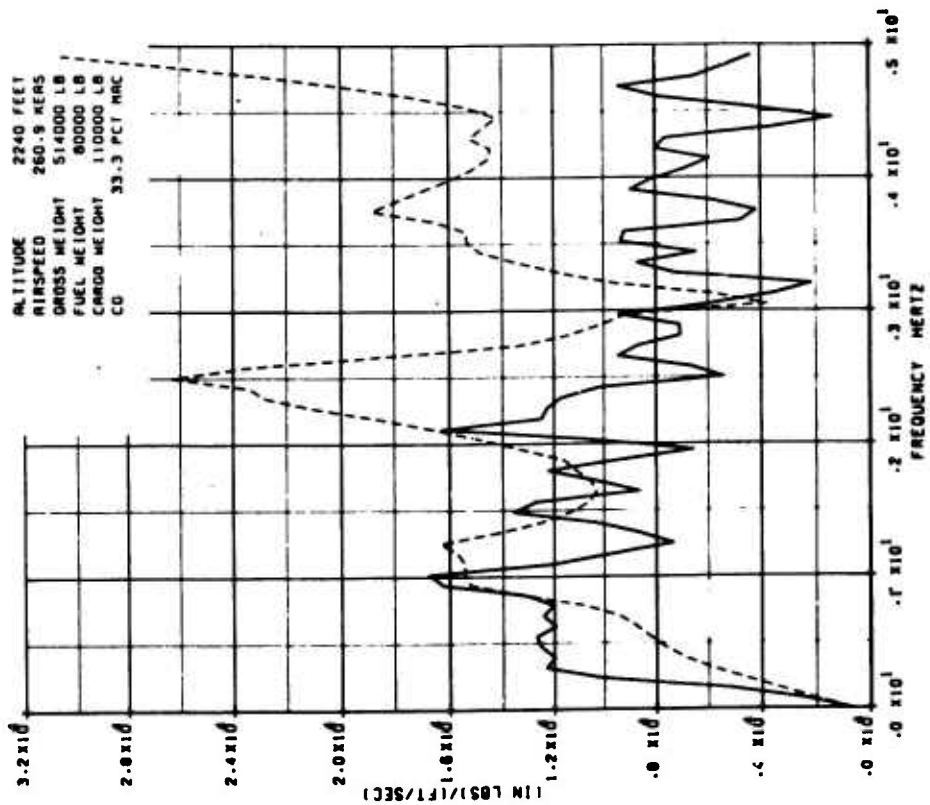
1-D GUST RESPONSE COMPARISON FOR C-5A AIRCRAFT

CROSS TRANSFER FUNCTION

OUTPUT- HORIZONTAL STABILIZER BENDING (NXP) AT MSS 232

INPUT- VERTICAL GUST VELOCITY

TEST --- THEORETICAL ---



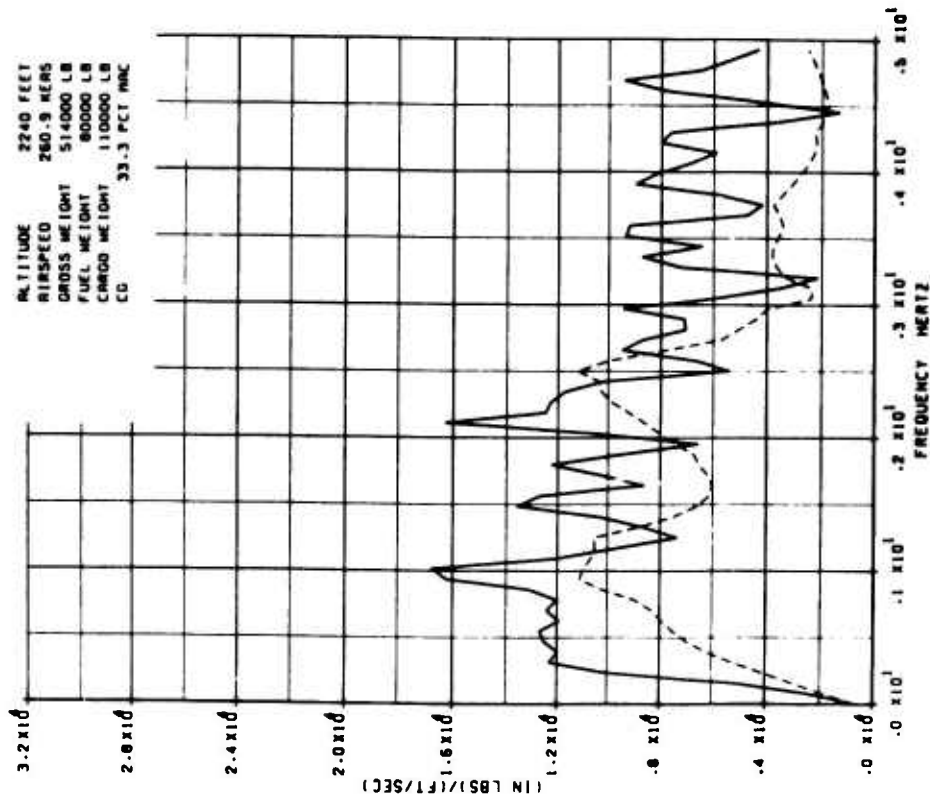
3-D GUST RESPONSE COMPARISON FOR C-5A AIRCRAFT

CROSS TRANSFER FUNCTION

OUTPUT- HORIZONTAL STABILIZER BENDING (NXP) AT MSS 232

INPUT- VERTICAL GUST VELOCITY

TEST --- THEORETICAL ---



1-D GUST RESPONSE COMPARISON FOR C-SA AIRCRAFT

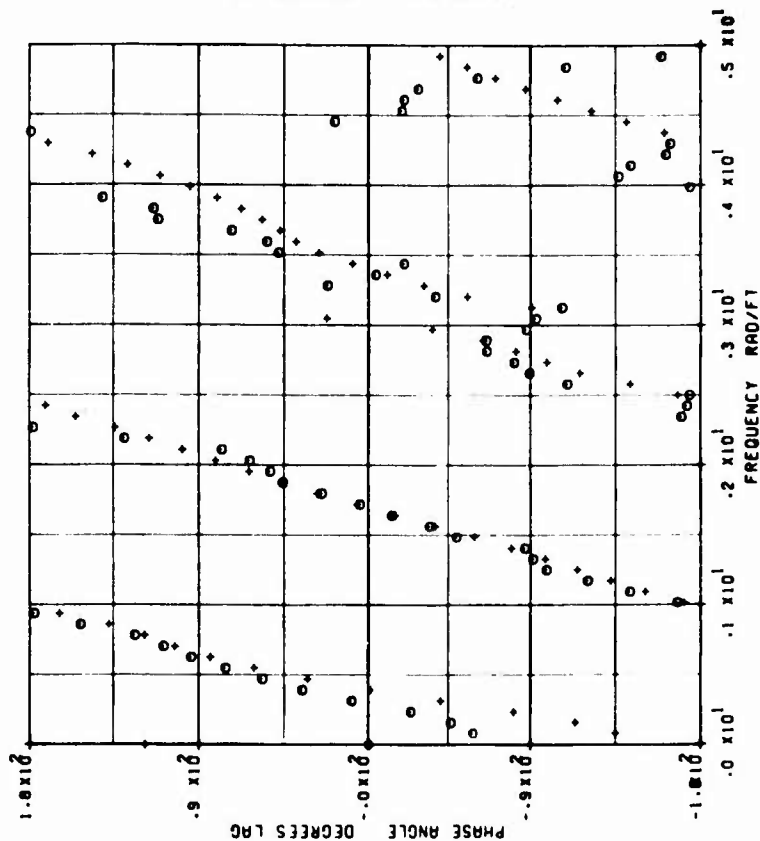
PHASE ANGLE

OUTPUT- HORIZONTAL STABILIZER BENDING (HXP) AT MSS 232

INPUT- VERTICAL GUST VELOCITY

TEST O THEORETICAL +

ALTITUDE 2240 FEET
AIRSPEED 260.9 KERS
GROSS WEIGHT 514000 LB
FUEL WEIGHT 80000 LB
CARGO WEIGHT 110000 LB
CG 33.3 PCT MAC



3-D GUST RESPONSE COMPARISON FOR C-SA AIRCRAFT

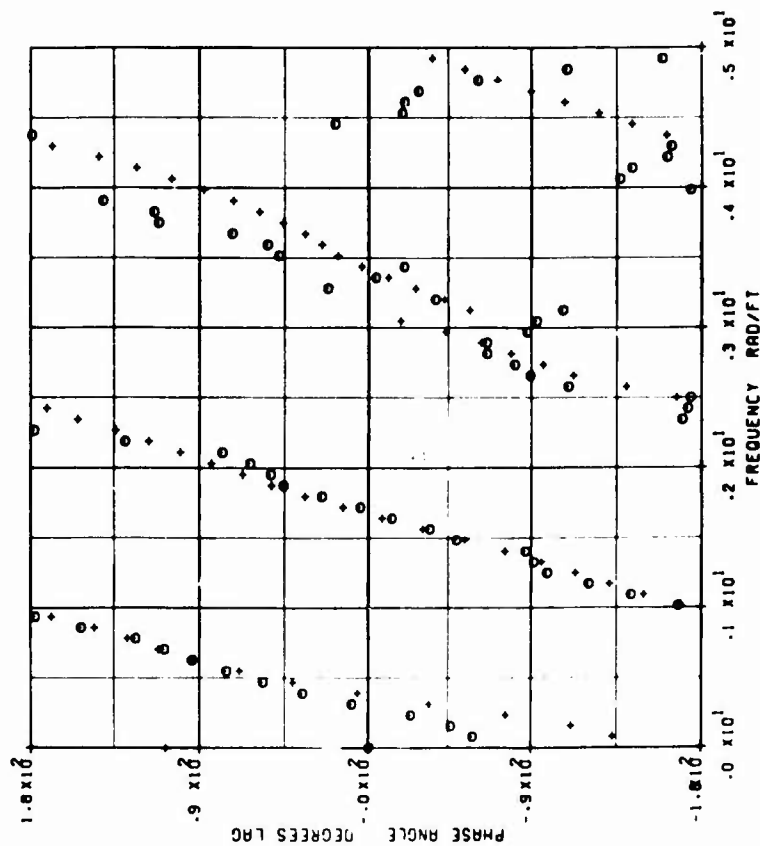
PHASE ANGLE

OUTPUT- HORIZONTAL STABILIZER BENDING (HXP) AT MSS 232

INPUT- VERTICAL GUST VELOCITY

TEST O THEORETICAL +

ALTITUDE 2240 FEET
AIRSPEED 260.9 KERS
GROSS WEIGHT 514000 LB
FUEL WEIGHT 80000 LB
CARGO WEIGHT 110000 LB
CG 33.3 PCT MAC



1-D DUST RESPONSE COMPARISON FOR C-5A AIRCRAFT

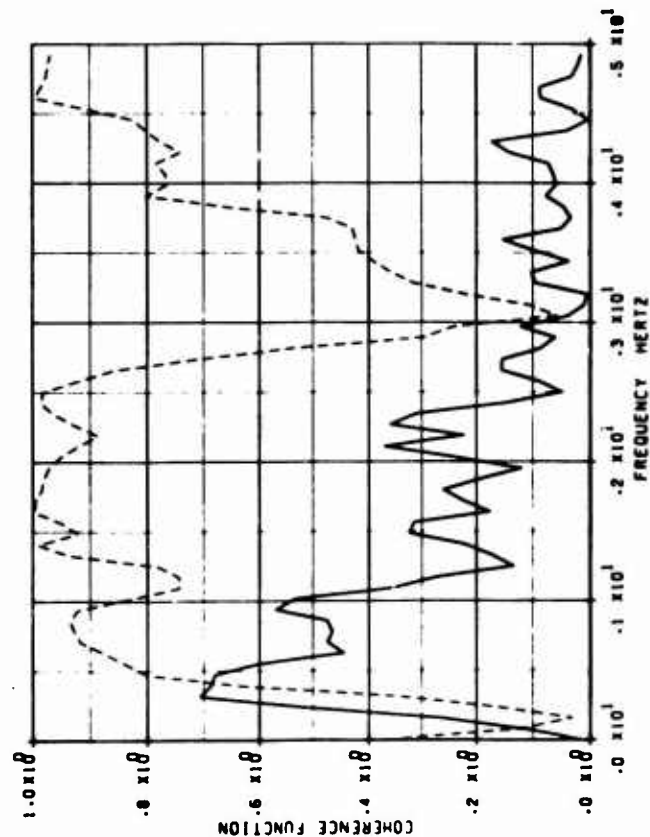
COHERENCE FUNCTION

OUTPUT- HORIZONTAL STABILIZER BENDING (INP) AT MSS 232

INPUT- VERTICAL GUST VELOCITY

TEST --- THEORETICAL --

ALTITUDE 2240 FEET
AIRSPEED 260.9 KERS
GROSS WEIGHT 514000 LB
FUEL WEIGHT 80000 LB
CARGO WEIGHT 110000 LB
CG 33.3 PCT MAC



3-D DUST RESPONSE COMPARISON FOR C-5A AIRCRAFT

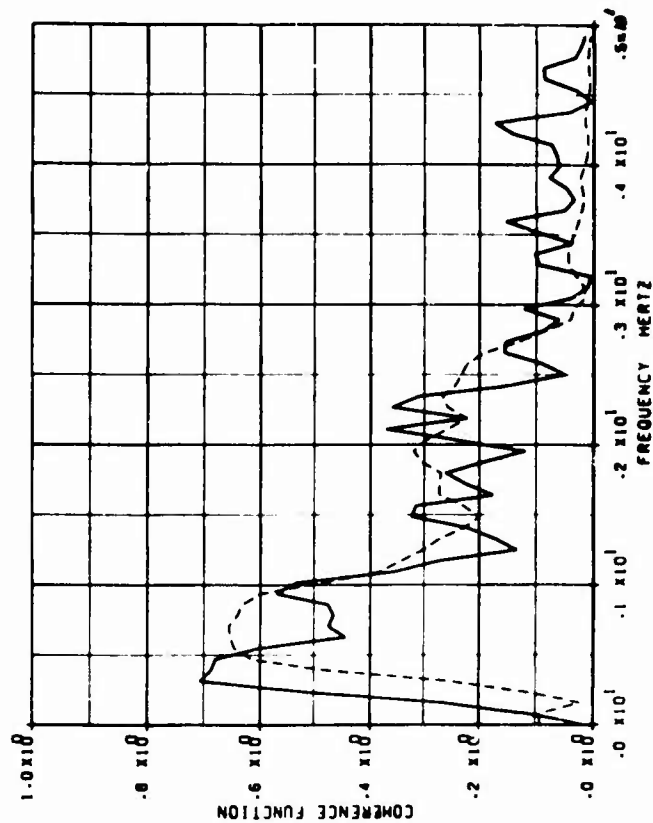
COHERENCE FUNCTION

OUTPUT- HORIZONTAL STABILIZER BENDING (INP) AT MSS 232

INPUT- VERTICAL GUST VELOCITY

TEST --- THEORETICAL --

ALTITUDE 2240 FEET
AIRSPEED 260.9 KERS
GROSS WEIGHT 514000 LB
FUEL WEIGHT 80000 LB
CARGO WEIGHT 110000 LB
CG 33.3 PCT MAC



SECTION VI

CONCLUSIONS AND RECOMMENDATIONS

Section V shows that variations in incremental loads resulting from the application of a 3-d rather than a 1-d turbulence representation to the gust response analysis of a large aircraft are far from uniform. Such changes cannot be approximated by adjusting the 1-d results by a single empirical correction factor as has sometimes been suggested. Furthermore, it is difficult to ignore load changes of the magnitude shown in Section V, particularly in fatigue design. For the simple power law S_N curve, the percent change in fatigue damage is many times greater than the percent change in the related incremental load for typical aircraft structural alloys.

The 3-d turbulence model presented in this report is derived from the same turbulence theory as the conventional 1-d model. No additional assumptions are introduced, and the only change which occurs in the transition to the 3-d case is that the gust coherence becomes dependent upon transverse separation. Moreover, this dependence is apparently quite insensitive to the specific spectral character of the turbulence field. For example, gust coherences derived from the von Karman and Dryden spectral models are almost indistinguishable according to Reference 4.

In effect, the 3-d model furnishes a transverse coherence description which is mathematically consistent with the longitudinal variation in the turbulence field that is reflected in the power spectra of the three gust velocity components. Since these spectra are measurable and their form is well established, the 3-d turbulence description does in no sense introduce a weak link in the gust response analysis. On the contrary, inherent defects in the structural and aerodynamic representation of the aircraft become more apparent because they are no longer obscured by the 1-d turbulence assumption. This is particularly evident in comparisons with flight test results where a gust probe has been employed.

It is therefore recommended that the effects of changes and refinements in the analytical model of the aircraft be explored within the context of the 3-d gust response analysis, using the flight test comparison procedures discussed in Section V. Development efforts in the following areas are also suggested: (1) introduction of special analytical methods to reduce the computational effort and volume of data which are ordinarily generated in gust design calculations, (2) adaptation of the current 3-d gust response method for time domain analysis to provide response time histories, (3) extension of the analytical aerodynamic model to permit the longitudinal gust component to be included, and (4) modification of the present 3-d gust response method to treat turbulence nonstationarities that are rapid enough to induce significant transient responses in the aircraft structure.

REFERENCES

1. Eichenbaum, F. D., "A New Method for Computing the Dynamic Response of Aircraft to Three-Dimensional Turbulence," Proceedings of the AIAA Structural Dynamics and Aeroelasticity Specialist Conference, New Orleans, Louisiana, Apr. 16-17, 1969
2. Eichenbaum, F. D., "Three-Dimensional Gust Response Correlation," Engineering Report 1036, Mar. 1970, Lockheed-Georgia Company
3. Eichenbaum, F. D., "A General Theory of Aircraft Response to Three-Dimensional Turbulence," Journal of Aircraft, Vol. 8, No. 5, May 1971, pp. 353-360
4. Eichenbaum, F. D., "Response of Aircraft to Three-Dimensional Random Turbulence," TR-72-28, Oct. 1972, Air Force Flight Dynamics Laboratory, Wright-Patterson Air Force Base, Ohio
5. Coupry, G., "Effect of Spanwise Variation of Gust Velocity on Airplane Response to Turbulence," Journal of Aircraft, Vol. 9, No. 8, Aug. 1972, pp. 569-574
6. Hinze, J. O., Turbulence: An Introduction to Its Mechanism and Theory, McGraw-Hill, New York, 1959, p. 183
7. Military Specification, "Airplane Strength and Rigidity Flight Loads," MIL-A-008861A (USAF), Mar. 1971, unclassified, p. 20
8. Military Specification, "Flying Qualities of Piloted Airplanes," MIL-F-8785B (ASG), Aug. 1969, unclassified, pp. 47-48
9. Bisplinghoff, R. L., and Ashley, H., Principles of Aeroelasticity, Wiley, New York, 1962, pp. 641-644

REFERENCES (Continued)

10. Ingram, C. T., and Eichenbaum, F. D., "A Comparison of C-141A Flight Test Measured and Theoretical Vertical Gust Responses," Journal of Aircraft, Vol. 6, No. 6, Nov.-Dec. 1969, pp. 532-536
11. Landahl, M. T., "Kernel Function for Nonplanar Oscillating Surfaces in a Subsonic Flow," AIAA Journal, Vol. 5, No. 5, May 1967, pp. 1045-1046
12. Eichenbaum, F. D., "An Improved Kernel Function Formulation for Unsteady Subsonic Flow," AIAA Journal, Vol. 11, No. 1, Jan. 1973, pp 124-124